Summer 8-13-2010

The Role of Altered Loading in Pathological Changes in the Long Head of the Biceps Tendon Following Rotator Cuff Tears in a Rat Model

Cathryn D. Peltz
University of Pennsylvania, cpeltz@seas.upenn.edu

The Role of Altered Loading in Pathological Changes in the Long Head of the Biceps Tendon Following Rotator Cuff Tears in a Rat Model

Abstract
Damage to the biceps tendon is common clinically and is frequently seen in the presence of rotator cuff tears. However, there is some debate over the role of the biceps tendon at the shoulder following a rotator cuff tear with some believing the biceps to play a significant role as a humeral head depressor while others believe the biceps plays no role at all. Therefore, controversy exists regarding its optimal treatment, with physicians relying mostly on anecdotal experience. Unfortunately, most clinical studies are not able to address the underlying causes in a controlled manner and cadaveric studies cannot monitor the injury process with time. Tendon degeneration and inflammation are both thought to play a role; however, the mechanisms responsible remain unknown, making clinical management of this problem difficult. Therefore, the objective of this study was to examine the effect of alterations in loading on the initiation of pathological changes in the long head of the biceps tendon following rotator cuff tears in order to determine its role as a mechanism for these changes. We hypothesized that rotator cuff tears result in altered loading that lead to degeneration of the biceps tendon, beginning at the insertion site and continuing along the length with time. Additionally, we hypothesized that increased loading following rotator cuff tears would result in further degeneration while decreased loading would result in improved tendon properties. We created an animal model of biceps tendon pathology in the presence of rotator cuff tears and utilized this model to examine the early, intermediate and late changes in histological, organizational, compositional and mechanical properties of the biceps tendon. We found that changes began in the intra-articular portion of the tendon before progressing to the extra-articular portion with time. We also investigated the effect of altered loading on these properties and found that increased loading resulted in further detrimental changes while decreased loading resulted in improved properties. These results indicate that the biceps tendon plays an increased role as a load bearing structure in the presence of rotator cuff tears and that these changes may be recoverable with decreased loading.

Degree Type
Dissertation

Degree Name
Doctor of Philosophy (PhD)

Graduate Group
Bioengineering

First Advisor
Louis J. Soslowsky

Keywords
biceps tendon, rotator cuff, animal model, altered loading, tendon pathology

Subject Categories
Biomechanics and Biotransport

THE ROLE OF ALTERED LOADING IN PATHOLOGICAL CHANGES IN THE LONG HEAD OF THE BICEPS TENDON FOLLOWING ROTATOR CUFF TEARS IN A RAT MODEL

Cathryn Peltz

A DISSERTATION

In

Bioengineering

Presented to the Faculties of the University of Pennsylvania

in Partial Fulfillment of the Requirements for the Degree of Doctor of Philosophy

2010

Supervisor of Dissertation

_____

Louis J. Soslowsky, PhD, Fairhill Professor, Orthopaedic Surgery

Graduate Group Chairperson

_____

Susan S. Margulies, PhD, Professor, Bioengineering

Dissertation Committee

Jason Burdick, PhD, Associate Professor, Bioengineering

Dawn Elliott, PhD, Associate Professor, Orthopaedic Surgery

David Glaser, MD, Associate Professor, Orthopaedic Surgery

Kurt Hankenson, DVM, PhD, Assistant Professor, Animal Biology

Acknowledgements

I would first like to thank my committee members for guiding me through my graduate experience. I would especially like to thank Dr. Louis Soslowsky, my advisor, for providing mentorship, support, knowledge, and insight throughout my time here. I thank Dr. David Glaser for surgical help and clinical insight throughout the development and duration of my thesis. I also thank Dr. Jason Burdick, Dr. Dawn Elliott, and Dr. Kurt Hankenson for their valuable comments and suggestions throughout my studies.

I would also like to thank my fellow members of the McKay Orthopaedic Research Laboratory. Dr. Joseph Sarver was the first person I worked with after joining the lab and has been my officemate for the past 3 years. His knowledge, advice and insight have been instrumental to my graduate education. I would like to thank LeAnn Dourte for not only being my REMO partner for several years, but for her continued support since. I would also like to thank Kris Miller for her enthusiasm and willingness to help and discuss ideas. I would also like to thank Stephanie Perry, who began as a mentor, grew to a colleague and continues to be a close friend. I would also like to acknowledge all the other graduate students, residents and post-docs, past and present, who I have exchanged not only scientific ideas, but life experiences with.

Finally, none of this would have been possible without the love and support of my family and friends. I thank my parents, Bill and Jane, who always encouraged me to go after anything I wanted and never wavered in their belief that I could do it.

ABSTRACT

THE ROLE OF ALTERED LOADING IN PATHOLOGICAL CHANGES IN THE LONG HEAD OF THE BICEPS TENDON FOLLOWING ROTATOR CUFF TEARS IN A RAT MODEL

Cathryn Peltz

Dr. Louis J. Soslowsky

Damage to the biceps tendon is common clinically and is frequently seen in the presence of rotator cuff tears. However, there is some debate over the role of the biceps tendon at the shoulder following a rotator cuff tear with some believing the biceps to play a significant role as a humeral head depressor while others believe the biceps plays no role at all. Therefore, controversy exists regarding its optimal treatment, with physicians relying mostly on anecdotal experience. Unfortunately, most clinical studies are not able to address the underlying causes in a controlled manner and cadaveric studies cannot monitor the injury process with time. Tendon degeneration and inflammation are both thought to play a role; however, the mechanisms responsible remain unknown, making clinical management of this problem difficult. Therefore, the objective of this study was to examine the effect of alterations in loading on the initiation of pathological changes in the long head of the biceps tendon following rotator cuff tears in order to determine its role as a mechanism for these changes. We hypothesized that rotator cuff tears result in altered loading that lead to degeneration of the biceps tendon, beginning at the insertion site and continuing along the length with time. Additionally, we hypothesized that

increased loading following rotator cuff tears would result in further degeneration while decreased loading would result in improved tendon properties. We created an animal model of biceps tendon pathology in the presence of rotator cuff tears and utilized this model to examine the early, intermediate and late changes in histological, organizational, compositional and mechanical properties of the biceps tendon. We found that changes began in the intra-articular portion of the tendon before progressing to the extra-articular portion with time. We also investigated the effect of altered loading on these properties and found that increased loading resulted in further detrimental changes while decreased loading resulted in improved properties. These results indicate that the biceps tendon plays an increased role as a load bearing structure in the presence of rotator cuff tears and that these changes may be recoverable with decreased loading.

TABLE OF CONTENTS

LIST OF TABLES

LIST OF FIGURES

Chapter 1: Introduction

A. Introduction

Musculoskeletal conditions cost our society an estimated $254 billion every year.[35] Shoulder injuries rank third in musculoskeletal clinical visits after back and neck pain.[11] Damage to the long head of the biceps tendon is common clinically and has often been identified as a source of shoulder pain. Although proximal long-head biceps tendon ruptures account for 96% of all biceps tendon ruptures[15], they rarely occur as an isolated injury and are often found in conjunction with pathologic conditions of the rotator cuff. Specifically, biceps tendon damage has been found in conjunction with rotator cuff tears and this damage is thought to increase with increasing tear size.[9,33] Considering that tears of the rotator cuff tendons are thought to occur in up to 50% of the population[11], damage to the long head of the biceps tendon is a very prevalent clinical problem.

What remains unknown is the mechanism responsible for the pathologic changes seen in the biceps tendon with a rotator cuff tear. Unfortunately, most clinical studies are not able to address the underlying cause of biceps tendon changes in the presence of rotator cuff tears in a controlled manner and cadaveric studies cannot monitor the injury process with time. In clinical studies, it is possible to biopsy a portion of the biceps tendon during a rotator cuff repair surgery. However, there are several complicating factors with this approach. First, the entire tendon cannot be removed and therefore regional differences in the tendon cannot be examined. Also, it would be extremely difficult to isolate a patient population with the same tear type and size as well as surgery that is performed at the same time post tear. Often in the clinic, the onset of symptoms

may not be representative of when the tear occurred therefore evaluating the effect of time post cuff tear would be difficult. In cadaveric studies, while one can harvest the entire tendon for analysis from a shoulder with a rotator cuff tear, little information exists on how long the tear has been present. In addition, cadaveric studies do not allow investigation of an in vivo time course of pathological changes following a known and reproducible rotator cuff tear.

Therefore, this study will begin to investigate the mechanisms of change by utilizing an animal model of biceps tendon pathology in the presence of rotator cuff tears to examine the effect of alterations in mechanical loading on the initiation of pathological changes in the biceps tendon.

B. Background

1. Shoulder Anatomy

The shoulder joint, or glenohumeral joint, can be described as a golf ball on a tee. In this scenario, the round golf ball (humeral head) sits on the slightly curved tee (glenoid), and while balanced is not fully enclosed. The bony architecture of the shoulder consists of the humerus, or upper arm bone, the scapula, or shoulder blade, and the clavicle (Figure 1.1). The humerus is able to rotate and translate in a shallow socket of

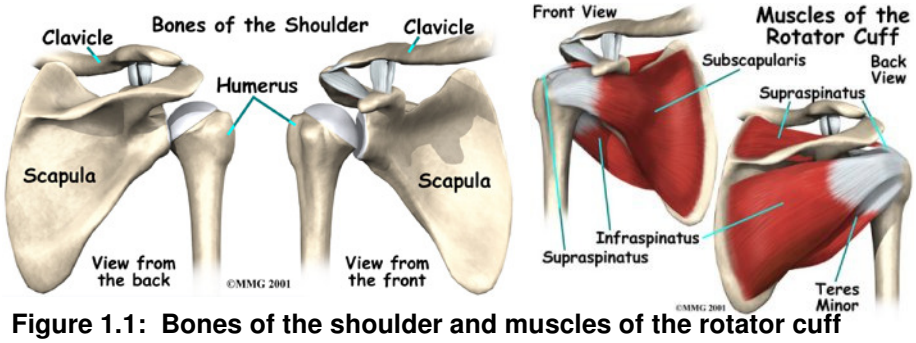

Figure 1.1: Bones of the shoulder and muscles of the rotator cuff (Image from eorthopod.com)

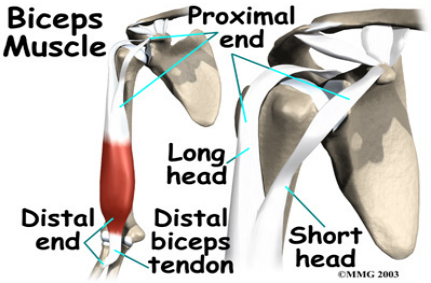

Figure 1.2: Proximal and distal ends of the biceps muscle (Image from eorthopod.com)

the scapula called the glenoid. The humerus is held into the glenoid and stabilized by a variety of soft tissues, including the glenohumeral ligaments, the rotator cuff and the long head of the biceps tendon. The rotator cuff is composed of 4 muscle-tendon units (the subscapularis, supraspinatus, infraspinatus, and teres minor) that originate on the scapula and insert on the humerus (Figure 1.1).[14,19] The subscapularis is the most anterior of the rotator cuff tendons, while the supraspinatus tendon is located under the coracoacromial arch. The infraspinatus and teres minor tendons are located posteriorly. Although the biceps tendon inserts at the elbow and most of its function occurs at this location, it also exists at the glenohumeral joint. The long head of the biceps tendon originates on the glenoid of the scapula and the short-head originates on the coracoid process before they join together and insert at the elbow (Figure 1.2). The long head of the biceps tendon runs across the humeral head and down the humerus, although the extent of its function in the shoulder joint is under debate and will be discussed in detail later.

2. Shoulder Function

The shoulder has the largest range of motion of any major joint in the human body. In general, the rotator cuff muscles and tendons are responsible for stabilization of the joint and many arm motions including humeral abduction, flexion, external and

internal rotation.[10,14,31,32] The subscapularis muscle is active as an internal rotator of the humerus and contributes to joint stability by providing an anterior restraint on external rotation. The supraspinatus muscle is mostly active in arm elevation. It functions to initiate arm abduction from 0º to 30º of elevation by compressing the humeral head against the glenoid fossa. The infraspinatus muscle is the second most active muscle of the rotator cuff and mainly functions in many aspects of external rotation by initiating the motion and preventing excessive rotation and hyperextension. It also contributes to joint stability and to arm elevation when the elbow is slightly flexed. Finally, the teres minor acts in parallel with the infraspinatus and serves as an external rotator of the humerus. While the rotator cuff muscles are usually identified as having primary activities as noted above, there is redundancy built into the system which allows for more than one muscle to perform certain functions. In fact, more recent studies suggest a cooperative role for many movements based on various factors including joint position, lines of action, and muscle capabilities.[17] While the function of the biceps tendon at the elbow is well-characterized, the function of the biceps in the shoulder is not. The general consensus is that the biceps tendon is a weak shoulder flexor. However, some debate on the exact role of the biceps in shoulder function exists and recent patient observation and biomechanical cadaver studies have proposed that the biceps tendon may also play a role as a humeral head depressor. [3,24,30,38,41]

3. Biceps Tendon

a. Anatomy

The biceps brachii tendon consists of 2 heads with a common insertion on the bicipital tuberosity of the radius. The biceps tendon originates at the supraglenoid

tuberosity of the scapula while the short-head originates on the coracoid process, also on the scapula. The two muscle bellies lie close to each other but are distinct until about 7cm from the elbow joint (Figure 1.2).[48] As seen in Figure 1.3, it runs obliquely across the top of the humeral head and then continues ventrally as it follows the humerus. The tendon then exits the articular capsule and enters the bicipital groove (intertubercular sulcus). Interestingly, the biceps tendon is intra-articular but extrasynovial. The outermost layer of the shoulder joint synovial sheath reflects back on itself to form a visceral sheath in which the biceps tendon is surrounded. This sheath permits the humeral head to glide along the biceps tendon. The cross-sectional area of the biceps tendon varies along its length. It is widest at its origin on the glenoid (8.5 X 2.8 mm) and narrows at the entrance to the bicipital groove (4.7 X 2.6 mm), with a similar area after exiting the groove, near the musculotendinous junction (4.5 X 2.8 mm).[12] The approximate tendon length is 9.2 cm.

The biceps tendon is unique in that it varies along its length due to changes in surrounding anatomy and types of loading seen in different areas. While bony landmarks help to contain the tendon within the groove, the majority of support for the biceps

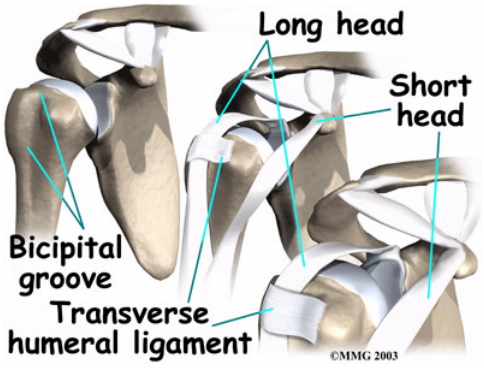

Figure 1.3: Bony anatomy and insertion locations of the short and long-heads of the biceps tendon (Image from eorthopod.com)

tendon is provided by surrounding soft tissues. The tendon is covered by the rotator cuff tendons near the glenoid and humeral head and the coracoacromial and transverse humeral ligaments help to retain the tendon in the groove distally. At the attachment of the biceps tendon on the glenoid, mostly compressive loading against the humeral head is seen. However, further away from the insertion site, the tendon is oriented longitudinally and mostly tensile loading is seen. A cadaveric study of normal biceps tendons by Kolts et al reinforced this idea, as structural differences were seen along the length of the tendon, with some fibrous cartilage features near the humeral head where compressive and shear forces are thought to occur and was more adapted to tensile loading as it approached the bicipital groove.[23]

b. Role at the shoulder

While the function of the biceps tendon at the elbow is well-characterized, the function of the biceps at the shoulder is not. Ruptures of the biceps tendon rarely occur as an isolated injury and therefore it is difficult to assess the associated functional deficits. The general consensus is that the biceps tendon is a weak shoulder flexor, although some studies suggest a larger role as a humeral head depressor or glenohumeral stabilizer.[3,24,30,38,41] This debate on the exact role of the biceps in shoulder function has led to a fair amount of patient observation and biomechanical cadaver studies to investigate its role.[1,24,26,28,36,41]

In a direct patient observation study by Warner and McMahon[41], they found that when the biceps is detached there appears to be an increase in superior translation of the humeral head with shoulder abduction and therefore concluded that the biceps tendon plays a significant role in the stability of the glenohumeral joint, specifically during

shoulder abduction in the superior-inferior plane. Kumar et al also noted that because abduction of the glenohumeral joint involves the sliding of the proximal humerus on the biceps tendon that the biceps tendon also plays a role as a humeral head depressor.[24] Electromyographic (EMG) studies have resulted in some conflicting results. For example, Sakurai et al found biceps activity at the shoulder to be present in 24 shoulder motions that increased with elevation.[36] They also concluded that the long head of the biceps can act as a humeral head stabilizer in both the superior and anterior directions. Conversely, Levy et al also tested biceps activity during abduction and concluded that the biceps is not active in shoulder motion and the role of the tendon must be passive.[26] It is interesting to note that both of these studies attempted to minimize elbow related activity using a brace to lock its position during shoulder movements. However, both authors acknowledge that many shoulder activities involve elbow motion and it is likely that minimizing elbow motion is probably not applicable to common activities of daily living. There have also been studies that attempt to evaluate the role of the biceps tendon in patients during shoulder surgery, also with conflicting results. Lippman et al concluded that it was only a passive structure[28]while Andrews et al observed that electrical stimulation resulted in compression of the humeral head against the glenoid.[1] As a result, there continues to be a wide range of opinions regarding the contribution of the biceps tendon to shoulder function, from those who believe it plays no role at all to those who consider it an important stabilizer.

c. Changes with rotator cuff tear

With rotator cuff tears, damage to the biceps tendon occurs.[33] Clinical observations note a widened, flattened or frayed biceps tendon at the time of cuff repair.[18]

Also, clinical studies have found that rotator cuff tear size correlates with advanced biceps tendon lesions.[9] However, not all studies have found pathology present.[8] The proposed role of the biceps tendon as a humeral head depressor is thought to be a significant contributor to changes seen in the biceps tendon with a rotator cuff tear, where one or more of the more significant superior stabilizers (supraspinatus and/or infraspinatus) would not be present. This could lead to an overload situation on the biceps tendon, impingement on the tendon or a combination of the two. EMG studies have studied the function of the biceps tendon in the presence of a rotator cuff tear with conflicting results.[21,49] Yamaguchi concluded no biceps activity was present in patients with rotator cuff tears[49]while Kido showed the biceps to be an active humeral head depressor when a tear was present.[21] The location of pathological changes is also somewhat controversial. Some believe that pathology occurs at the entrance to the bicipital groove, and suspect the tendon first becomes inflamed and then damaged when it has trouble sliding after it becomes hypertrophied. Neer has long believed that the biceps tendon is susceptible to impingement under the acromion after a rotator cuff tear occurs and that changes occur near the tendon's attachment to the glenoid on its bursal side. [34] It is also possible that changes may occur in this location but on the articular side, as increased compressive loading against the humeral head is present. A recent study by Joseph supports Neer's theory that changes begin at or near the insertion site. Joseph investigated both the intra- and extra-articular portions of tenotomized biceps tendons from shoulders with rotator cuff tears and found the intra-articular portions to have markedly different proteoglycan content and organization than the extra-articular portions.[20] However, the mechanisms responsible for biceps tendon changes in the

presence of a rotator cuff tear are difficult to address in a clinical study due to both the inability to harvest the entire biceps tendon during cuff repair and the complexity of evaluating the effect of time post-repair when the precise history including the exact instance of tear initiation is often unknown. Therefore, the use of an animal model would be beneficial.

These conflicting results have led to some clinical controversy surrounding treatment for the biceps tendon in the presence of a rotator cuff tear. The biceps tendon is thought to be a significant source of pain and therefore in some cases, is treated with a tenotomy (detachment) or tenodesis (detachment from scapula and reattachment elsewhere) even when the cuff tear is too massive to be repaired. However, if the biceps tendon does play an important functional role at the shoulder, retaining this tendon may be important. In the case of impingement, acromioplasty may be necessary. It is also unknown if the pathological changes in the biceps tendon due to an existing rotator cuff tear are recoverable with repair of the rotator cuff. Additionally, it is often not clear whether the changes in the biceps tendon are truly degenerate or are due to inflammation alone. It is therefore important to determine the initiating events and time course of damage that exists in this scenario.

d. Biceps tendon investigations in animal models

Currently, there are no animal models in use to investigate the biceps tendon. An animal model that mimics the clinical situation of biceps tendon changes following rotator cuff tears would allow for the mechanism by which these changes occur to be elucidated. There is also some clinical controversy over the appropriate treatment of the biceps tendon in the presence of a rotator cuff tear. With the mechanism of injury

identified, the best possible treatment to recover biceps tendon changes could be studied in an appropriate animal model.

4. Tendon Properties

a. Biology and composition

Tendons are soft connective tissues connecting muscle and bone. They consist of an extracellular matrix (ECM) constructed to bear tensile loads and contain fibroblasts. Fibroblasts are spindle shaped cells which align in rows between bundles of collagen fibers. In general, the gel-like matrix is primarily composed of collagens, proteoglycans, glycoaminoglycans (GAGs), elastin and water.[7,27,42-44,47] The collagen and elastic fibrils provide the structural (fibrillar) component, and the proteoglycans, GAGs, and water make up the gel-like matrix surrounding the fibrils. While a variety of collagens can be found in tendon, collagen type-I composes up to ~85% of tendon dry weight, with other collagens in supporting roles.[7,27,42-44,47] Proteoglycans, such as decorin, biglycan, aggrecan, fibromodulin, lumican, and versican, compose ~1-5% of dry weight.[7,27,42-44,47] Finally, elastin can compose up to ~2% of dry weight.[7,27,42-44,47] Water is a large component of tendons and composes ~60-80% of the wet weight.[7,27,42-44,47] The rotator cuff tendons have a slightly varied composition from what is considered the "general" description of tendons. Collagens type-XII and type-III play a larger role than in other tendons.[4,29] Also, the amount and distribution of proteoglycans is altered, with aggrecan being more prominent.[4,29] The composition of the biceps tendon has not been largely studied but it is thought to be similar to rotator cuff tendons in that compressive loads are thought to occur near the insertion and ovoid cells resembling chondrocyctes have been seen in this region.[23] It has also been shown that the proteoglycan content of the distal

region of the biceps tendon is markedly different than the proximal region, where the content was similar to the rotator cuff tendons.[2] Tendon composition is known to change with injury and therefore it is important to understand normal composition in order to correctly interpret results of immunohistochemical assays.

b. Structure and function

Tendons serve as the main force transmitter between muscles and bones. In general, an organized structure of collagen fibers is surrounded by a gel-like matrix. The collagen fibers are closely packed and aligned with the longitudinal axis of the tendon and display a wavy pattern, or crimp. This crimp pattern plays a large role in recruitment of the fibers and distribution of force during mechanical loading.[42,43,47] Due to this alignment of fibers along the longitudinal axis, tendons are generally strongest in tensile properties and poor in compression.

Biceps tendon structure differs slightly from typical. The tendon wraps around the humeral head before it inserts onto the scapula resulting in a complex loading environment at the insertion site. Cells near the tendon see high tensile loads and cells near the bone see more compressive loads. In order to provide proper joint function and prevent injury, the insertion site transfers these complex loads. Therefore, the properties of the tendons vary along their length to achieve normal function. In the proposed study, we expect the loading environment of the tendons to change with injury and therefore, we will measure variations in histological and immunohistochemical properties along the length of the tendon at the insertion site, in the intra-articular space and in the bicipital groove.

c. Mechanics

Tendon is an inhomogeneous, anisotropic, non-linear, viscoelastic material that undergoes large deformations.[7] The high proportion and longitudinal arrangement of the collagen type-I fibers make tendon one of the strongest tensile bearing soft tissues in the body.[42,47] The stress-strain behavior of tendon typically has an initial non-linear region, called the toe region, followed by a linear region until specimen yield and/or failure. The toe region is thought to be a result of the gradual recruitment of crimped fibers as the tendon is elongated.[13] During this time, there is a large amount of deformation with little load. After the toe region, the load-deformation curve is approximately linear since all of the fibers have become engaged and bear load. Tendon also exhibits viscoelastic behavior, which depends on both time and loading history. Proteoglycans and water, along with the inherent viscoelasticity of the collagen itself, are thought to be primarily responsible for the viscoelastic behavior of tendons.[42,47]

d. Injury and healing

After tendon injury, the basic components of general wound healing (inflammation, cell replication and migration, angiogenesis, matrix production and deposition / collagen protein formation, and remodeling) occur. These components happen during a significant reparative response, consisting of three phases.[25,27,42-44] It is important to note that these phases describe the tendon's response to an acute injury such as a tear, which is not happening in the biceps tendon in this study. However, the presence of these responses in the surrounding rotator cuff tendons that are detached may have a direct effect on the pathology of the biceps tendon.

The first phase, called the acute vascular-inflammatory response, occurs immediately after injury and lasts days.. This phase results in increased fibronectin,

GAGs, water, and type III collagen. The next phase, called the proliferative phase, begins a couple of days after injury and can last a week or so. While both type I and type III collagens are present, concentrations of type III collagen reach their peak during this stage and there is a notable increase in the ratio of collagen III to collagen I.[6,27] The final phase, called the remodeling phase, begins approximately 3 weeks after injury and can last over a year. Collagen I production has been seen to increase 15 to 22 times the normal rate during this period, which helps to return the ratio of type III to type I collagen back to normal.[42]

e. Remodeling and response to changes in loading

The remodeling response of a tendon has been shown to differ from its healing response after a transection.[40] Remodeling does not include the scar response discussed above in response to a transectional injury, but rather changes in collagen turnover and the balance and amount of proteins such as matrix metalloproteinases (MMPs) and their inhibitors (TIMPS), which play a large role in regulating the remodeling process.[22] Tendon is in a constant state of remodeling to maintain its matrix composition and properties, and normally the rate of degradation is equal to the rate of synthesis.[5]

Similar to other orthopaedic tissues, tendons have the ability to remodel and adapt their mechanical properties in response to an altered loading environment. When the mechanical demands on the tendon (both amount and type of loading) change, the tendon attempts to adapt to this change in load and the balance of this normally tightly regulated process is altered. Areas of tendons experiencing mostly tensile loading consist of more densely aligned collagen fibers and less proteoglycans.[47] Areas of the tendon exposed to compressive or shear loading typically consist of loosely aligned fibers and more

proteoglycans.[16] Previous studies have shown that immobilization or stress deprivation of the limb has a negative effect on the mechanical properties (tensile strength, modulus) of uninjured tendons.[16,37,42,47,50] Conversely, mechanical properties (modulus, ultimate load) and structural composition (crimp, collagen synthesis) of uninjured tendon have been positively effected by exercise.[16,37,45,46] Further, excessive increases in loading, or overuse, has been shown to have a negative effect on the mechanical properties (modulus) of tendon.[39] When an increase in physical activity happens, simultaneous degradation and synthesis of collagen is stimulated. With normal exercise, the rate of synthesis is greater than the rate of degradation, resulting in superior properties. Problems arise when the rate of degradation is greater than the rate of synthesis, such as in an overuse or disuse scenario. Additionally, the quality of the tissue present is important. A greater synthesis rate could be detrimental if poor quality tissue is being produced. In addition to changes in amount of loading, changes in type of loading could also be detrimental. A tendon adapted to tensile loading could be damaged when it is exposed to shear or compressive loads following injury. It is unclear what effect a reduction or increase in loading of the biceps tendon following a rotator cuff tear would have on the properties of this tendon but it is possible that the tendon can return to homeostasis and eventually its balanced state if it can successfully adapt to the change in loading or if the loading seen returns to normal levels.

C. <u>Specific Aims</u>

Pathological changes to the long head of the biceps tendon is a common clinical problem that has often been identified as a source of shoulder pain. This damage is also

frequently seen in the presence of rotator cuff tears. However, there role of the biceps tendon in the presence of a cuff tear is under some debate, with some studies suggesting the biceps plays a significant role as a humeral head depressor while others believe the biceps plays no role at the shoulder. Therefore, controversy exists regarding the optimal treatment for the damaged biceps tendon, with physicians relying mostly on anecdotal experience. Tendon degeneration and inflammation are both thought to play a role in this damage; however, the mechanisms which lead to biceps changes remain unknown which makes clinical management of this problem difficult. Determining the origin of pathology in location and type of change would help to identify the extrinsic mechanism by which these changes occur as well as the initiating biologic events that lead to tendon degeneration in this scenario.

The overall objective of this study is to examine the effect of alterations in mechanical loading on the initiation of pathological changes in the long head of the biceps tendon following rotator cuff tears in order to determine its role as a mechanism for these changes. To accomplish our objective, we will use an animal model of biceps tendon pathology in the presence of rotator cuff tears, both alone and in combination with additional changes in joint loading, to investigate the cause and effect relationships between changes in mechanical, histological and organizational properties along the length of the tendon. Our global hypothesis is that rotator cuff tears result in altered joint loading conditions that lead to degeneration of the long head of the biceps tendon, beginning at the insertion site and continuing along the tendon length with time.

Specific Aim 1: Identify the mechanical, histological and organizational changes in the long head of the biceps tendon following a combined supraspinatus and infraspinatus rotator cuff tendon tear in a rat model.

Hypothesis 1: Properties of normal biceps tendons will vary along the tendon length due to the different loading environments seen in each location.

Hypothesis 2: Following a rotator cuff tear, degeneration of the long head of the biceps tendon occurs, resulting in altered histological, organizational and mechanical properties.

Hypothesis 2a: Changes in histological and organizational properties will occur prior to, and result in, changes in biomechanical parameters.

Alterations in loading on the tendon as a result of rotator cuff tears will cause a change in collagen composition and decreased organization, which leads to increased area as the tendon attempts to remodel and produces more extracellular matrix. Eventually, decreased mechanical properties will result as the tendon cannot return to its original state and continues to produce more poor quality tissue.

Hypothesis 2b: Histological, organizational and mechanical changes in the long head of the biceps tendon following a rotator cuff tear will begin at the insertion site and progress along the tendon length with time post injury.

The origin of degeneration occurring at the insertion site is a direct result of increased loads seen by the tendon as its suspected role as a humeral head depressor is increased in the absence of supraspinatus and infraspinatus tendons.

Specific Aim 2: Determine the effect of changes in loading conditions on the long head of the biceps tendon following rotator cuff tears.

Hypothesis 3: Additional load on the long head of the biceps tendon (by short-head detachment and treadmill running) following a supraspinatus+infraspinatus rotator cuff tear will result in further pathologic changes.

Hypothesis 3a: Histological, organizational and mechanical changes in the long head of the biceps tendon will occur earlier when additional increases in load are seen in combination with rotator cuff tear.

Hypothesis 3b: Pathologic changes in the long head of the biceps tendon will be more severe at late time points when rotator cuff tears are combined with further increases in load compared to changes seen with a rotator cuff tear alone.

Hypothesis 4: Decrease in load on the long head of the biceps tendon (by immobilization) following a supraspinatus+infraspinatus rotator cuff tear will not result in pathologic changes.

Hypothesis 4a: At early time points, pathological changes in the long head of the biceps tendon will not be seen when load is removed following rotator cuff tear.

Immobilization following cuff tears will shield the biceps tendon from the increased loads seen with daily use following rotator cuff tears and the tendon will not show signs of degeneration.

Hypothesis 4b: At late time points, detrimental changes reflecting disuse, will be seen following rotator cuff tear with post-operative immobilization.

These studies will provide significant information on the effect of rotator cuff tears on the mechanical, histological and organizational properties of the biceps tendon. By determining the origin of these changes, both in type of change and location, we will provide insight into the possible mechanism for this change. Identification of the

contribution of altered loading as a mechanism of pathological changes in the biceps tendon in the presence of a rotator cuff tear will help guide surgeons in the optimal treatment for a biceps tendon that has been damaged as a result of a cuff tear. Future studies will use this animal model to evaluate possible treatment strategies and determine the likelihood of the recovery of these pathological changes.

D. Study Design

A total of 135 male Sprague-Dawley rats weighing 400-450 g were used for this study, as seen in Figure 1.4. In the study, surgical detachments of rotator cuff tendons will be performed both alone (Specific Aim 1) and in combination with additional increased or decreased load (Specific Aim 2) on the biceps tendon. Sham surgeries will also be performed to compare to detachments alone in Specific Aim 1. Additionally,

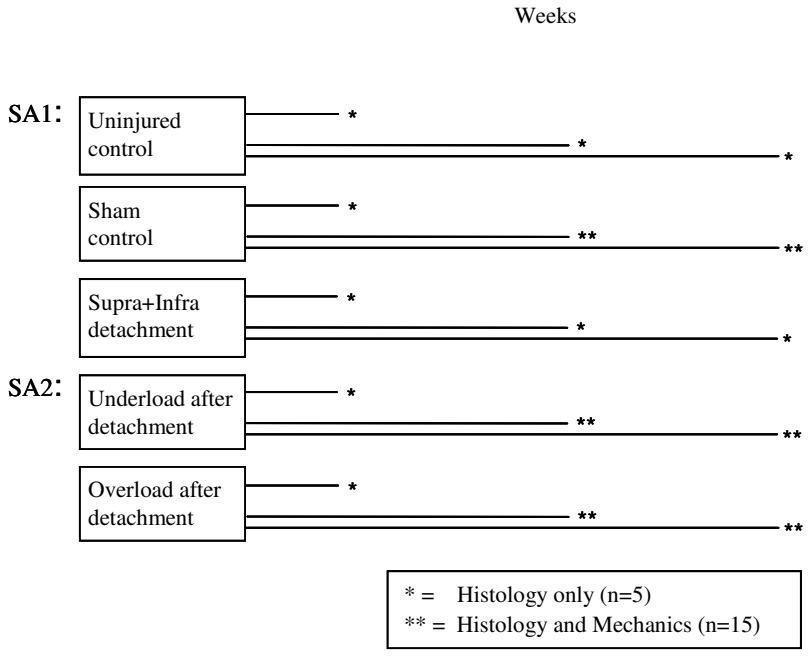

Figure 1.4: Study design to complete Specific Aims 1 (SA1) and 2 (SA2).

biomechanical, organizational, histological and immunohistochemical assays will be performed at specific time points. The later time points (4 and 8 weeks) were chosen to correspond with data from preliminary studies of biceps tendon pathology in the presence of a supraspinatus+infraspinatus detachment. Earlier time points were chosen in order to determine the origin of biceps tendon pathology. These studies will provide significant information on the effect of rotator cuff tears and the addition of post-operative altered loading on the mechanical, histological and organizational properties of the biceps tendon.

E. Chapter Overview

Chapter two describes the development of an animal model of biceps tendon pathology in the presence of rotator cuff tears and provides the methods, results, and discussion for the experimental studies performed to characterize the mechanical changes to the biceps tendon following multiple rotator cuff tear combinations in an animal model. Chapter three provides the methods, results, and discussion for the experimental studies performed to characterize the mechanical, histological, organizational and compositional changes to the biceps tendon following a supraspinatus+infraspinatus rotator cuff tear in an animal model compared to a sham injury. Chapter four provides the methods, results, and discussion for the experimental studies performed to determine the effect of alterations in loading following rotator cuff tears in an animal model on the mechanical properties of the biceps tendon. Chapter five provides the methods, results and discussion for the experimental studies performed to characterize the histological, organizational and compositional changes to the biceps tendon following rotator cuff

tears and altered loading in an animal model. Chapter six provides the provides the methods, results, and discussion for the experimental studies performed to characterize the mechanical changes to the biceps tendon following a supraspinatus+infraspinatus rotator cuff tear over time in an animal model. Finally, chapter seven summarizes the conclusions of the previous chapters and provides potential future directions in this area.

F. <u>References</u>

1. **Andrews, J. R.; Carson, W. G., Jr.; and McLeod, W. D.:** Glenoid labrum tears related to the long head of the biceps. *Am J Sports Med,* 13(5): 337-41, 1985.
2. **Berenson, M. C.; Blevins, F. T.; Plaas, A. H.; and Vogel, K. G.:** Proteoglycans of human rotator cuff tendons. *J Orthop Res,* 14(4): 518-25, 1996.
3. **Blasier, R. B.; Soslowsky, L. J.; Malicky, D. M.; and Palmer, M. L.:** Posterior glenohumeral subluxation: active and passive stabilization in a biomechanical model. *J Bone Joint Surg Am,* 79(3): 433-40, 1997.
4. **Blevins, F. T.; Djurasovic, M.; Flatow, E. L.; and Vogel, K. G.:** Biology of the rotator cuff tendon. *Orthop Clin North Am,* 28(1): 1-16, 1997.
5. **Buchanan, C. I., and Marsh, R. L.:** Effects of exercise on the biomechanical, biochemical and structural properties of tendons. *Comp Biochem Physiol A Mol Integr Physiol,* 133(4): 1101-7, 2002.
6. **Buckwalter, J. A.:** Activity vs. rest in the treatment of bone, soft tissue and joint injuries. *Iowa Orthop J,* 15: 29-42, 1995.
7. **Butler, D. L.; Juncosa, N.; and Dressler, M. R.:** Functional efficacy of tendon repair processes. *Annu Rev Biomed Eng,* 6: 303-29, 2004.

8. **Carpenter, J. E.; Wening, J. D.; Mell, A. G.; Langenderfer, J. E.; Kuhn, J. E.; and Hughes, R. E.:** Changes in the long head of the biceps tendon in rotator cuff tear shoulders. *Clin Biomech (Bristol, Avon),* 20(2): 162-5, 2005.

9. **Chen, C. H.; Hsu, K. Y.; Chen, W. J.; and Shih, C. H.:** Incidence and severity of biceps long head tendon lesion in patients with complete rotator cuff tears. *J Trauma,* 58(6): 1189-93, 2005.

10. **Friedman, R. J., and Knetsche, R. P.:** Biomechanics of the Rotator Cuff. In *Rotator Cuff Disorders*, pp. 45-58. Edited by Burkhead, W. Z., 45-58, Baltimore, Williams and Wilkins, 1996.

11. **Gomoll, A. H.; Katz, J. N.; Warner, J. J.; and Millett, P. J.:** Rotator cuff disorders: recognition and management among patients with shoulder pain. *Arthritis Rheum,* 50(12): 3751-61, 2004.

12. **Habermeyer, P., and Walch, G.:** The Biceps Tendon and Rotator Cuff Disease. In *Rotator Cuff Disorders*, pp. 142-159. Edited by Burkhead, W. Z., 142-159, Media, PA, Williams and Wilkins, 1996.

13. **Hansen, K. A.; Weiss, J. A.; and Barton, J. K.:** Recruitment of tendon crimp with applied tensile strain. *J Biomech Eng,* 124(1): 72-7, 2002.

14. **Harryman, D. T., 2nd, and Clark, J. M.:** Anatomy of the Rotator Cuff. In *Rotator Cuff Disorders*, pp. 23-35. Edited by Burkhead, W. Z., 23-35, Baltimore, Williams and Wilkins, 1996.

15. **Harwood, M. I., and Smith, C. T.:** Superior labrum, anterior-posterior lesions and biceps injuries: diagnostic and treatment considerations. *Prim Care,* 31(4): 831-55, 2004.

16. **Hyman, J., and Rodeo, S. A.:** Injury and repair of tendons and ligaments. *Phys Med Rehabil Clin N Am,* 11(2): 267-88, v, 2000.

17. **Iannotti, J. P.; Bernot, M. P.; Kuhlman, J. R.; Kelley, M. J.; and Williams, G. R.:** Postoperative assessment of shoulder function: a prospective study of full-thickness rotator cuff tears. *J Shoulder Elbow Surg,* 5(6): 449-57, 1996.

18. **Itoi, E.; Hsu, H. C.; Carmichael, S. W.; Morrey, B. F.; and An, K. N.:** Morphology of the torn rotator cuff. *J Anat,* 186 (Pt 2): 429-34, 1995.

19. **Jobe, C. M.:** Gross Anatomy of the Shoulder. In *The Shoulder*, pp. 34-87. Edited by Rockwood, C. A. J., and Matsen, F. A., 3rd, 34-87, Philadelphia, W.B Saunders Co., 1998.

20. **Joseph, M.; Maresh, C. M.; McCarthy, M. B.; Kraemer, W. J.; Ledgard, F.; Arciero, C. L.; Anderson, J. M.; Nindl, B. C.; and Mazzocca, A. D.:** Histological and molecular analysis of the biceps tendon long head post-tenotomy. *J Orthop Res*, 2009.

21. **Kido, T.; Itoi, E.; Konno, N.; Sano, A.; Urayama, M.; and Sato, K.:** The depressor function of biceps on the head of the humerus in shoulders with tears of the rotator cuff. *J Bone Joint Surg Br,* 82(3): 416-9, 2000.

22. **Kjaer, M.:** Role of extracellular matrix in adaptation of tendon and skeletal muscle to mechanical loading. *Physiol Rev,* 84(2): 649-98, 2004.

23. **Kolts, I.; Tillmann, B.; and Lullmann-Rauch, R.:** The structure and vascularization of the biceps brachii long head tendon. *Ann Anat,* 176(1): 75-80, 1994.

24. **Kumar, V. P.; Satku, K.; and Balasubramaniam, P.:** The role of the long head of biceps brachii in the stabilization of the head of the humerus. *Clin Orthop Relat Res,* (244): 172-5, 1989.

25. **Leadbetter, W. B.:** Cell-matrix response in tendon injury. *Clin Sports Med,* 11(3): 533-78, 1992.

26. **Levy, A. S.; Kelly, B. T.; Lintner, S. A.; Osbahr, D. C.; and Speer, K. P.:** Function of the long head of the biceps at the shoulder: electromyographic analysis. *J Shoulder Elbow Surg,* 10(3): 250-5, 2001.

27. **Lin, T. W.; Cardenas, L.; and Soslowsky, L. J.:** Biomechanics of tendon injury and repair. *J Biomech,* 37(6): 865-77, 2004.

28. **Lippmann, R. K.:** Bicipital Tenosynovitis. *NY State J Med*: 2235-2241, 1944.

29. **Malcarney, H. L., and Murrell, G. A.:** The rotator cuff: biological adaptations to its environment. *Sports Med,* 33(13): 993-1002, 2003.

30. **Malicky, D. M.; Soslowsky, L. J.; Blasier, R. B.; and Shyr, Y.:** Anterior glenohumeral stabilization factors: progressive effects in a biomechanical model. *J Orthop Res,* 14(2): 282-8, 1996.

31. **Matsen, F. A., 3rd; Arntz, C. T.; and Lippitt, S. B.:** Rotator Cuff. In *The Shoulder*, pp. 755-839. Edited by Rockwood, C. A. J., and Matsen, F. A., 3rd, 755-839, Philadelphia, W.B. Saunders Co., 1998.

32. **Morrey, B. F.; Itoi, E.; and An, K. N.:** Biomechanics of the Shoulder. In *The Shoulder*, pp. 233-276. Edited by Rockwood, C. A. J., and Matsen, F. A., 3rd, 233-276, Philadelphia, W.B. Saunders Co., 1998.

33. **Murthi, A. M.; Vosburgh, C. L.; and Neviaser, T. J.:** The incidence of pathologic changes of the long head of the biceps tendon. *J Shoulder Elbow Surg,* 9(5): 382-5, 2000.

34. **Neer, C. S., 2nd:** Anterior acromioplasty for the chronic impingement syndrome in the shoulder: a preliminary report. *J Bone Joint Surg Am,* 54(1): 41-50, 1972.

35. **Praemer, A.; Furner, S.; and Rice, D. P.:** Musculoskeletal Conditions in the United States. Edited, 182, Rosemont, IL, American Academy of Orthopaedic Surgeons, 1999.

36. **Sakurai, G.; Ozaki, J.; Tomita, Y.; Nishimoto, K.; and Tamai, S.:** Electromyographic analysis of shoulder joint function of the biceps brachii muscle during isometric contraction. *Clin Orthop Relat Res,* (354): 123-31, 1998.

37. **Sharma, P., and Maffulli, N.:** Tendon injury and tendinopathy: healing and repair. *J Bone Joint Surg Am,* 87(1): 187-202, 2005.

38. **Soslowsky, L. J.; Malicky, D. M.; and Blasier, R. B.:** Active and passive factors in inferior glenohumeral stabilization: a biomechanical model. *J Shoulder Elbow Surg,* 6(4): 371-9, 1997.

39. **Soslowsky, L. J.; Thomopoulos, S.; Tun, S.; Flanagan, C. L.; Keefer, C. C.; Mastaw, J.; and Carpenter, J. E.:** Neer Award 1999. Overuse activity injures the supraspinatus tendon in an animal model: a histologic and biomechanical study. *J Shoulder Elbow Surg,* 9(2): 79-84, 2000.

40. **Sun, H. B. et al.:** Cycle-Dependent Matrix Remodeling Gene Expression Response in Fatigue-Loaded Rat Patellar Tendons. *J Orthop Res*, 2010.

41. **Warner, J. J., and McMahon, P. J.:** The role of the long head of the biceps brachii in superior stability of the glenohumeral joint. *J Bone Joint Surg Am,* 77(3): 366-72, 1995.

42. **Woo, S. L.; An, K. N.; Frank, C. B.; Livesay, G. A.; Ma, C. B.; Zeminski, J.; Wayne, J. S.; and Myers, B. S.:** Anatomy, Biology, and Biomechanics of Tendon and Ligament. In *Orthopaedic Basic Science*, pp. 581-616. Edited by Buckwalter, J. A.; Einhorn, T. A.; and Simon, S. R., 581-616, Rosemont, IL, American Academy of Orthopaedic Surgeons, 2000.

43. **Woo, S. L., and Buckwalter, J. A.:** AAOS/NIH/ORS workshop. Injury and repair of the musculoskeletal soft tissues. Savannah, Georgia, June 18-20, 1987. *J Orthop Res,* 6(6): 907-31, 1988.

44. **Woo, S. L.; Debski, R. E.; Zeminski, J.; Abramowitch, S. D.; Saw, S. S.; and Fenwick, J. A.:** Injury and repair of ligaments and tendons. *Annu Rev Biomed Eng,* 2: 83-118, 2000.

45. **Woo, S. L.; Gelberman, R. H.; Cobb, N. G.; Amiel, D.; Lothringer, K.; and Akeson, W. H.:** The importance of controlled passive mobilization on flexor tendon healing. A biomechanical study. *Acta Orthop Scand,* 52(6): 615-22, 1981.

46. **Woo, S. L.; Gomez, M. A.; Woo, Y. K.; and Akeson, W. H.:** Mechanical properties of tendons and ligaments. II. The relationships of immobilization and exercise on tissue remodeling. *Biorheology,* 19(3): 397-408, 1982.

47. **Woo, S. L.; Livesay, G. A.; Runco, T. J.; and Young, E. P.:** Structure and Function of Tendons and Ligaments. In *Basic Orthopaedic Biomechanics*, pp.

514. Edited by Mow, V. C., and Hayes, W. C., 514, Philadelphia, Lippincott-Raven, 1997.

48. **Yamaguchi, K.; Keener, J.; and Galatz, L.:** Disorders of the Biceps Tendon. In *Disorders of the Shoulder: Diagnosis and Management*, pp. 217-260. Edited by Iannotti, J. P., and Williams, G. R., 217-260, Philadelphia, Lippincott, 2007.

49. **Yamaguchi, K.; Riew, K. D.; Galatz, L. M.; Syme, J. A.; and Neviaser, R. J.:** Biceps activity during shoulder motion: an electromyographic analysis. *Clin Orthop Relat Res,* (336): 122-9, 1997.

50. **Yasuda, K., and Hayashi, K.:** Changes in biomechanical properties of tendons and ligaments from joint disuse. *Osteoarthritis Cartilage,* 7(1): 122-9, 1999.

Chapter 2: Development of an animal model for biceps tendon pathology in the presence of rotator cuff tears

A. Introduction

This chapter will discuss the development of an animal model for biceps tendon pathology in the presence of multiple rotator cuff tear combinations in the rat model.

Biceps tendon pathology is a common clinical problem that is also thought to be a significant source of shoulder pain. Although proximal biceps tendon pathology (at the shoulder) is known to account for the majority biceps tendon damage, it rarely occurs in isolation.[11] Clinically, damage to the biceps tendon has been found often in conjunction with rotator cuff tears.[3,12,13] Clinical observations have described the biceps tendon as being flattened, widened, and/or frayed at the time of rotator cuff repair surgery[12] and this damage has also been seen to increase with increasing tear size.[3] Since rotator cuff tears can occur in up to 50% of the population over the age of 65[9], this area is of great clinical concern. The further damage with increasing tear size is also problematic as while most rotator cuff tears include the supraspinatus tendon, only half are isolated in that one tendon alone.[10]

Unfortunately, most clinical studies are unable to address the underlying cause of biceps tendon changes in the presence of rotator cuff tears in a controlled manner, and cadaveric studies cannot monitor the injury process with time. Currently, no animal models are available on this topic. However, the rat has previously been identified as an appropriate model for studies involving the rotator cuff.[16] The rat was chosen partly for

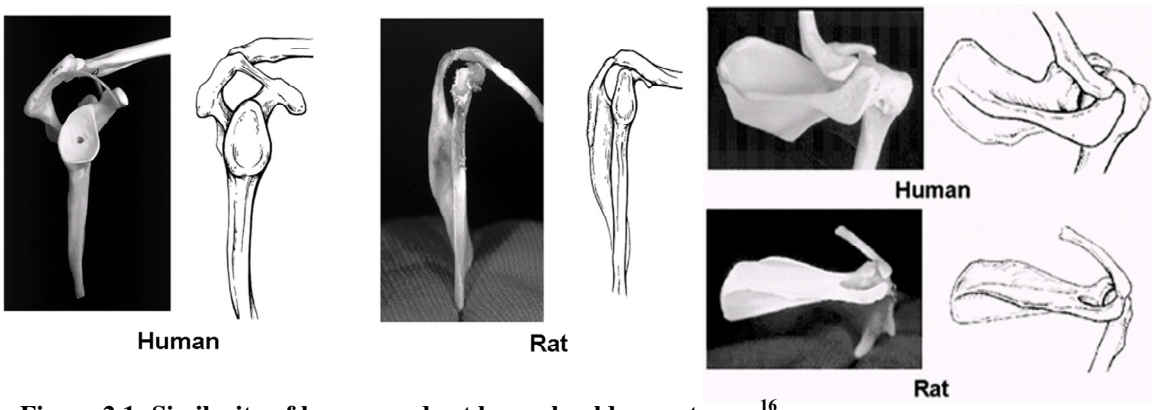

Figure 2.1: Similarity of human and rat bony shoulder anatomy. [16]

its similarity to the human in bony shoulder anatomy (Figure 2.1). The anatomy of the biceps tendon is also very similar in the rat and the human (Figure 2.2). In both the rat and the human, the long-head of the biceps tendon originates at the superior aspect of the glenoid and passes through the bicipital groove (Figure 2.2). Additionally, the histology of the rat biceps tendon (Figure 2.3) is similar to the human in that its insertion site is markedly less organized when compared to the distal tendon.

A previous study in our laboratory used a rat model of multiple tendon tears to

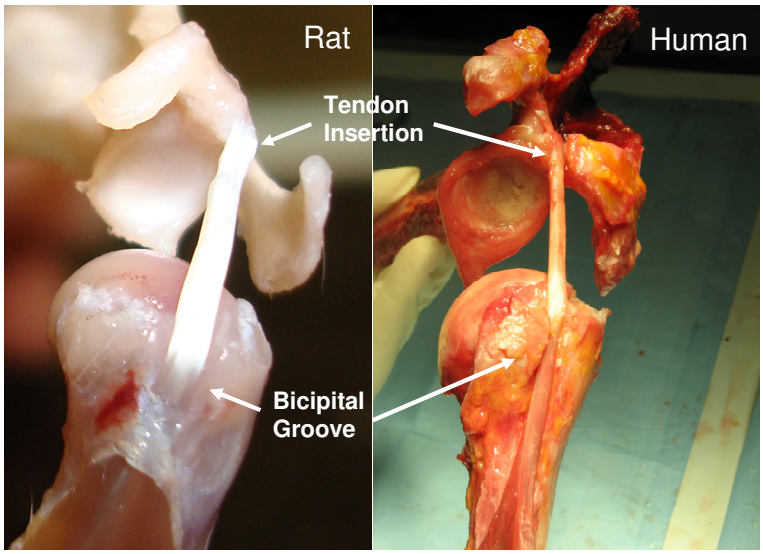

Figure 2.2: Comparison of rat and human biceps tendon anatomy. Note similarity of bicipital groove and tendon insertion on superior aspect of the glenoid.

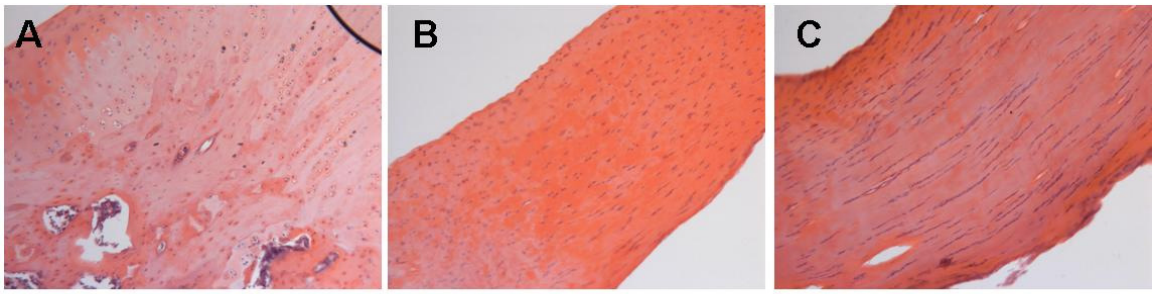

Figure 2.3: Histological images along the length of a normal rat biceps tendon. A: insertion site, B: intra-articular space, C: bicipital groove.

investigate their effect on the remaining intact rotator cuff tendons.[14] This study showed that the intact rotator cuff tendons were detrimentally affected by the presence of rotator cuff tears, and therefore the objective of this study was to utilize the rat model for rotator cuff tendon tears to develop an animal model of biceps tendon pathology in the presence of rotator cuff tears. Our hypotheses were that, in the rat model: 1) an increase in the number of rotator cuff tendons torn would result in further decreased mechanical properties of the biceps tendon, 2) these mechanical properties would continue to decrease over time and 3) a two tendon tear involving the infraspinatus would result in lower mechanical properties than those involving the subscapularis.

B. Methods

Seventy-eight Sprague-Dawley rats (400-450 g) were used in this study. These rats were divided into 4 groups, and within each group were sacrificed at both 4 and 8 weeks after tendon detachments. The treatment groups consisted of: uninjured control (n=10 at 4 weeks, n=10 at 8 weeks), supraspinatus tendon detachment (n=10 at 4 weeks, n=10 at 8 weeks), supraspinatus+infraspinatus tendon detachments (n=10 at 4 weeks, n=9 at 8 weeks), and supraspinatus+subscapularis tendon detachments (n=9 at 4 weeks, n=10 at 8 weeks). In the tendon detachment groups, a unilateral surgery was performed on the

animal's left shoulder to detach the prescribed rotator cuff tendons from their bony insertion on the humerus. The method for supraspinatus tendon detachment is well-established and has been used in this lab extensively.[4,6-8,14,15,18] This technique has been recently expanded to include additional detachments of the other major rotator cuff tendons, the infraspinatus and subscapularis.[4,14]

The surgical detachment begins with a 2-cm skin incision made over the glenohumeral joint with the arm in external rotation. This incision was then followed by blunt dissection through the deltoid muscle down to the rotator cuff musculature. The rotator cuff was then exposed and the tendons and their insertions onto the humerus were visualized. The tendons were then identified as: the subscapularis, the most anterior and broadest of the rotator cuff tendons; the supraspinatus, which passes under the bony arch of the acromion, coracoid and clavicle; and the infraspinatus, posterior to the others with an insertion similar to the supraspinatus. A traction suture was then passed underneath the acromion to facilitate further exposure of the tendons. The supraspinatus tendon was then separated from the other rotator cuff tendons anteriorly and posteriorly before sharply detaching it with a scalpel blade from its insertion on the greater tuberosity. In the two-tendon detachment groups, the other tendon (infraspinatus or subscapularis) was detached in the same manner. Any remaining fibrocartilage was left intact at the insertion site and detached tendons were allowed to freely retract. The overlying muscle was then closed with suture and the overlying skin with staples. The rats were allowed unrestricted cage activity until sacrifice at 4 or 8 weeks.

After sacrifice, the scapula-biceps tendon-muscle segments were dissected out. The associated muscle was removed by gentle scraping and the tendon was fine dissected

under a stereomicroscope. In order to optically determine the distribution of strain along the tendon, Verhoeff stain lines were then placed along the tendon length using 6-0 silk suture. The first stain line was placed at the insertion of the tendon onto the scapula, and the remaining stain lines were placed 1.5, 3.5, 8.5 and 11.5 mm distally from the insertion in order to denote the proximal tendon insertion site (0-1.5 mm), intra-articular space (1.5-3.5 mm), and portion of the tendon in the bicipital groove (3.5-8.5 mm) (Figure 2.4). The last stain line was placed at 11.5 mm, denoting placement of the grip for mechanical testing. These positions were determined from a preliminary study consisting of dissection of two rats, where the length and position of the tendon in the bicipital groove was determined with the animals arm at its side in neutral rotation. Two additional shoulders were fixed, decalcified, embedded, sectioned and stained with hematoxylin and

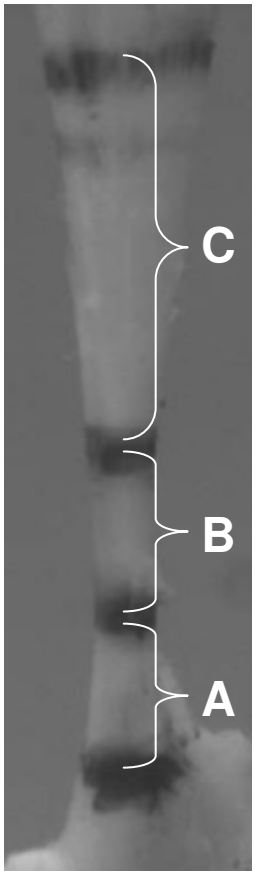

Figure 2.4: Image obtained during biomechanical testing illustrating regions of biceps tendon denoted by stain lines. (A) insertion site; (B) intra-articular space; (C) bicipital groove.

eosin. These sections were then examined under a microscope and the length of the tendon cross-sectional area for each location. After this measurement, the scapula was embedded in polymethylmethacrylate for biomechanical testing. The embedded scapula was placed into a custom designed testing fixture and the proximal end of the tendon (stain line at 11.5 mm) was held in a screw clamp lined with fine grit sandpaper. The specimen was then immersed in a 39ºC PBS bath and preloaded to 0.1 N before preconditioning for 10 cycles from 0.1 to 0.5N at a rate of 1%/second. The tendon was then held for 300 seconds before a stress-relaxation experiment that elongated the specimen to 4% strain at 5%/second (0.575 mm/sec) followed by a 600 second relaxation period. Following this relaxation period, the specimen was returned to its initial preload displacement and held for 60 seconds before ramp to failure at 0.3%/second was applied. This mechanical testing procedure can be seen in Figure 2.5.

Local tissue strain in each portion of the tendon was measured optically using the applied stain lines and a custom MATLAB program. Briefly, this program determines the difference in gray scale intensity between the stain line and the surrounding tendon through the images collected during the ramp to failure test. Elastic properties, such as stiffness and modulus, were calculated using the linear portion of the load-displacement and stress-strain curves, respectively. Maximum stress at the insertion was calculated only for specimens that failed at the insertion site and not for specimens that failed at any other location, such as the grip or midsubstance. Viscoelastic properties (peak and equilibrium load, percent relaxation) were determined from the stress relaxation curve for each specimen.

Significance was assessed between groups at each time point using one-way ANOVAs with Bonferroni post-hoc correction. After it was determined that control tendons exhibited a difference between time points, a bootstrapping approach was used to randomly pair 4 and 8 week data from each group.[17] The difference in each property over time (from 4 to 8 weeks) was then compared between groups using a one-way ANOVA and Bonferroni correction. To correct for the number of comparisons, significance was set at $p<0.0125$ (0.05/4) and trends at $p<0.025$ (0.1/4).

C. Results

Four weeks after tendon detachments, biceps tendon areas in all locations were higher in the supraspinatus and supraspinatus+infraspinatus detachment groups when compared to control (Table 2.1). Biceps tendon areas in the supraspinatus+subscapularis group were increased over control in the intra-articular space and bicipital groove (Table 2.1). Interestingly, biceps tendons in the presence of a supraspinatus tendon tear were larger than those in the presence of a supraspinatus+subscapularis tear at this time point (Table 2.1). At the insertion site, a supraspinatus+infraspinatus tendon tear resulted in a

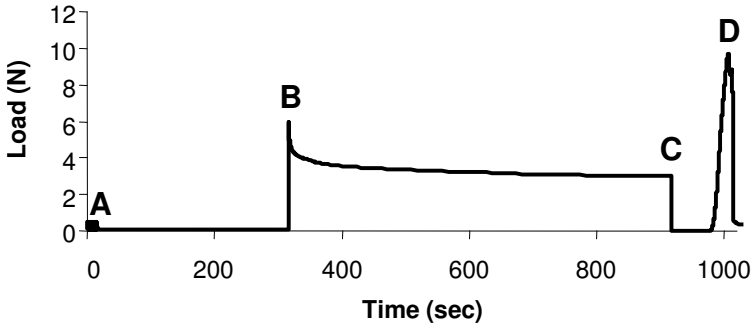

Figure 2.5: Mechanical testing protocol: (A) pre-conditioning; (B) stress-relaxation; (C) return to pre-load displacement; (D) ramp to failure.

Table 2.1: Biceps area is increased at 4 and 8 weeks and modulus decreased at 8 weeks following rotator cuff detachments

	Time post detachment (weeks)	Insertion Site Area (mm^2)	Intra-Articular Space Area (mm^2)	Bicipital Groove Area (mm^2)	Insertion Site Modulus (MPa)	Intra-articular Space Modulus (MPa)	Bicipital Groove Modulus (MPa)
Control	4	0.79±0.19	0.58±0.14	0.61±0.10	202±95	267± 90	313±51
	8	054±0.05	0.37±0.04	0.47±0.07	281±82	451±117	632±155
Supra Detach	4	1.16±0.35*	0.96±0.20*	0.87±0.13*	115±66#	235±159	312±159
	8	1.08±0.25*	0.95±0.19*	0.89±0.13*	243±144	284±167*	454±159*
Supra+Subscap detach	4	0.90±0.20‡	0.75±0.17†,#	0.73±0.17#,‡	193±56†	312±155	344±154
	8	1.09±0.18*	0.87±0.08*	0.74±0.06*,†	185±69*	217±91*	466±161#
Supra+Infra detach	4	1.09±0.21*,##	0.84±0.19*	0.81±0.14*	152±66	245±80	321±117
	8	1.45±0.44*,‡,##	1.19±0.21*,†, ‡‡	1.06±0.26*,‡‡,‡	133±80*	195±71*	366±193*

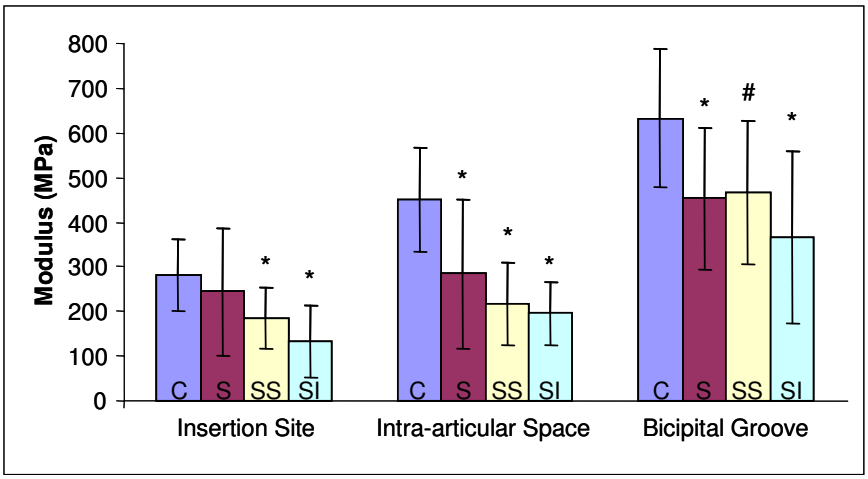

Figure 2.6: Biceps moduli at the insertion site, intra-articular space, and bicipital groove were decreased 8 weeks following rotator cuff detachments. C-control, S-supraspinatus detachment, SS-supraspinatus +subscapularis detachment, SI-supraspinatus+infraspinatus detachment. (*sig from control, #trend from control)

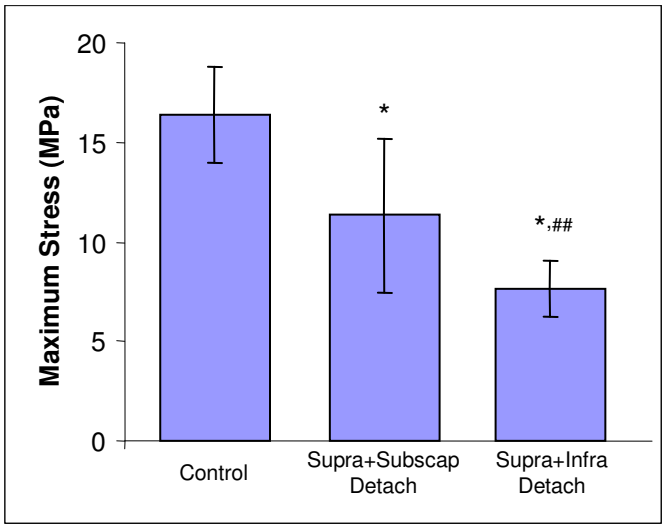

Figure 2.7: Maximum stress of the biceps tendon decreased with two-tendon tears and was further decreased with the involvement of the infraspinatus as opposed to the subscapularis. (*sig from control, ## trend from supra+subscap detachment)

larger biceps than a supraspinatus+subscapularis tear (Table 2.1). Insertion site modulus of the biceps tendon was decreased with a supraspinatus tear compared to control and supraspinatus+subscapularis groups (Table 2.1). There were no differences in stiffness or viscoelastic properties four weeks following detachments.

Eight weeks after rotator cuff tendon detachments, biceps tendons from the one and two tendon detachment groups had significantly larger areas in all three locations compared to control tendons (Table 2.1). Modulus of the biceps tendon in the intra-articular space and bicipital groove were decreased in all detachment groups compared to control tendons (Figure 2.6). Maximum stress and insertion site modulus from both two tendon detachment groups were significantly decreased compared to control tendons (Figures 2.6, 2.7). Interestingly, tendons from the supraspinatus only detachment group did not fail at the insertion site, therefore maximum stress could not be calculated. There was a trend for larger area values in the two tendon detachment groups compared to the one tendon detachment group (Table 2.1). Biceps tendons from the supraspinatus+infraspinatus tendon detachment group had a larger area in all portions of the tendon (Table 2.1) and lower maximum stress (Figure 2.7) compared to tendons from the supraspinatus+subscapularis tendon detachment group. Finally, there were no

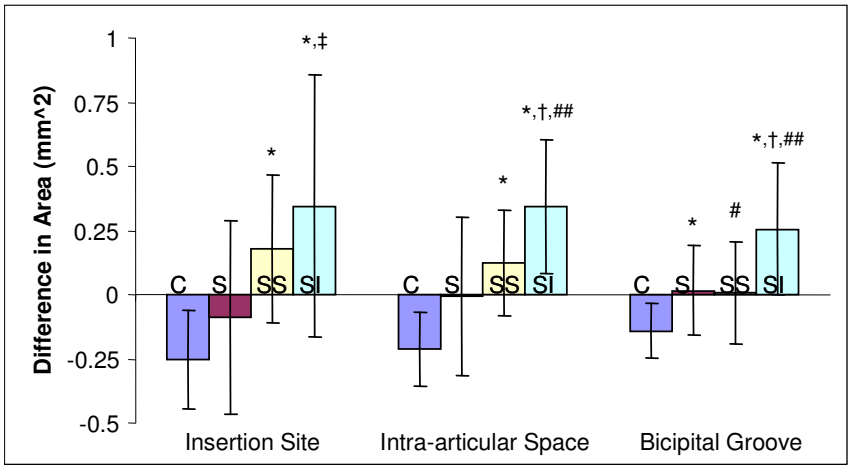

Figure 2.8: The change in area from 4 to 8 weeks, presented relative to control, was significantly higher in the two-tendon detachment groups compared to control at the insertion site, intra-articular space and bicipital groove. (*sig from control, #trend from control, †sig from supra detachment, ‡trend from supra detachment, ##trend from supra+subscap detachment)

differences in stiffness or viscoelastic properties at the 8 week time point.

Between 4 and 8 weeks, the areas of all three tendon portions increased for both two-tendon groups compared to control (Figure 2.8). In addition, the area of the biceps tendons in the supraspinatus+infraspinatus group increased over time compared to control than in the supraspinatus group in all 3 portions and increased compared to the supraspinatus+subscapularis group in the intra-articular space and bicipital groove (Figure 2.8). The tendon modulus decreased over time compared to control in all three locations for both the supraspinatus+infraspinatus and supraspinatus+subscapularis tear groups (Figure 2.9).

D. Discussion

This is the first animal study to examine the long-head of the biceps tendon after one and two rotator cuff tendon detachments. Results support our first hypothesis that mechanical properties of the long-head of the biceps tendon would decrease with

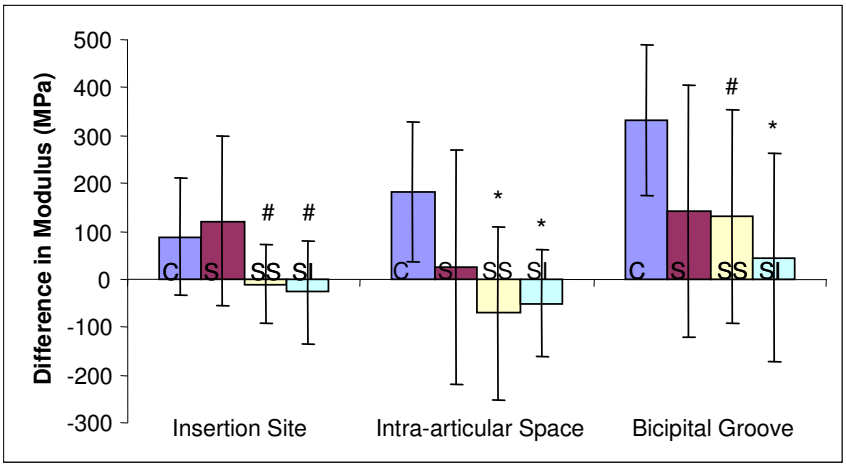

Figure 2.9: Biceps tendon modulus, presented relative to control, decreased between 4 and 8 weeks in both two-tendon detachment groups compared to control. (*sig from control, #trend from control)

increasing rotator cuff tear size. This finding agrees with several clinical studies that note a widened or frayed biceps at the time of rotator cuff repair.[12] Clinical studies have also shown increasing biceps tendon lesions with multiple rotator cuff tendon tears.[3] Changes in biceps tendons in the presence of rotator cuff tears may be due to altered joint loading scenarios including use as a humeral head depressor, functional compensations, or stress shielding due to disuse. Degeneration of the biceps tendon in the presence of a rotator which would be enhanced with a tear or subacromial impingement. It could also be the result of the cuff tear may be due to the role of the biceps as a humeral head stabilizer, biceps tendon being required to perform new functions with altered mechanical loading at the shoulder when the tendons that would normally perform those functions are damaged or no longer present. It is also interesting to note that biceps tendons in the presence of a supraspinatus tear did not fail at the insertion site. Tendons in this group exhibited an increase in area but no decrease in insertion modulus. This could mean that with a supraspinatus tear alone, the biceps tendon quality has not yet become substantially altered.

Our second hypothesis was also supported in that biceps tendon area and modulus significantly worsened over time in both two tendon detachment groups, despite the spread in the data. This result correlates with a clinical study which found that all biceps tendons with cuff tears considered "chronic" (those over 3 months) had associated pathology.[3] At four weeks, changes were primarily in tendon area. This correlates with clinical findings of an inflamed tendon.[13] However, clinical studies cannot measure mechanical properties of these tendons and it is not known if the tendon tissue has become degenerate, nor its time course. In our study, we measured a progression from a

tendon with increased area at 4 weeks to a tendon with increased area and decreased modulus at 8 weeks. We also found that biceps tendons in the presence of two-tendon rotator cuff tears degenerated significantly between 4 and 8 weeks, as shown by increased area and decreased modulus. This degeneration with time is supported by other studies in our laboratory that have shown supraspinatus only tendon tears to be mostly healed by 8 weeks[8], while multiple tendon tears continue to have decreased mechanical properties at this time.[4] This increase in degeneration with time may also be due in part to a self-limitation in use or a functional loss by the rat at early time points. Previous studies in our laboratory have evaluated functional changes by measuring rat ambulation parameter post-injury. In these studies, we have found that rat ambulation was altered up to 4 weeks post supraspinatus detachment.[15] Rat ambulation was further altered with 2 tendon tears, and this alteration persisted up to 8 weeks.[15] In addition, we also have found that the mechanical properties of the uninjured rotator cuff tendons are altered 4 and 8 weeks after single and multiple tendon tears, which may be due to changes in shoulder kinematics.[14] With time, remaining tendons would learn to compensate for functions normally performed by detached tendons, resulting in further decreases in mechanical properties.

Finally, our third hypothesis was supported as a supraspinatus+infraspinatus tear had decreased mechanical properties compared to a supraspinatus+subscapularis tear. This expectation was based on clinical data suggesting biceps tendonitis following the involvement of the infraspinatus tendon in rotator cuff tears[3]as well as the biceps role as a humeral head depressor when two superior stabilizers (supraspinatus and infraspinatus) are torn. Following four weeks post rotator cuff tears, only the area of the biceps

insertion site was increased with an infraspinatus tear as opposed to a subscapularis tear. However, at 8 weeks all 3 areas as well as maximum stress of the biceps tendon were significantly worse in the supraspinatus+infraspinatus group. While both two tendon tears got progressively worse over time, areas in the supraspinatus+infraspinatus group progressed significantly more than the supraspinatus only and supraspinatus+subscapularis tear groups.

It is also interesting to note that the tendon modulus varied along the length of the tendon. The modulus was lowest at the insertion site, increased in the intra-articular space and was highest in the bicipital groove. This could be due to the different functions and loading environments seen in each of these areas. This reiterates the general concept that the material properties of tendon vary depending on location and that average whole tissue properties may not be an accurate representation of each portion of the tissue. We also did not find any differences in viscoelastic properties in this study, which due to the nature of testing was only possible to determine for the whole tendon and not for each location. Viscoelastic properties of the biceps tendon have not been investigated before, and it is possible that these properties are not affected due to the presence of rotator cuff tears. However, it is possible that viscoelastic changes may be present if we were able to more rigorously examine them.

It should be acknowledged that the rotator cuff tendon tears in this study were made acutely and do not represent the most common human condition where degeneration is thought lead to tendon rupture. Biceps tendon changes however, do develop over time as they are thought to be due to the changes in joint kinematics and altered loading that result from rotator cuff tears. Clinically, these changes would occur

slowly over time and not instantaneously as in this study. Also, the addition of a later time point would be interesting to see if degeneration of the biceps tendon in this model leads to eventual tendon rupture.

The results of this study are important because they define the rat rotator cuff injury model as consistent with the biceps tendon pathology seen clinically with rotator cuff tears. The role of the biceps tendon is not well characterized and there is some debate to the extent of its function.[2] Some clinicians believe that the biceps tendon has little function and therefore retaining an abnormal biceps tendon in the presence of a rotator cuff tear will affect functional outcome more than the loss of that tendon, but no clinical studies have been done to address this theory.[1] The identification of an animal model of biceps tendon pathology with rotator cuff tears allows for controlled studies to investigate the etiology of this problem as well as potential treatment strategies.

References

1. **Ahrens, P. M., and Boileau, P.:** The long head of biceps and associated tendinopathy. *J Bone Joint Surg Br,* 89(8): 1001-9, 2007.
2. **Burkhead, W. Z., Arcand, Michel A., Zeman, Craig, Habermeyer, Peter and Walch, Giles:** The Biceps Tendon. In *The Shoulder*, pp. 1009-1063. Edited by Rockwood, C. A., 1009-1063, Philadelphia, W.B. Saunders, 1998.
3. **Chen, C. H.; Hsu, K. Y.; Chen, W. J.; and Shih, C. H.:** Incidence and severity of biceps long head tendon lesion in patients with complete rotator cuff tears. *J Trauma,* 58(6): 1189-93, 2005.

4. **Dourte, L. M.; Perry, S. M.; Getz, C. L.; and Soslowsky, L. J.:** Tendon Properties Remain Altered in a Chronic Rat Rotator Cuff Model. *Clin Orthop Relat Res*.

5. **Favata, M.:** Scarless healing in the fetus: Implications and strategies for postnatal tendon repair. In *PhD Thesis: Bioengineering*, pp. 216. Edited, 216, Philadelphia, University of Pennsylvania, 2006.

6. **Gimbel, J. A.; Mehta, S.; Van Kleunen, J. P.; Williams, G. R.; and Soslowsky, L. J.:** The tension required at repair to reappose the supraspinatus tendon to bone rapidly increases after injury. *Clin Orthop Relat Res,* (426): 258-65, 2004.

7. **Gimbel, J. A.; Van Kleunen, J. P.; Lake, S. P.; Williams, G. R.; and Soslowsky, L. J.:** The role of repair tension on tendon to bone healing in an animal model of chronic rotator cuff tears. *J Biomech,* 40(3): 561-8, 2007.

8. **Gimbel, J. A.; Van Kleunen, J. P.; Mehta, S.; Perry, S. M.; Williams, G. R.; and Soslowsky, L. J.:** Supraspinatus tendon organizational and mechanical properties in a chronic rotator cuff tear animal model. *J Biomech,* 37(5): 739-49, 2004.

9. **Gomoll, A. H.; Katz, J. N.; Warner, J. J.; and Millett, P. J.:** Rotator cuff disorders: recognition and management among patients with shoulder pain. *Arthritis Rheum,* 50(12): 3751-61, 2004.

10. **Harryman, D. T., 2nd; Sidles, J. A.; Harris, S. L.; and Matsen, F. A., 3rd:** The role of the rotator interval capsule in passive motion and stability of the shoulder. *J Bone Joint Surg Am,* 74(1): 53-66, 1992.

11. **Harwood, M. I., and Smith, C. T.:** Superior labrum, anterior-posterior lesions and biceps injuries: diagnostic and treatment considerations. *Prim Care,* 31(4): 831-55, 2004.

12. **Itoi, E.; Hsu, H. C.; Carmichael, S. W.; Morrey, B. F.; and An, K. N.:** Morphology of the torn rotator cuff. *J Anat,* 186 (Pt 2): 429-34, 1995.

13. **Murthi, A. M.; Vosburgh, C. L.; and Neviaser, T. J.:** The incidence of pathologic changes of the long head of the biceps tendon. *J Shoulder Elbow Surg,* 9(5): 382-5, 2000.

14. **Perry, S. M.; Getz, C. L.; and Soslowsky, L. J.:** After rotator cuff tears, the remaining (intact) tendons are mechanically altered. *J Shoulder Elbow Surg,* 18(1): 52-7, 2009.

15. **Perry, S. M.; Getz, C. L.; and Soslowsky, L. J.:** Alterations in function after rotator cuff tears in an animal model. *J Shoulder Elbow Surg,* 18(2): 296-304, 2009.

16. **Soslowsky, L. J.; Carpenter, J. E.; DeBano, C. M.; Banerji, I.; and Moalli, M. R.:** Development and use of an animal model for investigations on rotator cuff disease. *J Shoulder Elbow Surg,* 5(5): 383-92, 1996.

17. **Soslowsky, L. J.; Thomopoulos, S.; Esmail, A.; Flanagan, C. L.; Iannotti, J. P.; Williamson, J. D., 3rd; and Carpenter, J. E.:** Rotator cuff tendinosis in an animal model: role of extrinsic and overuse factors. *Ann Biomed Eng,* 30(8): 1057-63, 2002.

18. **Yokota, A.; Gimbel, J. A.; Williams, G. R.; and Soslowsky, L. J.:** Supraspinatus tendon composition remains altered long after tendon detachment. *J Shoulder Elbow Surg,* 14(1 Suppl S): 72S-78S, 2005.

Chapter 3: Mechanical, histological, organizational and compositional changes in the biceps tendon following a rotator cuff tear in a rat model

A. Introduction

This chapter will investigate the regional changes in mechanical, histological, organizational and compositional properties of the long head of the biceps tendon following rotator cuff tears in a rat model at early, intermediate and late time points.

Biceps tendon damage is a common clinical problem that is often found in the presence of rotator cuff tears.[2,10] However, there is some debate over the role of the biceps tendon at the shoulder following a rotator cuff tear. Some believe the biceps plays a significant role as a humeral head depressor while others believe it plays no role at all.[8,14] Therefore, controversy exists regarding its optimal treatment, with physicians relying mostly on anecdotal experience. Tendon degeneration, inflammation and altered loading are all thought to play a role in the development of this pathology; however, the mechanisms which lead to biceps changes remain unknown which makes clinical management of the problem difficult.

Clinicians have noted the biceps tendon to be flattened, widened and/or frayed at the time of rotator cuff repair[6] and the damage has also been seen to increase with increasing tear size.[2] However, it is often not clear whether the changes are truly degenerate or are due to inflammation alone. The location where pathologic changes begin is also somewhat controversial. Some believe that pathology occurs at the entrance to the bicipital groove, and suspect the tendon first becomes inflamed and then damaged when it is has trouble sliding when hypertrophied. Neer has long believed that the biceps

tendon is susceptible to impingement under the acromion after a rotator cuff tear occurs and that changes begin near the tendon's attachment to the glenoid on its bursal side.[11] It is also possible that changes may occur in this location but on the articular side, as increased compressive loading against the humeral head is present.

The composition of the biceps tendon in a shoulder with an intact rotator cuff has been shown to be similar to rotator cuff tendons near its insertion site.[9] Both tensile and compressive loading is seen at this location and therefore the insertion site of a biceps tendon in an intact shoulder is less organized and expresses different amounts of various collagens and proteoglycans than the rest of the tendon. Away from the insertion site, the composition is markedly different and the collagen fibers are organized along the long axis of the tendon as the tendon experiences mostly tensile loading in this location.[1] It is unknown what the effect of rotator cuff tears is on the histological, compositional and organizational properties along the entire length of the biceps tendon.

Little is also known about the effect of rotator cuff tendon tears on the regional histological properties of the biceps tendon over time. These questions are difficult to address in clinical studies due to both the inability to harvest the entire biceps tendon during surgery and the complexity of evaluating the effect of time post-repair when the precise history including the exact instance of tear initiation is often unknown. In addition, it would not be possible to obtain many specimens at time points soon after a rotator cuff tear occurs. In Chapter 2, we compared biceps tendons in the presence of rotator cuff tears to control tendons from uninjured animals in a rat model.[12] This study looked at only biomechanical changes and found increased area after 4 weeks and increased area and decreased modulus after 8 weeks.[12] Assays focusing on biological

changes at these and earlier time points were not performed and the mechanism responsible for these changes remains unknown.

However, when looking at earlier time points, it is possible that there may be effects of the surgical exposure itself. Therefore, the objective of this study was to determine the histological, organizational, compositional and mechanical changes in the biceps tendon following a rotator cuff tear compared to a sham surgery at early, intermediate and late time points. Our hypotheses were that: 1) histological and compositional changes will appear before organizational changes, and both will appear before mechanical changes and 2) changes in all properties will begin at the insertion site and proceed along the length of the tendon at later time points.

B. Methods

Sixty-five male Sprague-Dawley rats (400-450g) were used in this IACUC approved study and separated into two treatment groups: supraspinatus+infraspinatus tendon detachments (n=34) and sham surgery (n=31). Animals were sacrificed at 1, 4 and 8 weeks post-surgery for histological analysis (n=4 or 5 per group and time point) and at 4 and 8 weeks post-surgery for mechanical testing (n=8-10 per group and time point). The animals used for mechanical testing at 4 and 8 weeks are the same as those discussed in Chapter 2.

In both groups, a unilateral surgery was performed on the animal's left shoulder. The surgical procedure is the same as discussed in Chapter 2 but will be repeated here for completeness. Briefly, with the arm in external rotation, a 2 cm skin incision was made followed by blunt dissection down to the rotator cuff musculature. The rotator cuff was

exposed and the tendons were visualized at their insertion on the humerus. The sham surgery ended here and the overlying muscle and skin were closed. In the supraspinatus+infraspinatus detachment group, the surgery continued with separation of the supraspinatus tendon from the other rotator cuff tendons before sharp detachment at its insertion on the greater tuberosity using a scalpel blade. The infraspinatus tendon was then detached in the same manner. Any remaining fibrocartilage at the insertion was left intact and detached tendons were allowed to freely retract without attempt at repair creating a gap ~4 mm from their insertion sites. The overlying muscle and skin were closed and the animals in both groups were allowed unrestricted cage activity.

Animals were sacrificed for mechanical testing at 4 and 8 weeks following surgery. The mechanical testing procedure is the same as reported in Chapter 2, but will be repeated here for completeness. The scapula, long-head of the biceps tendon and associated muscle were removed and the tendons were fine dissected under a microscope. Five Verhoeff stain lines were then placed along the length of each tendon denoting the insertion site (0-1.5mm), the portion of the tendon in the intra-articular space (1.5-3.5mm), and the portion in the bicipital groove (3.5-8.5mm). A fifth stain line was placed at 11.5mm to identify grip placement and these stain lines were used to determine the distribution of strain along the length of the tendon. These positions were determined using histology to identify the length of the insertion site and gross dissections to determine the portion in the bicipital groove.[12] Tendon geometry was measured in each tendon portion using a laser based system.[4]

The scapula was then embedded in a holding fixture using polymethylmethacrylate (PMMA) and inserted into a specially designed fixture. The

proximal end of the tendon was then held at the fifth stain line (11.5mm) in a screw clamp lined with fine grit sandpaper. The specimen was then immersed in a 39°C PBS bath, preloaded to 0.1N, preconditioned for 10 cycles from 0.1N to 0.5N at a rate of 1%/sec, and held for 300sec. Immediately following, a stress relaxation experiment was performed by elongating the specimen to a strain of 4% at a rate of 5%/sec (0.575 mm/sec) followed by a 600sec relaxation period. Specimens were then returned to the initial preload displacement and held for 60 seconds and ramp to failure was then applied at a rate of 0.3%/sec. Using the applied stain lines, local tissue strain in each tendon portion was measured optically with a custom program (MATLAB). Elastic properties, such as stiffness and modulus, were calculated using linear regression from the visually determined linear region of the load-displacement and stress-strain curves, respectively. Peak and equilibrium load were determined from the stress relaxation test and percent relaxation was then calculated from these values.

Animals were sacrificed for histological analyses 1, 4 and 8 weeks following surgery. Cross-sectional area was also measured along the length of the tendon in the 1 week specimens. Each tendon was analyzed in 4 locations: the insertion site (0-1.5mm), the intra-articular space (1.5-3.5mm), the proximal bicipital groove (3.5-6mm) and the distal bicipital groove (6-8.5mm). Sagittal sections (7μm) were collected serially and stained with hematoxylin and eosin. Quantitative polarized light microscopy was used to determine collagen fiber orientations on these H&E stained sections.[5] Briefly, a rotatable λ compensator was used and a set of grayscale images (100x mag.) were taken at each tendon location at 10º increments as the crossed analyzer and polarizer were simultaneously rotated through 90º. Next, a set of color images was taken at 10º

increments as the compensator and crossed analyzer and polarizer were rotated through 90º. A custom MATLAB program was then used to analyze approximately 120 points for each set of pictures to determine the collagen organization. The grayscale images were used to calculate the extinction angle and the color images to determine the orientation of the collagen. The angular deviation (AD) of the collagen orientation, a measure of the fiber distribution spread, in each tendon location for each specimen was then calculated as used previously.[16]

H&E stained sections were also analyzed for changes in cell shape and cellularity. Histological grading standards for cellularity and cell shape were produced by first organizing images for each tendon location from either least to most cellular or most elongated to more rounded cell shape. These images were then divided into four quadrants and the middle image from each quadrant was chosen as the representative image for that quadrant and assigned a grade of 0, 1, 2 or 3. Images were then assigned grades by 3 blinded graders who compared each image to these standards for each location. The median grade between the 3 blinded graders for each image was then assigned to that image.

Finally, the distribution of various extra-cellular matrix proteins was localized in the biceps tendon using immunohistochemistry. The same specimens were used as for histological and polarized light analyses and one section from each specimen was stained for collagens type I, II, III and XII as well as proteoglycans aggrecan, biglycan and decorin (Table 3.1). Briefly, standard 7μm sections were first dewaxed and rehydrated followed by blocking and antibody reactions.[15] Sections for aggrecan were pretreated with 10-mmol/L dithiothreitol-50mmol/L tris-hydrocholic acid and 200 mmol/L sodium

Table 3.1: Primary antibodies used for immunohistochemical staining.

Protein Target	Antibody	Host	Type	Enzyme pretreatment	Dilution	Incubation Period (h)	Source
Collagen I	AB755P	Rabbit	Polyclonal	Hyaluronidase	1:200	16	Chemicon (Temecula, CA)
Collagen II	II-116B3	Mouse	Monoclonal	Hyaluronidase	1:4	16	DSHB (Iowa City, IA)
Collagen III	c7805	Mouse	Monoclonal	Hyaluronidase	1:50	38	Sigma (St. Louis, MO)
Collagen XII	LB-1200	Rabbit	Polyclonal	Hyaluronidase	1:100	16	Cosmo-bio (Tokyo, Japan)
Aggrecan	LF-113	Rabbit	Polyclonal	Chondroitinase ABC	1:200	16	L. Fisher (Bethesda, MD)
Biglycan	LF-159	Rabbit	Polyclonal	Chondroitinase ABC	1:200	38	L. Fisher
Decorin	JSCATE	Rabbit	Polyclonal	Chondroitinase AC	1:300	38	J. Sandy (Chicago, IL)

chloride for 2 hours at 37ºC and then alkylated with 40 mmol/L iodoacetamide-1 mol/L PBS for 1 hour at 37ºC. Sections for collagen type III were pretreated for 4 minutes with Protease K at room temperature. For all antibodies, various enzyme incubations were carried out at 37ºC (Table 1). Endogenous peroxidase activity was blocked in all sections by treatment with 3% hydrogen peroxide in methanol for 10 minutes, and non-specific binding of the secondary antibody was blocked with both 5% skim milk-PBS for 30 minutes and appropriate serum (goat or horse) for 20 minutes. Tissue sections were then incubated with primary antibodies for up to 38 hours (Table 3.1) at 4ºC. Negative control sections were incubated with nonimmune horse serum diluted to the same protein content. The sections were then exposed to biotin-conjugated secondary antibodies (1:100 rat anti-mouse monoclonal antibody or 1:200 goat anti-rabbit polyclonal antibody) for 30 minutes, and then avidin-biotinylated peroxidase complex reagent was applied for 30 minutes at room temperature. Finally, sections were incubated with 3,3'-diaminobenzidine for 4 minutes.

The same 4 regions were analyzed for immunohistochemical staining as for polarized light analysis and histological grading. Images were taken at 100x and evaluated semi-quantitatively using a custom DAB intensity measurement program (MATLAB).[13,17] Briefly, quartiles were produced for each tendon location using the total

target DAB intensity ranges for each protein target, which were determined as the difference between the most and least stained specimens in each group. Each quartile was assigned a value of undetectable (0), low (1), moderate (2) or high (3) and each image was assigned one of these grades.

Mechanical testing parameters and angular deviation were compared between groups at each time point using students t-tests and this data is presented as average +/- standard deviation. For histological and immunohistochemical analyses, median grades were compared for each tendon location between groups at each time point using a non-parametric Mann-Whitney test and therefore, this data is presented as median and interquartile ranges.

C. Results

After 1 week, area was unchanged at the insertion site (Figure 3.1), intra-articular space (Figure 3.2) and bicipital groove (Figure 3.3) compared to sham. However, at 4 and 8 increased at all locations (Figures 3.1-3.3). Modulus was not different at any

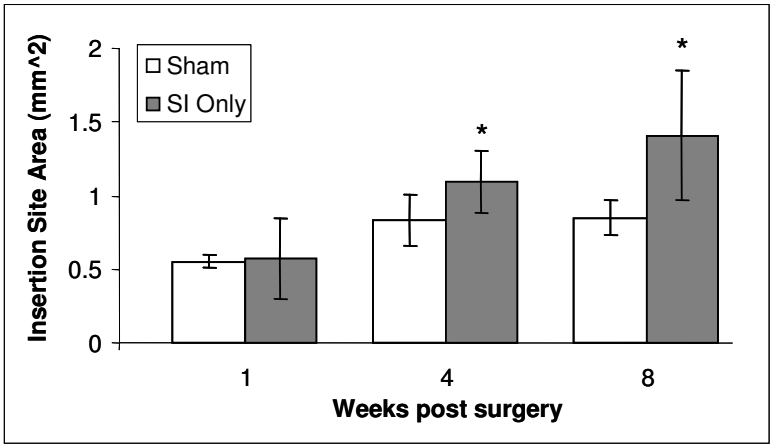

Figure 3.1: Biceps tendon insertion site area is increased at 4 and 8 weeks post detachment. (*sig from Sham)

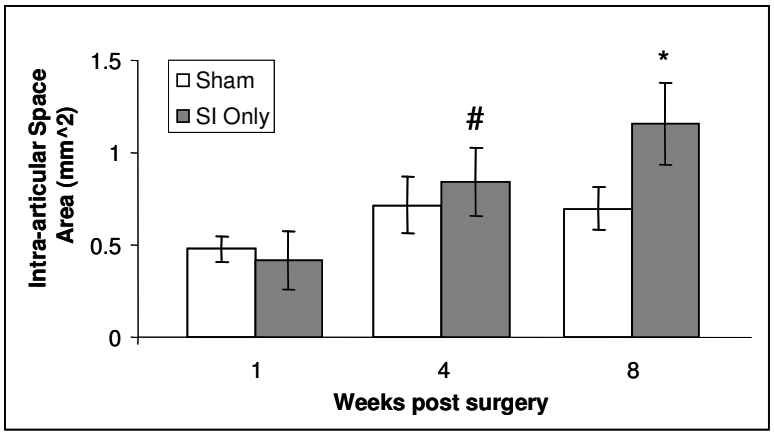

Figure 3.2: Area in the intra-articular space is increased at 4 and 8 weeks. (*sig from Sham, #trend from Sham)

location 4 weeks post detachments (Figure 3.4) and at 8 weeks modulus was decreased in the intra-articular space compared to sham (Figure 3.5). There were no differences in viscoelastic parameters at either time point.

Angular deviation was increased in the intra-articular space at both 1 (Figures 3.6 and 3.9) and 4 weeks following detachments (Figures 3.7 and 3.10). After 8 weeks, angular deviation was increased at all locations compared to sham surgery (Figures 3.8 and 3.13).

Changes in cell shape and cellularity were seen with histological grading. At 1 week, a more rounded cell shape was seen in the intra-articular space with rotator cuff

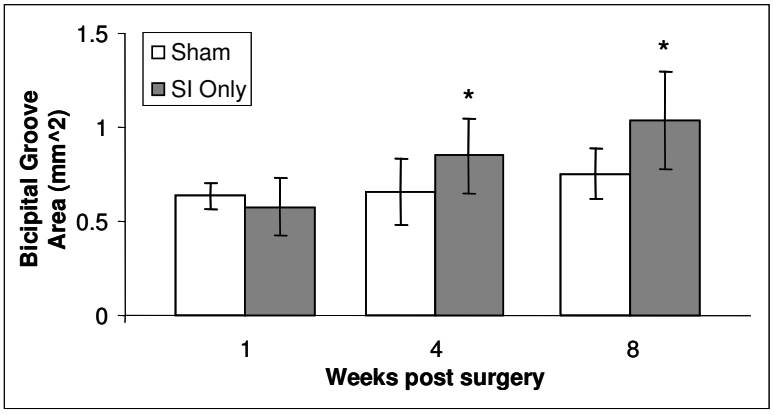

Figure 3.3: Area of the biceps in the bicipital groove is increased at 4 and 8 weeks. (*sig from Sham)

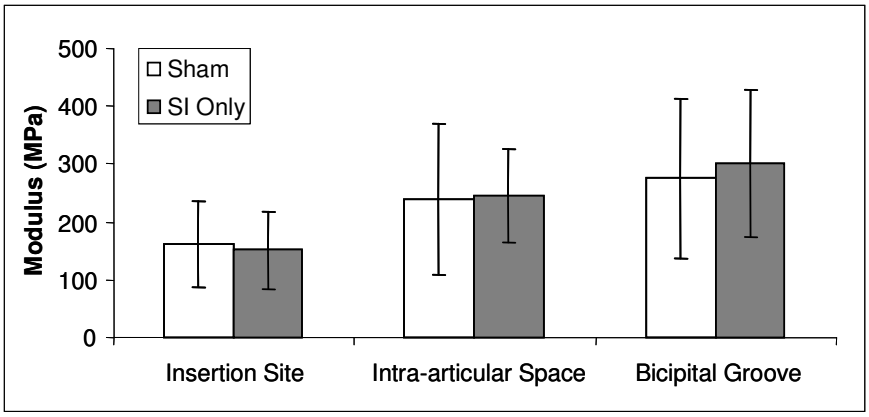

Figure 3.4: After 4 weeks, modulus is unchanged at all locations.

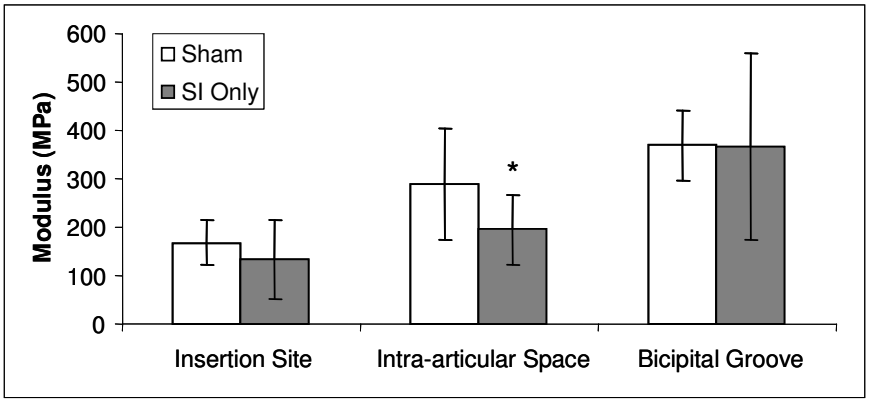

Figure 3.5: After 8 weeks, modulus is decreased in the intra-articular space. (*sig from Sham)

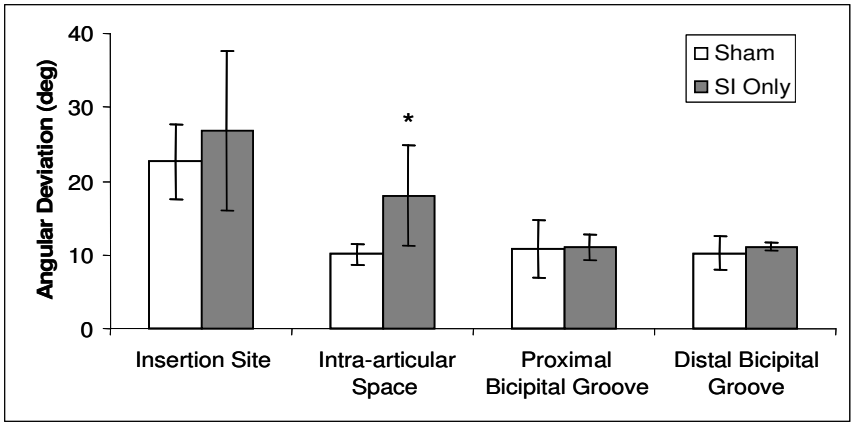

Figure 3.6: Angular deviation is increased in the intra-articular space after 1 week. (*sig from Sham)

detachments (Figure 3.9). Four weeks following detachments, cellularity was increased (Figures 3.10 and 3.11) and a more rounded cell phenotype was found along the entire length of the tendon (Figures 3.10 and 3.12). Cellularity continued to be increased at all tendon locations at 8 weeks (Figures 3.13 and 3.14), and a more rounded cell shape was seen in the intra-articular space as well as proximal and bicipital grooves (Figures 3.13 and 3.15).

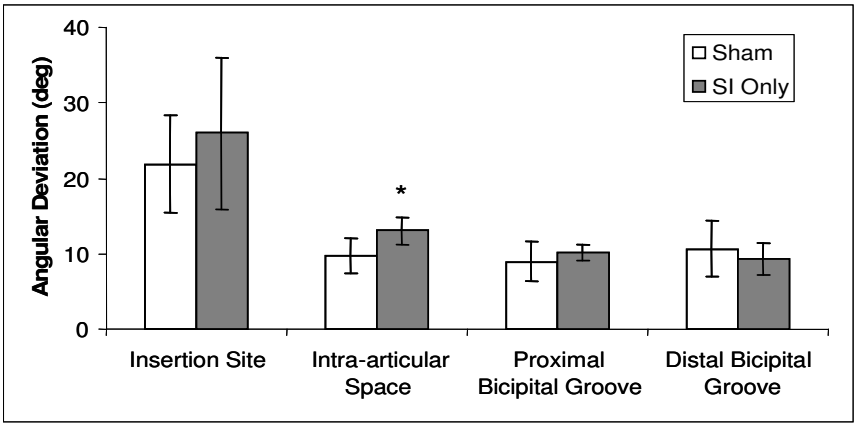

Figure 3.7: After 4 weeks, angular deviation continues to be increased in the intra-articular space. (*sig from Sham)

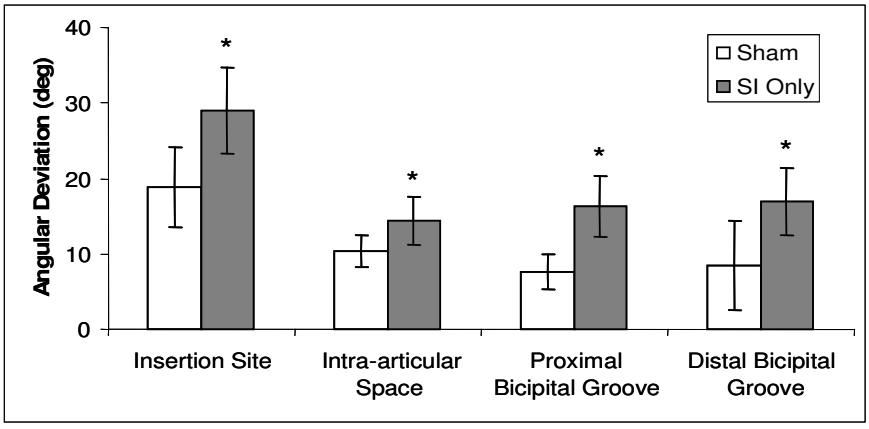

Figure 3.8: After 8 weeks, angular deviation is increased along the entire tendon length. (*sig from Sham)

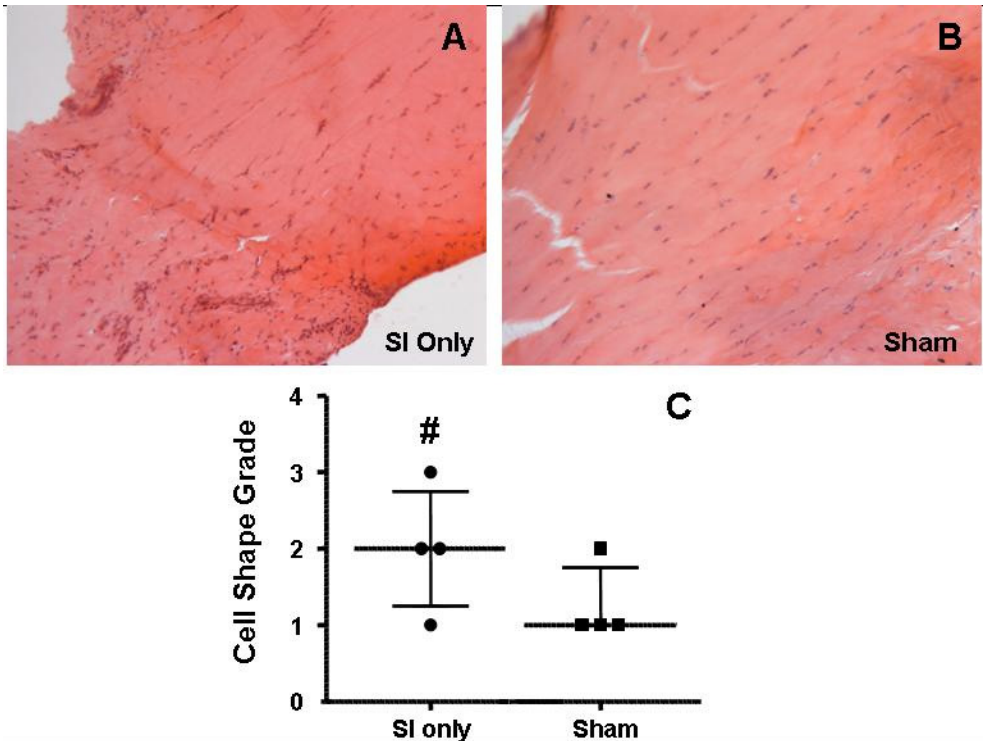

Figure 3.9: After 1 week, a more rounded cell phenotype was seen in the intra-articular space with SI only (A) compared to sham (B). The median and inter-quartile ranges of the histological grading is seen in panel C. Also notice the more organized fibers in the sham image at this time point. (#trend from Sham)

Changes in protein expression were found with immunohistochemical staining. At 1 week, aggrecan was increased along the entire tendon length (Figure 3.16). Also at 1 week, biglycan and collagens I and XII were increased at the insertion site (Figure 3.17). Four weeks following detachments, aggrecan was increased in the proximal bicipital groove. Biglycan was increased in the intra-articular space and decorin was increased in the intra-articular space and proximal and distal grooves. Collagens III and XII were increased at the insertion site. Finally, 8 weeks post detachments, there were trends for increased aggrecan in the distal bicipital groove and increased biglycan was increased along the entire tendon length (Figure 3.18). Decorin was increased at the insertion site and in the intra-articular space. Collagen I was increased along the entire tendon length and Collagen XII was increased at the insertion site.

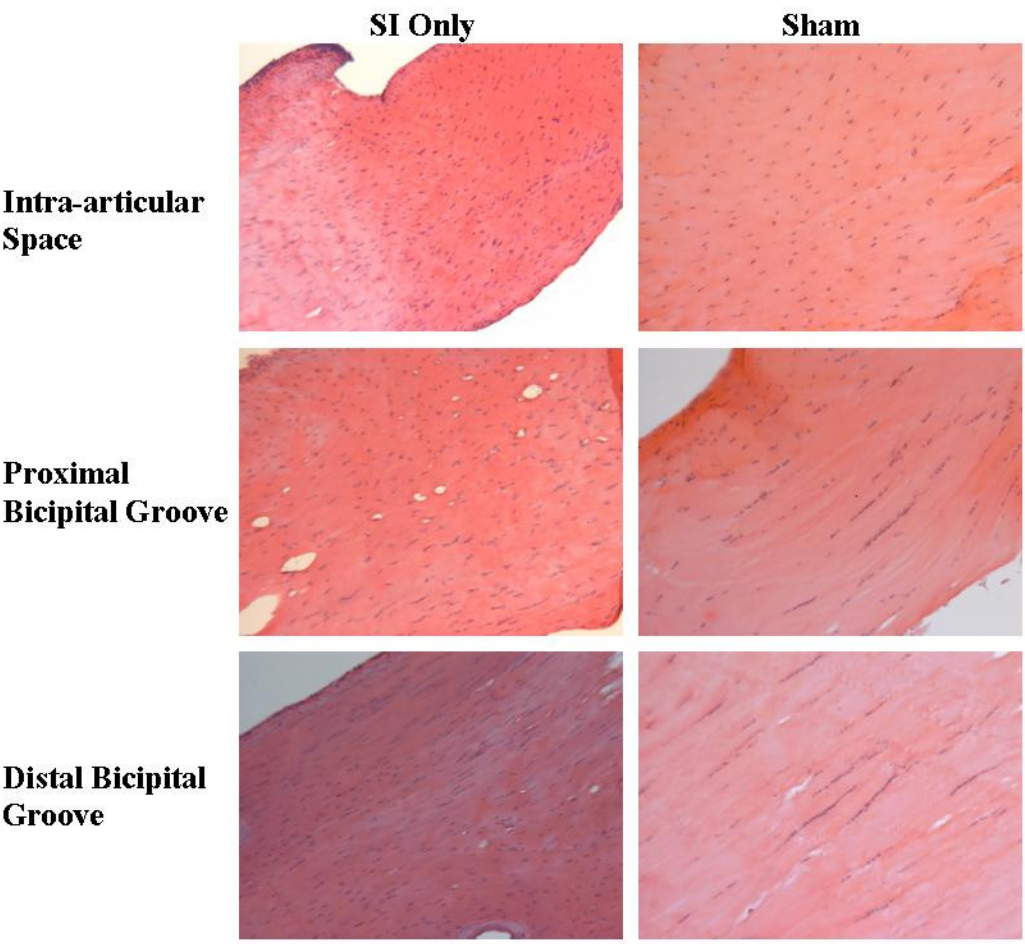

Figure 3.10: Cell shape and cellularity are increased in the intra-articular space and proximal and distal bicipital groove 4 weeks following detachments. Also note the more disorganized collagen in the intra-articular space in the SI only images.

D. Discussion

Results do not support our hypothesis that compositional changes would precede organizational changes but do support the hypothesis that organizational changes precede changes in mechanics. Changes in both composition and organization were found at the earliest time point investigated in this study. However, more disorganized tissue was seen in the intra-articular space at 1 and 4 weeks followed by a decrease in modulus in the intra-articular space 8 weeks following detachment. Increased cellularity was not

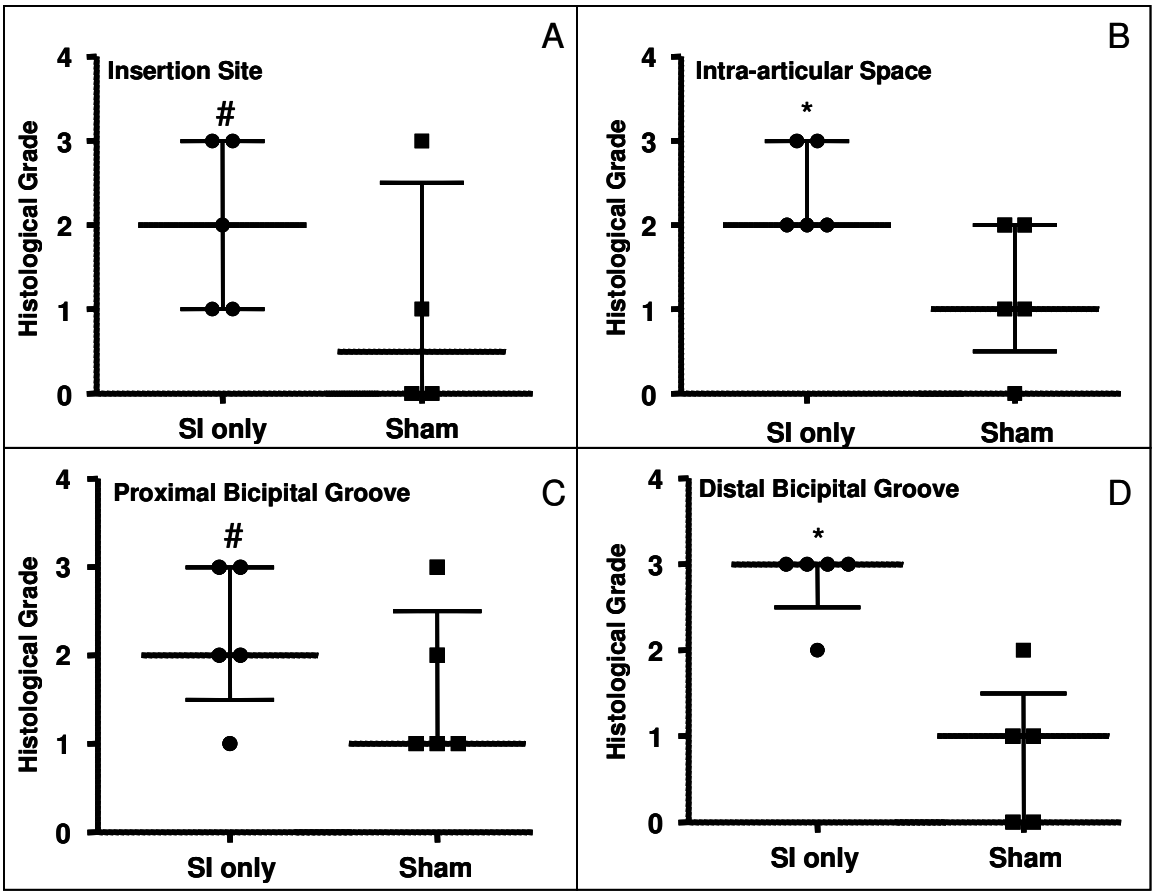

Figure 3.11: After 4 weeks, cellularity is increased along the entire length of the tendon compared to sham surgery. Data is presented as median with interquartile ranges. (*sig from Sham, #trend from Sham)

seen until the 4 and 8 week time points, at which increases were seen along the entire tendon length. However, it is possible that cellularity was increased after 1 week with both the sham and rotator cuff detachment surgeries, which decreased in the sham animals but not in the presence of detachments.

It is also interesting to note that changes in histological grading support changes seen in organization. After 1 week, a more disorganized tendon was seen in the intra-articular space. Also at this time point, there was a trend toward a more rounded cell phenotype at this location. After 4 weeks, it seems that cell shape changes precede organizational changes as again the tendon was only disorganized in the intra-articular

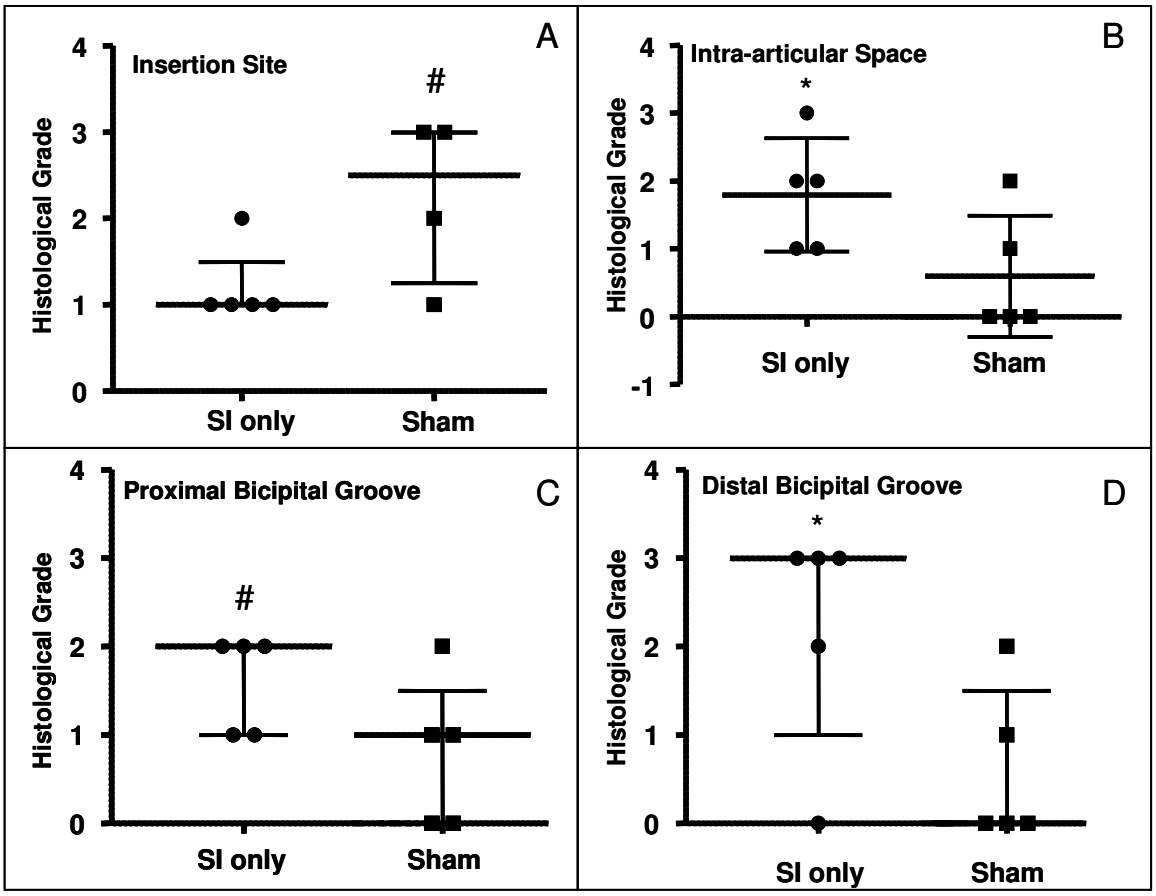

Figure 3.12: Compared to sham, cell shape is more elongated at the insertion site (A) and more rounded in the intra-articular space (B), proximal bicipital groove (C) and distal bicipital groove (D) 4 weeks following detachments. Data is presented as median with interquartile ranges. (*sig from Sham, #trend from Sham)

space but a more rounded cell shape was seen along the entire tendon length. Finally, after 8 weeks decreased organization and a more rounded cell phenotype were present along the entire tendon length. This more rounded cell shape and decreased organization, characteristics seen at a tendon insertion site which is exposed to a complex loading environment, could be the result of increased compressive loading seen by the tendon against the humeral head and in the bicipital groove. When the most significant superior stabilizers of the humeral head (supraspinatus and infraspinatus) are detached, we speculate that the biceps tendon plays an increased role in compressive loading as a

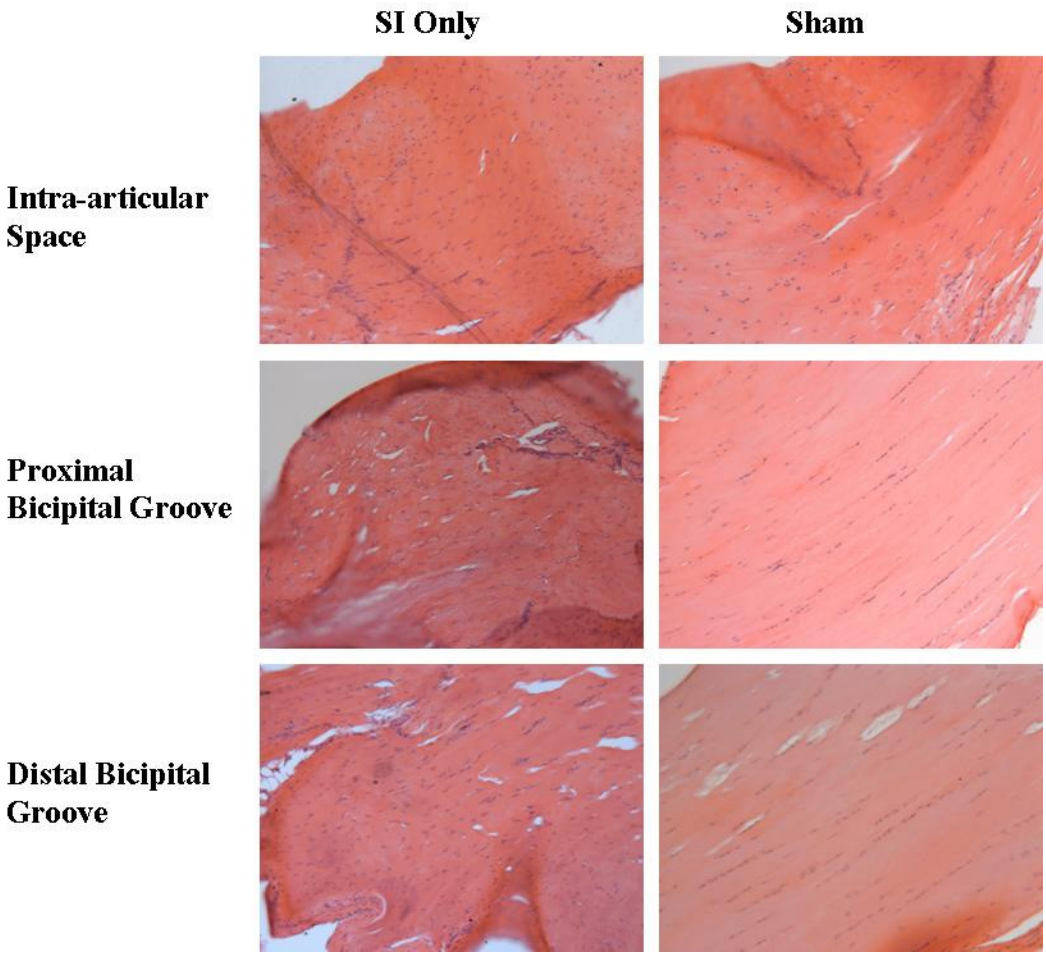

Figure 3.13: Cell shape and cellularity are increased in the intra-articular space and proximal and distal bicipital groove 8 weeks following detachments. Also note the more disorganized collagen at all locations in the SI only images.

humeral head depressor and stabilizer, therefore seeing more multi-directional loading along its length rather than the pure tensile loading it sees with an intact rotator cuff.

This theory is supported by the increase in aggrecan (a proteoglycan found most often in cartilage) at 1 week post detachments. Biglycan, an ECM protein associated with injury, was also increased at the insertion site after 1 week. Increased biglycan expression progressed along the length of the tendon with time as increased expression was seen at 4 weeks in the intra-articular space and at 8 weeks along the entire tendon length. This finding supports the theory that a degenerative process is occurring in the

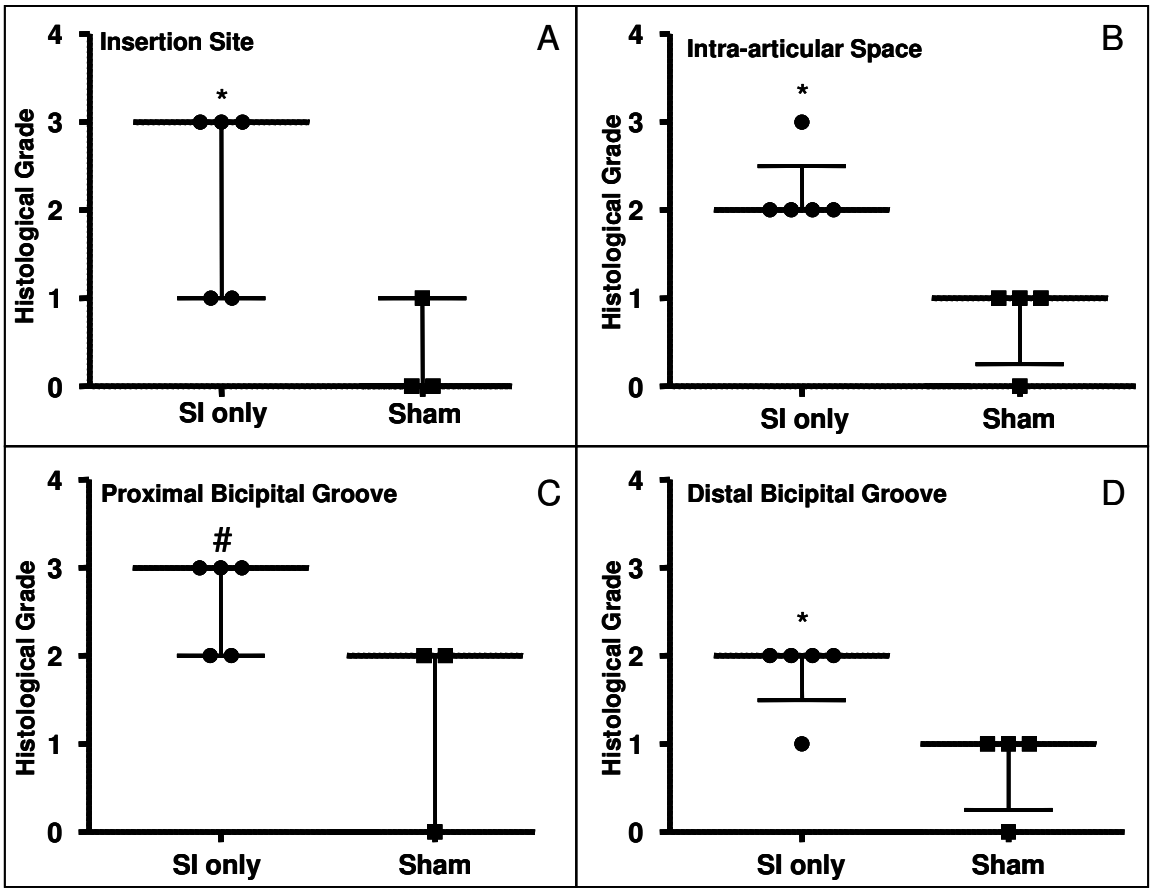

Figure 3.14: After 8 weeks, cellularity remains increased along the entire tendon length. Data is presented as median with interquartile ranges. (*sig from Sham, #trend from Sham)

tendon, and it is not solely becoming inflamed in the presence of the rotator cuff tear. Collagen I, the most prevalent collagen seen in tendons, was increased at the insertion site at 1 week and along the entire tendon length at 8 weeks, perhaps indicating that the tendon is trying to return its properties to normal by producing more collagen adapted to tensile loading.

Immunohistochemical results support our hypothesis that changes begin at the insertion site as, other than aggrecan, all changes at 1 week were only at the insertion site. However, histological grading and organizational results indicate changes may begin in the intra-articular space. The lack of changes in organization seen at the insertion site may be due simply to the fact that a disorganized collagen matrix already exists at this

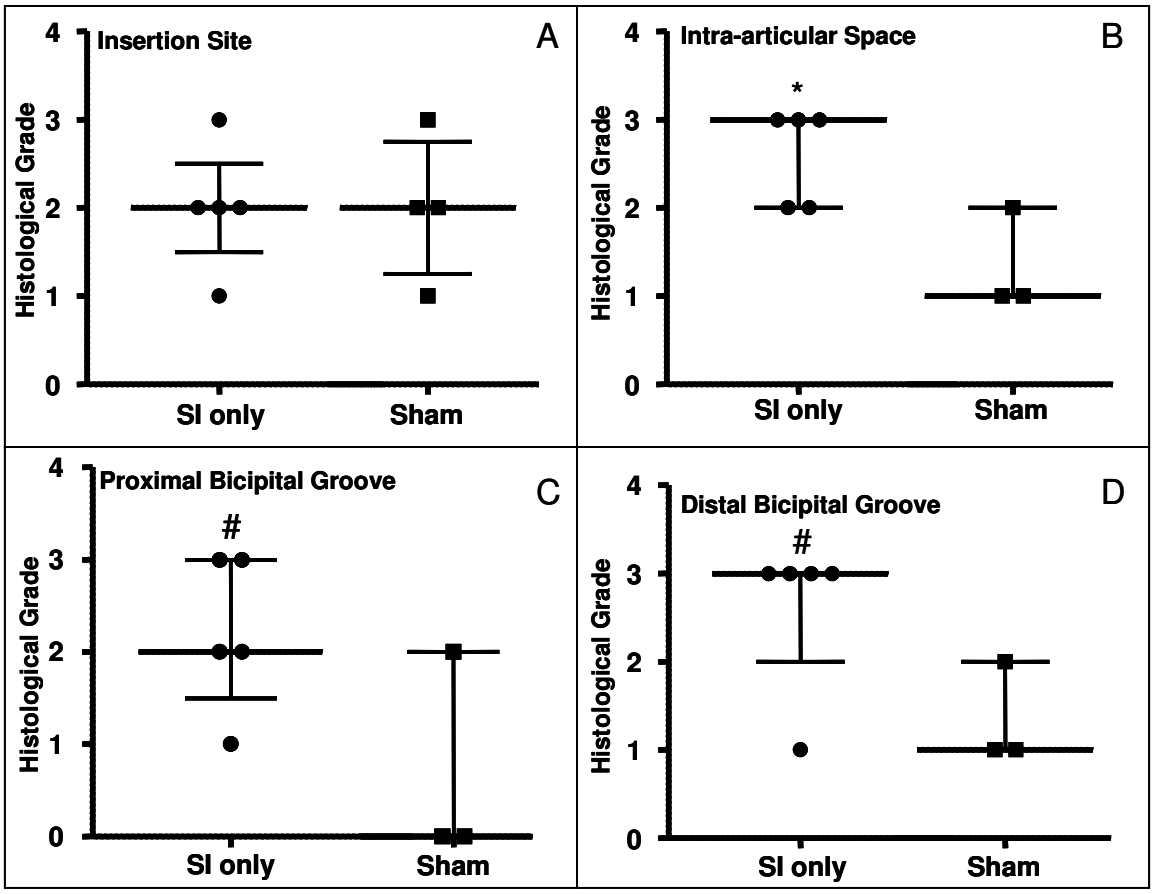

Figure 3.15: After 8 weeks, a more rounded cell phenotype was seen in the intra-articular space (B) and proximal (C) and bicipital (D) grooves. Data is presented as median with interquartile ranges. (*sig from Sham, #trend from Sham)

location and further disorganization may be difficult to detect. Following sham surgery, the organization is the same in the intra-articular space and proximal and distal bicipital grooves whereas following rotator cuff detachments the intra-articular space is more disorganized than the more distal locations, perhaps indicating it is experiencing types of loading more like that seen at the insertion site.

While not all changes occur first at the insertion site, it was consistently shown that changes appear in the intra-articular portion of the tendon before the extra-articular portion. These results are supported by the recent work of Joseph et al, who found the intra- and extra-articular portions of the biceps tendon to be markedly different when in

the presence of rotator cuff tears.[7] However, this study did not compare to uninjured tendons and therefore there may be some differences in the intra- and extra-articular portions that are inherent to the tendon and not a result of rotator cuff tears. In this study, it was possible to compare to a sham surgery and therefore any changes seen are the direct result of the rotator cuff tear.

Additionally, the scope of histological analyses used in this study was extremely broad, including histological grading, immunohistochemical staining, and quantification of collagen organization. Blinded histological grading was done semi-quantitatively and those grades were subsequently analyzed using rigorous non-parametric statistics. Immunohistochemical staining images were also analyzed with non-parametric statistics after being assigned grades based on the pixel intensity of the stain. Changes in this study were often seen in more than one of these assays, giving further confidence in the conclusions drawn here that degenerative changes are present in the biceps tendon following rotator cuff tears.

Furthermore, there are clearly a variety of biological changes occurring in this model that could be investigated in depth in the future. Specifically, although an increase in cellularity and more rounded cell shape were seen here following cuff tears, the source of these cells was not determined and whether the rounded cell shape was the result of an infiltration of new rounded cells or a change in the phenotype of the elongated cells found in normal tendons is not known. While we controlled for inflammation due to surgery by comparing to a sham, it is possible that inflammatory cells may participate at later time points due to the injury and healing response following rotator cuff tendon detachments. Future studies could determine the types of cells that are present when

cellularity is increased as well as investigate inflammatory factors such as FLAP and COX-2.

This study is not without limitation. The rotator cuff tendon tears in this study were made acutely, which may be considered a shortcoming of this model. However, biceps tendon pathology occurs over time without surgical injury to the tendon itself. It is also possible that additional biological changes may be taking place that were not detected with the immunohistochemical staining performed in this study. A group of targets were selected that, according to previous studies, would be expected to show differences across both time and the length of the tendon and have been extensively used for rotator cuff tendons in the rat model. Future work with this model may include additional biological assays such as PCR or staining for targets involved in collagen turnover. We also did not examine the tendons for calcium deposits, which are sometimes found in degenerative rotator cuff tendons and are thought to be secondary to subacromial impingement.[3] In this study, we found that changes began in the intra-articular portion of the tendon first, suggesting that perhaps impingement under the

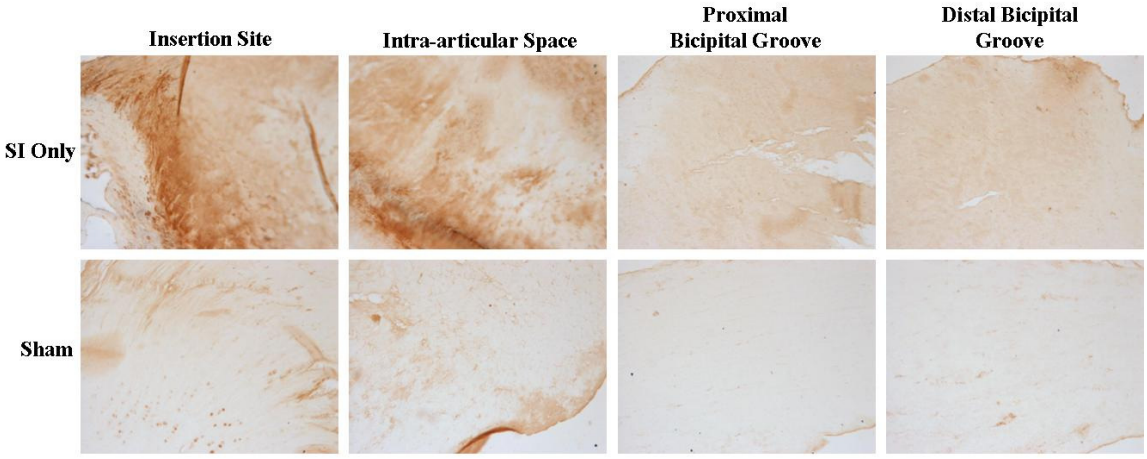

Figure 3.16: Aggrecan expression is increased along the entire tendon length 1 week following rotator cuff detachments.

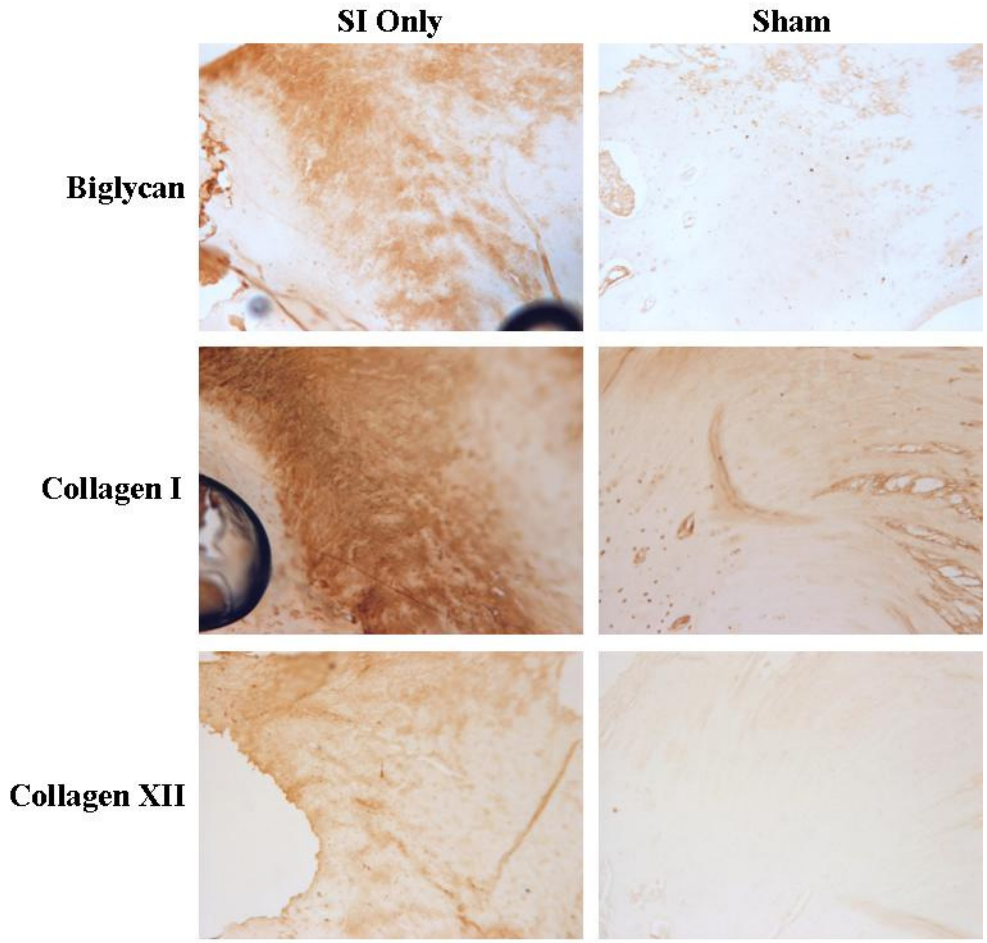

Figure 3.17: After 1 week, biglycan, collagen I and collagen XII are all increased at the insertion site compared to sham surgery.

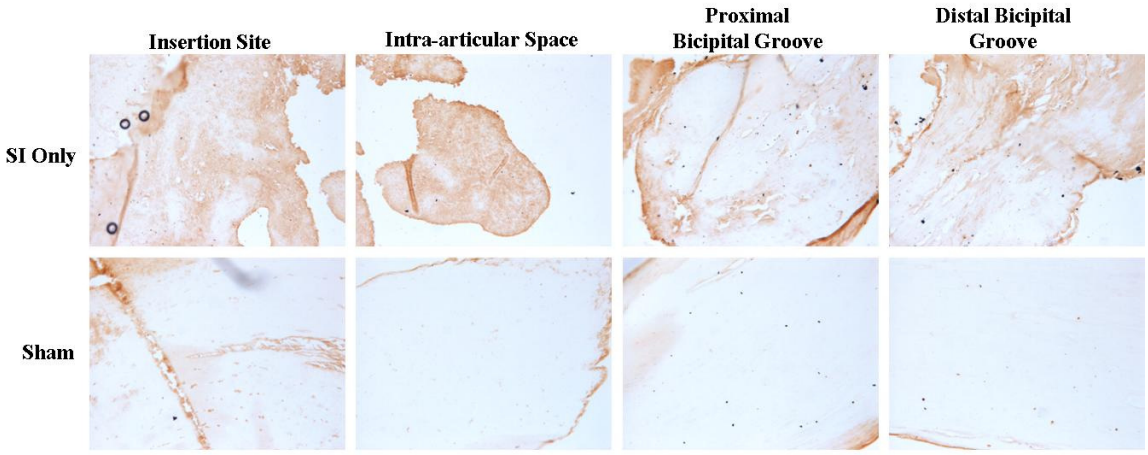

Figure 3.18: Biglycan was increased along the entire tendon length 8 weeks following detachments compared to sham surgery.

acromion in the intra-articular space is one of the possible mechanisms for biceps tendon pathology in the presence of rotator cuff tears. Therefore, it would be interesting to determine if calcium deposits are present in this model. Additionally, the effect of altered loading scenarios in addition to rotator cuff detachments on all properties measured here will be investigated.

In summary, it was shown here that organizational and compositional changes precede changes in area, which in turn precede changes in mechanical properties. In addition, it was shown that organizational and mechanical property changes begin in the intra-articular space while most immunohistochemical changes began at the insertion site. These results illustrate that changes in the biceps tendon occur gradually over time and represent true degenerative changes and not inflammation alone. This model can now be used to rigorously investigate the mechanism responsible for biceps tendon pathology in the presence of rotator cuff tears.

E. References

1. **Berenson, M. C.; Blevins, F. T.; Plaas, A. H.; and Vogel, K. G.:** Proteoglycans of human rotator cuff tendons. *J Orthop Res,* 14(4): 518-25, 1996.
2. **Chen, C. H.; Hsu, K. Y.; Chen, W. J.; and Shih, C. H.:** Incidence and severity of biceps long head tendon lesion in patients with complete rotator cuff tears. *J Trauma,* 58(6): 1189-93, 2005.
3. **Depalma, M. J., and Johnson, E. W.:** Detecting and treating shoulder impingement syndrome: the role of scapulothoracic dyskinesis. *Phys Sportsmed,* 31(7): 25-32, 2003.

4. **Favata, M.:** Scarless healing in the fetus: Implications and strategies for postnatal tendon repair. In *PhD Thesis: Bioengineering*, pp. 216. Edited, 216, Philadelphia, University of Pennsylvania, 2006.

5. **Gimbel, J. A.; Van Kleunen, J. P.; Mehta, S.; Perry, S. M.; Williams, G. R.; and Soslowsky, L. J.:** Supraspinatus tendon organizational and mechanical properties in a chronic rotator cuff tear animal model. *J Biomech,* 37(5): 739-49, 2004.

6. **Itoi, E.; Hsu, H. C.; Carmichael, S. W.; Morrey, B. F.; and An, K. N.:** Morphology of the torn rotator cuff. *J Anat,* 186 (Pt 2): 429-34, 1995.

7. **Joseph, M.; Maresh, C. M.; McCarthy, M. B.; Kraemer, W. J.; Ledgard, F.; Arciero, C. L.; Anderson, J. M.; Nindl, B. C.; and Mazzocca, A. D.:** Histological and molecular analysis of the biceps tendon long head post-tenotomy. *J Orthop Res*, 2009.

8. **Kido, T.; Itoi, E.; Konno, N.; Sano, A.; Urayama, M.; and Sato, K.:** The depressor function of biceps on the head of the humerus in shoulders with tears of the rotator cuff. *J Bone Joint Surg Br,* 82(3): 416-9, 2000.

9. **Kolts, I.; Tillmann, B.; and Lullmann-Rauch, R.:** The structure and vascularization of the biceps brachii long head tendon. *Ann Anat,* 176(1): 75-80, 1994.

10. **Murthi, A. M.; Vosburgh, C. L.; and Neviaser, T. J.:** The incidence of pathologic changes of the long head of the biceps tendon. *J Shoulder Elbow Surg,* 9(5): 382-5, 2000.

11. **Neer, C. S., 2nd:** Anterior acromioplasty for the chronic impingement syndrome in the shoulder: a preliminary report. *J Bone Joint Surg Am,* 54(1): 41-50, 1972.

12. **Peltz, C. D.; Perry, S. M.; Getz, C. L.; and Soslowsky, L. J.:** Mechanical properties of the long-head of the biceps tendon are altered in the presence of rotator cuff tears in a rat model. *J Orthop Res,* 27(3): 416-20, 2009.

13. **Wurgler-Hauri, C. C.; Dourte, L. M.; Baradet, T. C.; Williams, G. R.; and Soslowsky, L. J.:** Temporal expression of 8 growth factors in tendon-to-bone healing in a rat supraspinatus model. *J Shoulder Elbow Surg,* 16(5 Suppl): S198-203, 2007.

14. **Yamaguchi, K.; Riew, K. D.; Galatz, L. M.; Syme, J. A.; and Neviaser, R. J.:** Biceps activity during shoulder motion: an electromyographic analysis. *Clin Orthop Relat Res,* (336): 122-9, 1997.

15. **Yokota, A.; Gimbel, J. A.; Williams, G. R.; and Soslowsky, L. J.:** Supraspinatus tendon composition remains altered long after tendon detachment. *J Shoulder Elbow Surg,* 14(1 Suppl S): 72S-78S, 2005.

16. **Zar, J. H.:** Biostatistical Analysis. Edited, Princeton, Prentice Hall, 1984.

17. **Zgonis, M.; Wurgler-Hauri, C. C.; Perry, S. M.; and Soslowsky, L. J.:** The effect of rest after overuse on extracellular matrix proteins in rat supraspinatus tendon: An immunohistochemical analysis. In *Transactions of the Orthopaedic Research Society*, pp. 854. Edited, 854, San Diego, 2007.

Chapter 4: Altered loading affects the regional mechanical properties of the biceps tendon following rotator cuff tears in a rat model

A. Introduction

This chapter will investigate the effect of altered loading on regional changes in mechanical properties of the long head of the biceps tendon following rotator cuff tears in a rat model.

Damage to the long head of the biceps tendon is a common clinical condition that has often been identified as a source of shoulder pain. Although proximal long-head biceps tendon ruptures account for 96% of all biceps tendon ruptures[10], they rarely occur as isolated injuries and are often found in conjunction with pathologic conditions of the rotator cuff. Specifically, biceps tendon damage has been found in conjunction with rotator cuff tears and this damage is thought to increase with increasing tear size.[5,17] Considering that tears of the rotator cuff are thought to occur in up to 50% of the population[9], damage to the long head of the biceps tendon is a very prevalent clinical problem. However, there is some debate over the role of the biceps tendon at the shoulder following a rotator cuff tear. Some believe the biceps plays a significant role as a humeral head depressor[15] while others believe the biceps plays no functional role.[30] Therefore, controversy exists regarding the optimal treatment for the damaged biceps tendon, with physicians relying mostly on anecdotal experience.

The proposed role of the biceps tendon as a humeral head depressor is thought to be a significant contributor to changes seen in the biceps tendon with a rotator cuff tear, where one or more of the significant superior stabilizers (supraspinatus and/or

infraspinatus) would not be present. This could lead to an overload situation on the biceps tendon, impingement of the tendon against the acromion, or a combination of the two. The location where pathologic changes begin is also somewhat controversial. Some believe that pathology occurs at the entrance to the bicipital groove, and suspect the tendon first becomes inflamed and then damaged when it is has trouble sliding when hypertrophied. Neer has long believed that the biceps tendon is susceptible to impingement under the acromion after a rotator cuff tear occurs and that changes begin near the tendon's attachment to the glenoid on its bursal side.[19] It is also possible that changes may occur in this location but on the articular side, as increased compressive loading against the humeral head is present.

However, the mechanisms responsible for biceps tendon changes in the presence of rotator cuff tears are difficult to address in a clinical study due to both the inability to harvest the entire biceps tendon during surgery and the complexity of evaluating the effect of time post-repair when the precise history including the exact instance of tear initiation is often unknown. In Chapter 2, the established rotator cuff rat model was used to investigate the effect of multiple rotator cuff tear combinations on the long-head of the biceps tendon.[21] In this study, we found that the presence of rotator cuff tears led to a biceps tendon with increased area and eventually decreased modulus.[21] We also found that two tendon tears resulted in more pathologic changes than a one tendon (supraspinatus) tear, and that a combination of the supraspinatus and infraspinatus was worse than a supraspinatus and subscapularis combination. The results of this study showed that the rat model correlates well with the clinical condition in that pathology exists and increases with increasing tear size.

Therefore, the objective of this study was to use this established rat model to investigate the effect of altered loading on the biceps tendon following rotator cuff tears in order to begin to elucidate the mechanism by which these pathologies occur. Our hypotheses were that: 1) changes will begin near the insertion site and progress along the tendon length with time, 2) increased loading will result in further detrimental changes and 3) decreased loading will result in superior properties to those in the presence of a rotator cuff tear alone.

B. Preliminary Studies

Before investigating the effects of altered loading following rotator cuff tears on the biceps tendon, studies were done to determine appropriate methods for both increasing and decreasing the load on the biceps tendon following rotator cuff tears.

a. Increased loading

Previously in the rat, functional overload of the plantaris muscle has been achieved by removal of the gastocnemius and soleus muscles.[1,2,24,25] Similarly, we sought to overload the long-head of the biceps by detachment of the short-head from its insertion. We hypothesized that the long-head of the biceps muscle would show markers of hypertrophy 4 weeks following surgical detachment of the short-head, and that a greater degree of hypertrophy would be seen when short-head detachment was followed by 4 weeks of exercise by treadmill running. Four groups (n=4 in each) were included in this study: uninjured control (CTL), sham surgery (SHAM), short-head detachment followed by cage activity (CA) and short-head detachment followed by exercise (EX). Exercise consisted of treadmill running at a moderate speed (10 m/min) that gradually

increased up to an hour per day by the end of 2 weeks and continued at 1 hr/day until the end of the study.

All animals were sacrificed 4 weeks after surgery and their biceps muscles were removed. The short-head and long-head muscles were separated and wet weight of the long-head was determined. Long-head muscles were then frozen in isopentane cooled by liquid nitrogen and stored at -80ºC. Transverse sections were cut on a cryostat (10 µm) at -20ºC, fixed and stained with hematoxylin and eosin (H&E). Stained sections were then viewed on microscope and the number of centrally located nuclei per high power field (HPF) was counted. An average of values from 3 sections for each animal was obtained. Differences between groups in both long-head muscle mass and number of centrally located myonuclei were compared using a one-way ANOVA with Bonferroni correction. Significance was set at $p<0.05$.

An increase in muscle mass was seen when short-head detachment was followed by treadmill running compared to all other groups (Figure 4.1). There were no

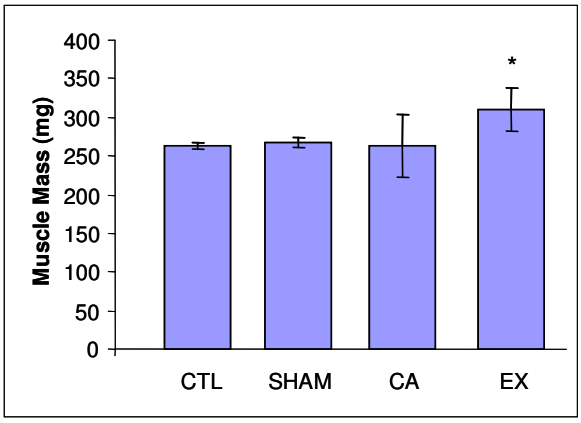

Figure 4.1: Long-head of the biceps muscle mass increased significantly when detachment of the short-head was followed by exercise (*=sig from CTL, SHAM and CA)

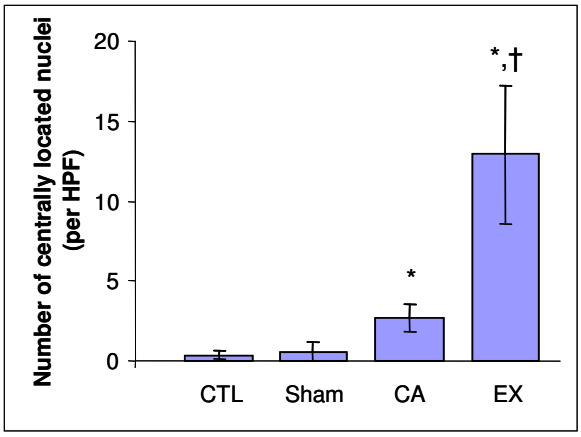

Figure 4.2: Increases in the number of centrally located myonuclei were seen with detachment of the short-head of the biceps followed by cage activity and exercise. (*sig from CTL and Sham, †=sig from CA)

differences in muscle mass between CTL, SHAM and CA groups. Additionally, there was no difference in the number of centrally located myonuclei between SHAM and CTL groups. There was, however, a significant increase in animals with a short-head detachment followed by either CA or EX compared to both SHAM and CTL (Figure 4.2). Additionally, there were significantly more centrally located myonuclei in animals that exercised following short-head detachment compared to those with cage activity (Figure 4.2). Centrally located myonuclei are generally considered a marker of muscle remodeling, and have been seen to occur in combination with hypertrophy in studies of testosterone administration[14] and correlated with an increase in muscle fiber size following vibration exposure in the rat.[18] We feel that the increase in muscle mass seen with detachment and exercise along with an increase in centrally located myonuclei confirms that the long-head of the biceps muscle is injured. In these animals, the short head of the biceps is detached and they are performing daily treadmill exercise, therefore we are confident that the combination of these 2 factors results in increased loading of the biceps tendon in this model.

b. **Decreased loading**

Our laboratory has extensive experience in immobilization of the rat shoulder following rotator cuff tendon repair.[20,22,26,28] Previous studies have used immobilization as a method of altered loading environment following supraspinatus detachment and repair in order to determine the effect on tendon to bone insertion site healing.[22,28] These studies have shown that long periods of immobilization resulted in superior tendon to bone healing, presumably due to better reformation of the healing insertion site when decreased loading is present.

Recently, a study was performed in order to investigate the effect of immobilization on shoulder range of motion. All animals had their left supraspinatus tendon detached (injured) and repaired as described[22] and were divided into cage activity (CA, n=21) and immobilization (IM, n=27) groups. Immediately after surgery, the CA group received cage activity for 6 weeks while the IM group shoulders were immobilized for 6 weeks as described.[23] Briefly, Webril (Tyco Healthcare) was placed around the injured arm and upper torso, forming a modified sling. This Webril sling was then covered in a layer of adhesive bandage (Vetrap, Penn Vet Supply). After these first 6 weeks of CA or IM, all animals underwent a protocol of controlled and gradual remobilization which began with short time periods (7 minutes) of moderate treadmill running (10m/min) and slowly increased in time up to 1 hour per day by the end of 4 weeks and continued at 1 hour per day until the end of the remobilization period at 12 weeks.

Range of motion (ROM) was measured for all animals prior to injury and repair,

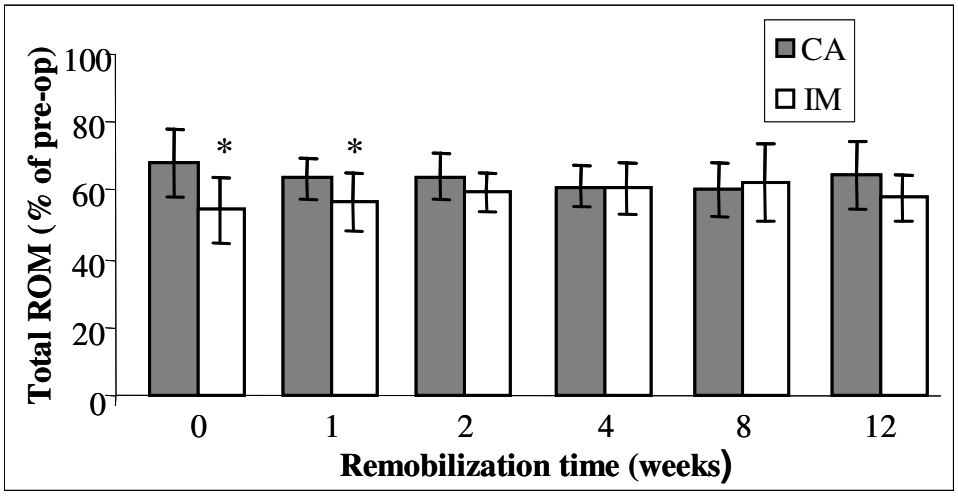

Figure 4.3: Total ROM is significantly decreased with post-operative immobilization (IM) compared to cage activity (CA) at the end of immobilization (0 weeks) and after 1 week of remobilization but IM and CA are not different after 2, 4, 8 or 12 weeks. (*=sig from CA)

at the end of their respective cage activity and immobilization periods (referred to as time 0), as well as at 1, 2, 4, 8 and 12 weeks of the remobilization period, as described.[26] Briefly, at each time point, each animal was anesthetized and its arm placed in a rotating clamp at 0º of abduction and 90º of elbow flexion. This position was defined as neutral, consistent with that position in humans, and a torque was applied to the arm for three internal and external rotation loading and unloading cycles to a prescribed torque target. ROM was determined using data from all three cycles. ROM was decreased in the IM group at the end of the immobilization period as well as one week later (Figure 4.3). By 2 weeks after the end of immobilization, there were no longer any differences between CA and IM groups. An initial decrease in ROM following immobilization is consistent with an environment of decreased loading in that joint. These results support our ability to create an environment of decreased loading on the shoulder joint following rotator cuff injury in the rat model. It is important to note, however, that the actual joint reaction forces at the shoulder or loads on the tendons during immobilization are unknown in this model. We also acknowledge that muscle activity during immobilization was not mesaured. Therefore, it is possible that some level of muscle firing may still be occurring in these animals. Despite this possibility, previous studies in the rat, although not in the shoulder, have found muscle atrophy of the soleus, plantaris, and gastrocnemius muscles following cast immobilization[11,16] and therefore we are confident that decreased loading in the shoulder is indeed experienced following immobilization in this model.

C. Methods

Fifty-nine Sprague-Dawley rats (Charles River, 400-450g) were used in this study approved by the University of Pennsylvania Institutional Animal Care and Use Committee. Rats were divided into 3 groups sacrificed at 4 and 8 weeks after surgical tendon detachments: supraspinatus+infraspinatus detachment only (n=10 at 4 wks, n=10 at 8 wks), supraspinatus+infraspinatus tendon detachment followed by decreased loading (n=10 at 4 wks, n=10 at 8 wks), and supraspinatus+infraspinatus tendon detachment followed by increased loading (n=10 at 4 wks, n=9 at 8 wks). All animals in the detachment only group are the same as those previously reported in Chapter 2. In all groups, a unilateral surgery was performed to sharply detach the rotator cuff tendons from the heir bony insertion, as previously described in Chapters 2 and 3, but included here for completeness.[21] Briefly, with the arm in external rotation, a 2 cm skin incision was made followed by blunt dissection down to the rotator cuff musculature. The rotator cuff was exposed and the tendons were visualized at their insertion on the humerus. The supraspinatus was first separated from the other rotator cuff tendons before sharp detachment at its insertion on the greater tuberosity using a scalpel blade before detaching the infraspinatus tendon in the same manner. Any remaining fibrocartilage at the insertion was left intact and detached tendons were allowed to freely retract without attempt at repair creating a gap ~4 mm from their insertion sites. The overlying muscle and skin were closed.

Animals in the supraspinatus and infraspinatus detachment only group (SI Only) were then allowed unrestricted cage activity. Animals in the post-detachment decreased loading group (SI+DEC) were immediately immobilized post-operatively using Vetrap.[20,22] Animals in the post-detachment increased loading group (SI+INC) had an

additional surgical detachment of the short-head of the biceps tendon immediately following rotator cuff detachments. Additionally, these same animals were prescribed a moderate treadmill running protocol (10 m/min) beginning 3 days after surgery. This protocol began initially at 10 minutes on the first day and increased over a 2 week period to 1 hour/day and continued at this time until the end of the study at 4 or 8 weeks.

After sacrifice, the scapula and the long-head of the biceps tendon were removed. Preparations for mechanical testing and the mechanical testing procedure are the same as those reported in Chapters 2 and 3, but are repeated here for completeness. The associated muscle was removed, and the tendons were fine dissected under a microscope. Five Verhoeff stain lines were then placed along the length of each tendon denoting the insertion site (0-1.5mm), the portion of the tendon in the intra-articular space (1.5-3.5mm), and the portion in the bicipital groove (3.5-8.5mm). A fifth stain line was placed at 11.5mm to identify grip placement and these stain lines were used to determine the distribution of strain along the length of the tendon. These positions were determined using histology to identify the length of the insertion site and gross dissections to determine the portion in the bicipital groove.[21] Tendon geometry was measured in each tendon portion using a laser based system.[6]

For biomechanical testing, the scapula was embedded in a holding fixture using polymethylmethacrylate (PMMA). The holding fixture was inserted into a specially designed testing fixture. The proximal end of the tendon was then held at the fifth stain line (11.5mm) in a screw clamp lined with fine grit sandpaper. The specimen was then immersed in a 39°C PBS bath, preloaded to 0.1N, preconditioned for 10 cycles from 0.1N to 0.5N at a rate of 1%/sec, and held for 300sec. Immediately following, a stress

relaxation experiment was performed by elongating the specimen to a strain of 4% at a rate of 5%/sec (0.575 mm/sec) followed by a 600sec relaxation period. Specimens were then returned to the initial preload displacement and held for 60 seconds and ramp to failure was then applied at a rate of 0.3%/sec. Using the applied stain lines, local tissue strain in each tendon portion was measured optically with a custom program (MATLAB). Elastic properties, such as stiffness and modulus were calculated using linear regression from the visually determined linear region of the load-displacement and stress-strain curves, respectively. Peak and equilibrium load were determined from the stress relaxation test and percent relaxation was then calculated from these values.

The non-linear load-displacement data were also analyzed with a structurally based elastic model first developed by Lanir[27] and recently adapted by our laboratory for rat supraspinatus tendon.[22] This function assumes that tendon is comprised of a population of linearly elastic fibers that un-crimp as the tendon is lengthened. After un-crimping, the fiber contributes to the force in a linear fashion, and the length at which the fiber un-crimps is referred to as the fiber's slack length. The tendon's non-linear force-length behavior, therefore, is the result of the non-linear distribution in fiber slack-lengths, which can be described by a cumulative probability distribution function (such as a Gaussian) described in the following:

$$p(L_0) = \frac{1}{\sigma\sqrt{2\pi}} \int_{-\infty}^{L_0} e^{\frac{-(t-\mu)^2}{\sigma}} \qquad (1)$$

Where p is the cumulative probability of a fiber being uncrimped, or recruited (between 0 and 100%), σ is the standard deviation of the fiber slack-lengths (mm), L_0 is the fiber slack-length (mm) and μ is the average fiber slack length (mm). A fiber is then

uncrimped (recruited) once the tendon length has exceeded the fiber's slack-length according to:

$$F(x) = K_{avg} \sum_{i=1}^{N} (x - L_0^i) \cdot H(x - L_0^i) \qquad (2)$$

where K_{avg} is the average fiber stiffness (N/mm), x is the tendon length (mm), L_0^i is the slack length of fiber i, and H is the heavy side step function (which is defined as 0 when $x< L_0^i$, and 1 when $x>=L_0^i$). This model has been used by Lanir and others to describe the non-linear elastic behavior of a variety of tissues. Generally speaking, disorganized tissues, such as skin, have a long flat toe-region, resulting in a large slack length mean and standard deviation; whereas, highly aligned tissue, such as ligament, have a relatively short sharp toe-region, resulting in a small slack length mean and standard deviation.[3,12] Thus, the more aligned or organized the tissue, the smaller the slack length standard deviation, Force displacement data from the ramp-to-failure portion of the test were fit to this structurally based model using the nonlinear least squares function in MATLAB to determine slack length distribution parameters (mean and standard deviation) and average fiber stiffness.

Lastly, data from the stress-relaxation portion of the test were analyzed using quasi-linear viscoelastic (QLV) theory. Quasi-linear viscoelastic theory separates the instantaneous non-linear elastic behavior from the time-dependent relaxation behavior according to:

$$F(t) = \int_0^t G(t - \tau) \frac{\partial F^e}{\partial \tau} d\tau \qquad (3)$$

where F(t) is the tendon force, G(t) is the relaxation function, and dFe/dt is the time derivative of the elastic function. In a manner consistent with Lanir[27], we used the structurally based elastic function in our QLV model. Specifically, we slightly modified Lanir's formulation by using the reduced relaxation function originally proposed by Fung[7], since it is more commonly used in tendon and ligament literature[29]:

$$G(t) = \frac{1 + C\left[E_1(t/\tau_2) - E_1(t/\tau_1)\right]}{1 + C\ln(\tau_2/\tau_1)} \qquad (4)$$

where G is the reduced relaxation function, t is time, C is the relaxation factor, E is the exponential integral function, and τ_1 and τ_2 are the short and long relaxation time constants, respectively. Load displacement data from the stress relaxation test were fit using the nonlinear least squares function in MATLAB to determine slack length distribution parameters (mean and standard deviation), average fiber stiffness, as well as the reduced relaxation function constants (C, τ_1 and τ_2).

Significance was assessed between groups at each time point using one-way ANOVAs with Bonferroni post-hoc comparisons. To correct for the number of comparisons, significance was set at $p<0.017$ (0.05/3) and trends at $p<0.033$ (0.1/3).

D. Results

At the insertion site, area increased with increased loading 4 weeks following a supraspinatus+infraspinatus tear (Figure 4.4). Also with increased loading, stiffness (Figure 4.5) and modulus (Figure 4.6) decreased at the insertion site. With decreased loading, there was an increase in stiffness at the insertion site (Figure 4.5). In the intra-

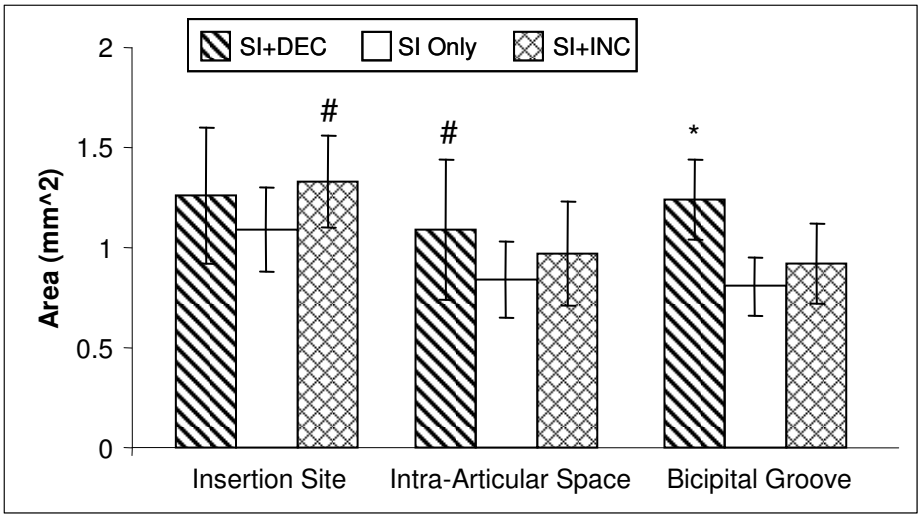

Figure 4.4: Area changes with altered loading 4 weeks following rotator cuff detachments. (*sig from SI only, #trend from SI only)

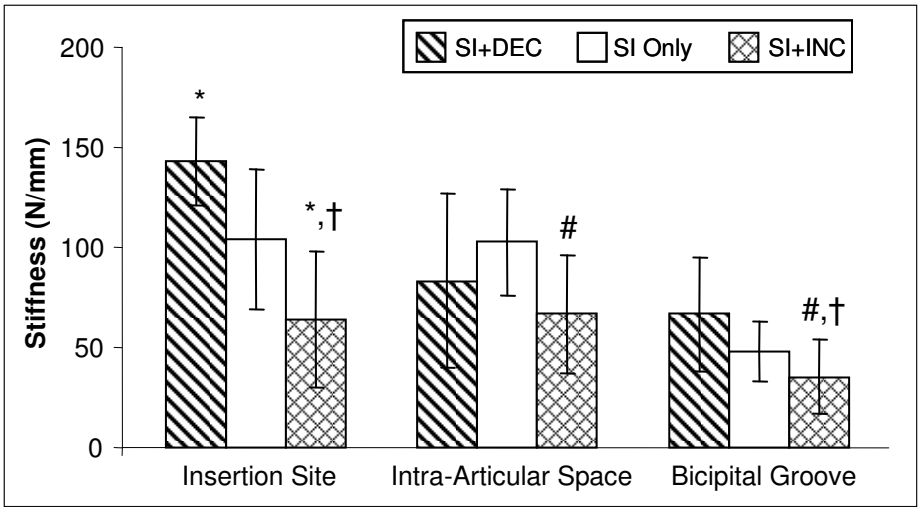

Figure 4.5: Four weeks following detachments, stiffness is decreased with increased loading at all locations and increased with decreased loading at the insertion site. (*sig from SI only, #trend from SI only, †sig from SI+DEC)

articular space, stiffness and modulus were decreased with increased loading (Figures 4.5 and 4.6, respectively). Decreased loading resulted in increased area (Figure 4.4) and decreased modulus (Figure 4.6) in the intra-articular space. Finally, in the bicipital groove, modulus and stiffness decreased with increased loading (Figures 4.5 and 4.6). With decreased loading, area increased in the bicipital groove (Figure 4.4).

There were also changes in QLV and structural fit parameters measured during

the stress-relaxation test and structural fit parameters measured during the ramp to failure test 4 weeks after detachments. During the stress-relaxation test, percent relaxation was increased with increased loading and peak and equilibrium load were decreased with increased loading (Table 4.1). Several structural fit parameters were also significantly altered during the stress-relaxation test (Table 4.1). Slack length mean and standard deviation (Table 4.1) were increased with decreased loading while average fiber stiffness during the stress- relaxation test (Figure 4.7) was decreased with increased loading. There was also an increase in the relaxation constant C with increased loading (Table 4.1). Time constants (tau1 and tau2) were decreased with increased loading compared to decreased loading (Table 4.1). During the ramp to failure test, slack length mean was increased with increased loading compared to decreased loading (Table 4.2) and slack length standard deviation was increased with increased loading compared to both detachment alone and decreased loading (Table 4.2). Whole tendon average fiber stiffness during the ramp to failure test decreased with increased loading (Figure 4.7).

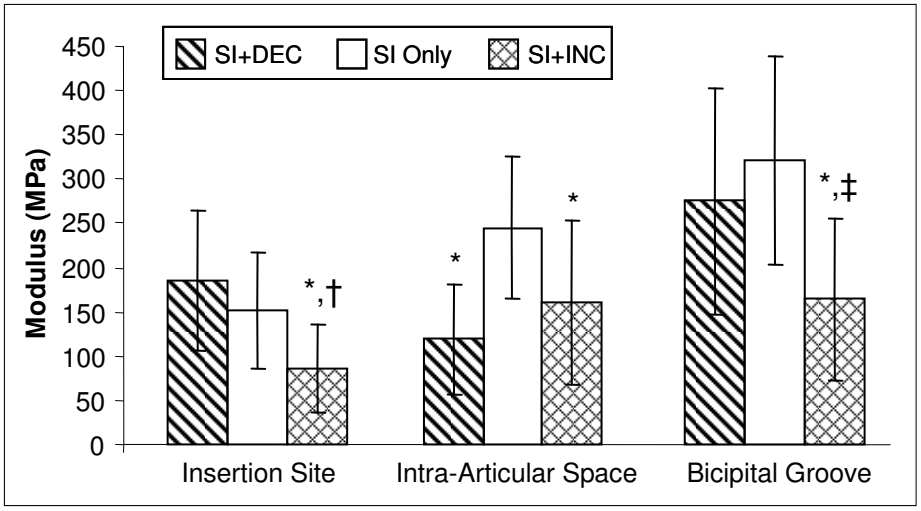

Figure 4.6: Modulus is decreased at all locations with increased loading and in the intra-articular space with decreased loading 4 weeks following detachments. (*sig from SI only, †sig from SI+DEC, ‡trend from SI+DEC)

Table 4.1: Parameters from QLV and structural fit analyses during the stress-relaxation test change with altered loading 4 weeks following detachments. (*sig from SI only, #trend from SI only, †sig from SI+DEC, ‡trend from SI+DEC)

	Peak Load (N)	Eq. Load (N)	Percent Relaxation	Slack Length Mean (mm)	Slack Length StDev (mm)	Stiffness (N/mm)	C	Tau1 (sec)	Tau2 (sec)
SI+DEC	4.0±1.2	1.9±0.8	0.51±0.05	0.17±0.05*	0.19±0.03*	15.2±5.4	0.15±0.03	0.15±0.09	417±174
SI Only	4.4±0.9	1.9±0.7	0.52±0.04	0.13±0.02	0.14±0.03	14.5±2.3	0.15±0.02	0.10±0.09	405±228
SI+INC	3.1±1.1*	1.3±0.6#,‡	0.59±0.05*,†	0.14±0.09†	0.15±0.03†	10.1±3.9*,†	0.19±0.06#	0.05±0.05†	269±110‡

Table 4.2: Structural fit parameters during the ramp to failure test are altered with increased loading 4 weeks following detachments. (*sig from SI only, #trend from SI only, ‡trend from SI+DEC)

	Slack Length Mean (mm)	Slack Length StDev (mm)	Stiffness (N/mm)
SI+DEC	0.27±0.04	0.14±0.04	12.2±4.1
SI Only	0.27±0.03	0.15±0.02	14.9±4.7
SI+INC	0.29±0.07	0.19±0.08#	9.1±2.7*,‡

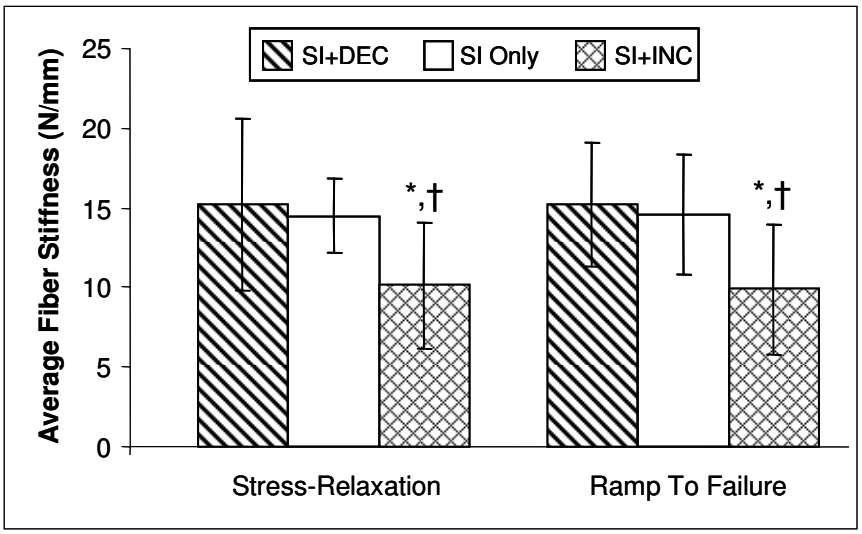

Figure 4.7: Four weeks following detachments, whole tendon average fiber stiffness was decreased with increased loading during both the stress-relaxation and ramp to failure tests. (*sig from SI only, †sig from SI+DEC)

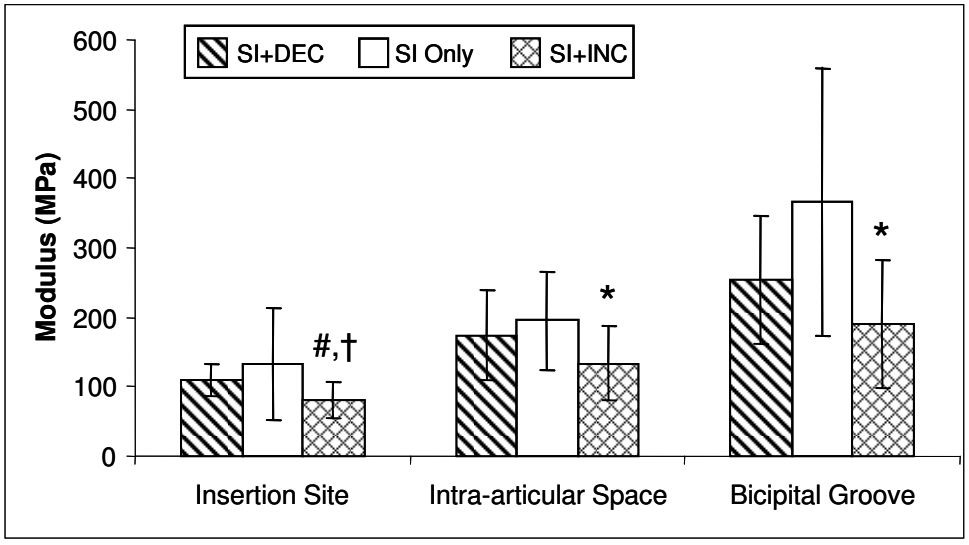

Figure 4.8: Eight weeks following detachments, modulus is decreased with increased loading at all tendon locations. (*sig from SI only, #trend from SI only, †sig from SI+DEC)

Eight weeks following a supraspinatus+infraspinatus tear, modulus (Figure 4.8) and stiffness (Figure 4.9) were decreased at all locations (insertion site, intra-articular space and bicipital groove) with increased loading. There were no changes in area at 8 weeks. Viscoelastic parameters were also altered with increased loading 8 weeks following detachments. Percent relaxation were decreased with decreased loading and increased with increased loading (Figure 4.10) and peak and equilibrium load were decreased with increased loading (Table 4.3). Average fiber stiffness during the stress-relaxation test was decreased (Figure 4.11) and the relaxation constant C was increased with increased loading (Table 4.3). During the ramp to failure test, whole tendon average fiber stiffness was decreased (Figure 4.11) and slack length standard deviation increased with increased loading (Table 4.4). There were no detrimental changes with decreased loading compared to detachment alone at any tendon location in modulus (Figure 4.8) or stiffness (Figure 4.9) 8 weeks following detachments. There were also no differences in

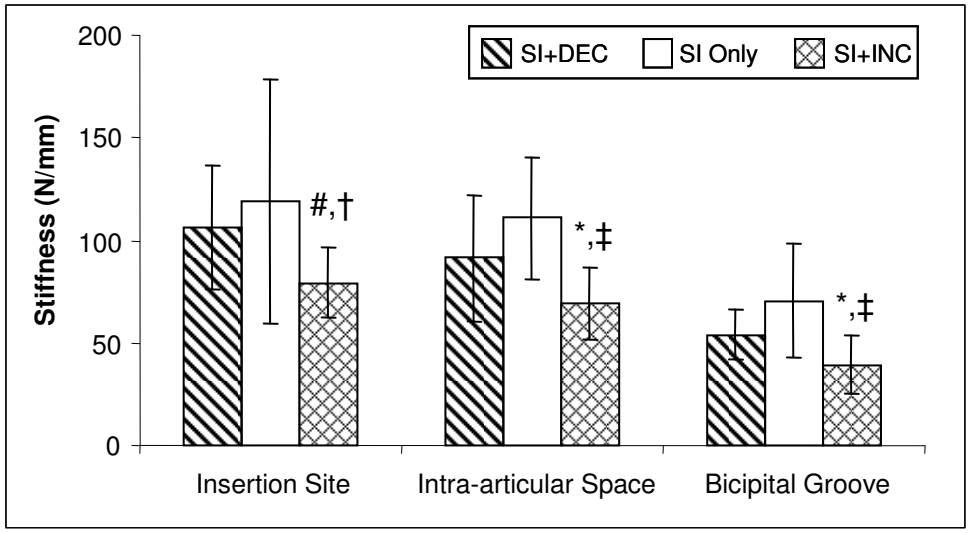

Figure 4.9: Stiffness is decreased at all tendon locations with increased loading compared to both detachment only and decreased loading 8 weeks following detachments. (*sig from SI only, #trend from SI only, †sig from SI+DEC, ‡trend from SI+DEC)

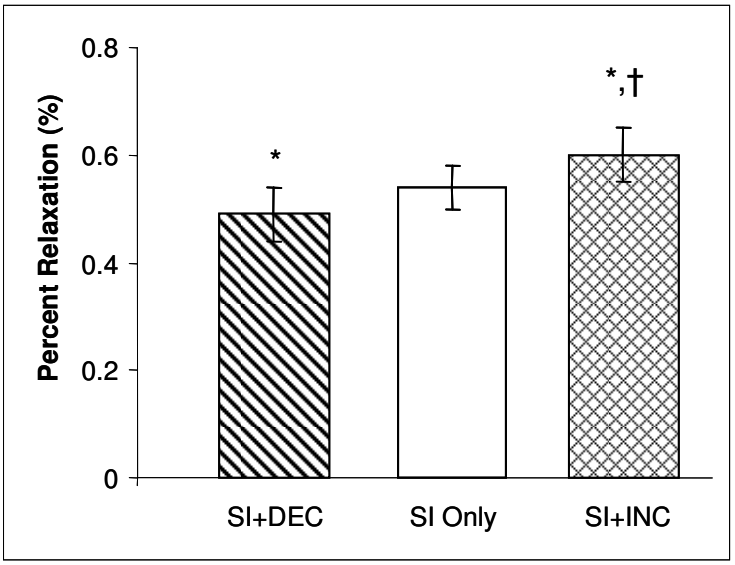

Figure 4.10: Percent relaxation is increased with increased loading and decreased with decreased loading 8 weeks after detachments. (*sig from SI only, †sig from SI+DEC)

structural fit parameters during stress-relaxation (Table 4.3, Figure 4.11) during the ramp to failure test (Table 4.4, Figure 4.11) after 8 weeks of decreased loading.

E. Discussion

Our first hypothesis was that tendon changes with alterations in loading would begin at the insertion site and progress along the tendon length with time. Unfortunately, the results of this study do not allow us to conclude where tendon changes begin. After 4 weeks of altered loading, detrimental changes were seen with increased loading and improved properties were seen with decreased loading at the insertion site. However, detrimental changes were also seen with increased loading along the entire tendon length. Also, the results regarding decreased loading differed at other locations, where detrimental changes were found such as increased area and decreased modulus in the intra-articular space and increased area in the bicipital groove. After 8 weeks of altered

Table 4.3: QLV and structural fit parameters determined from stress-relaxation data 8 weeks following rotator cuff tendon detachments. (*sig from SI only, #trend from SI only, †sig from SI+DEC, ‡trend from SI+DEC)

	Peak Load (N)	Eq. Load (N)	Percent Relaxation	Slack Length Mean (mm)	Slack Length StDev (mm)	Stiffness (N/mm)	C	Tau1 (sec)	Tau2 (sec)
SI+DEC	3.6±1.5	1.8±0.7	0.49±0.05*	0.16±0.03	0.17±0.03	14.4±5.8	0.15±0.03	0.12±0.08	360±95*
SI Only	5.0±1.4	2.4±0.7	0.54±0.04	0.19±0.07	0.18±0.05	19.7±5.4	0.14±0.03	0.11±0.07	561±193
SI+INC	3.1±1.2*	1.3±0.6*	0.60±0.06*,†	0.17±0.09	0.18±0.06	11.8±3.6*	0.21±0.06*,‡	0.14±0.1	391±150#

Table 4.4: Structural fit parameters from the ramp to failure test are altered with increased loading 8 weeks following detachments. (*sig from SI only, #trend from SI only, ‡trend from SI+DEC)

	Slack Length Mean (mm)	Slack Length StDev (mm)	Stiffness (N/mm)
SI+DEC	0.27±0.04	0.14±0.04	12.2±4.1
SI Only	0.27±0.03	0.15±0.02	14.9±4.7
SI+INC	0.29±0.07	0.19±0.08#	9.1±2.7*,‡

loading, the results were more consistent, with decreased properties along the entire tendon length with increased loading and no differences between decreased loading and detachment alone at any location.

While the location at which changes first occur was not determined, it was shown that regional differences do exist. While the changes were more uniform after 8 weeks, earlier changes varied by tendon location. In our study, if only the insertion site at 4 weeks would have been evaluated, the data would have shown that decreased loading was helpful while had the only the intra-articular space been examined, it would have been concluded it was harmful. It is also possible that differences may be missed if the entire

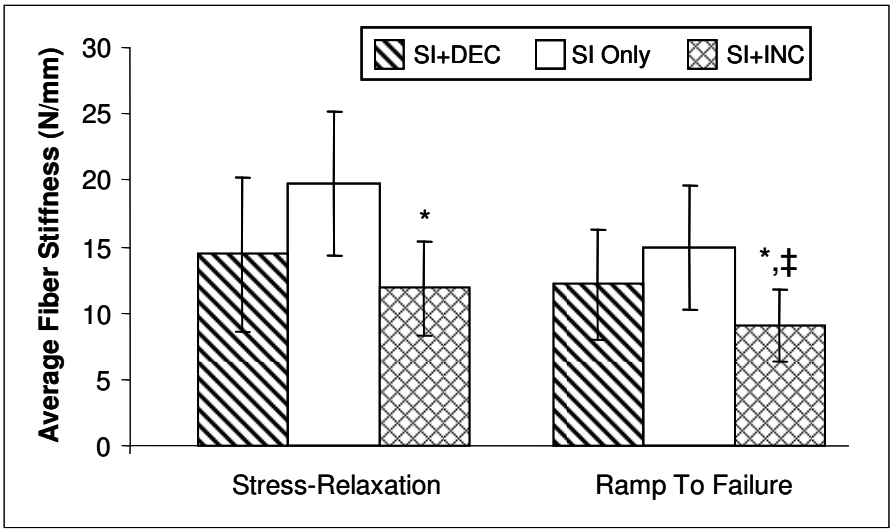

Figure 4.11: Whole tendon average fiber stiffness was decreased with increased loading during both stress-relaxation and ramp to failure tests 8 weeks following detachments. (*sig from SI only, ‡trend from SI+DEC)

tendon is analyzed as the modulus has been found to vary along the length, making an "average modulus," a parameter that may have very high variations. This may help to explain some of the conflicting results of other studies investigating the effect of rotator cuff tears on pathology of the long head of the biceps tendon. For example, one study found no differences in area or material properties in biceps tendons from cadaveric shoulders with and without rotator cuff tears.[4] However, in that study, only stamped central portions of the tendons were tested. Conversely, another recent study[13] looked separately at the intra- and extra-articular portions of tenotomized biceps tendons from shoulders with rotator cuff tears. In this study, the intra-articular portion of the tendon had a significantly higher proteoglycan content, decreased organization and increased expression of collagen III and MMP-1 and 3 compared to the extra-articular portion.

Results regarding the effect of increased loading supported our second hypothesis that increased loading would result in further detrimental changes compared to detachment alone. At both 4 and 8 weeks, significantly decreased modulus and stiffness were found at the insertion site, in the intra-articular space and in the bicipital groove. Increased area was also shown at the insertion site at 4 weeks. In Chapter 2[21], only increased area was found 4 weeks following a supraspinatus+infraspinatus tear and d decreased modulus was not seen until 8 weeks following detachment. Changes in stiffness were not observed in that study. Viscoelastic parameters, which could only be measured for the whole tendon, were also altered with increased loading. Stiffness during the stress-relaxation test was decreased at both 4 and 8 weeks, while percent relaxation and relaxation constant C were increased at 8 weeks. From these results, insight into the role increased loading may play as a mechanism for biceps damage in the

presence of a rotator cuff tear can be obtained. Future studies will continue to elucidate this role by examining histological, organizational and compositional changes at these and other timepoints.

Our third hypothesis was that decreased loading would cause positive changes in mechanical properties compared to supraspinatus+infraspinatus detachment alone. After 4 weeks of altered loading, conflicting results were found in different portions of the tendon. At the insertion site, stiffness was increased with decreased loading compared to detachment alone, which is generally considered to be an improvement in tendon properties. In the intra-articular space, negative changes were seen with increased area and decreased modulus. Finally, area increased in the bicipital groove, which is most likely a negative change. However, at 8 weeks, there were no differences between the decreased loading and detachment alone groups. This may be due to the an initial decrease in tendon properties that are now attempting to return to normal with increased immobilization time. Although investigating the effect of immobilization on tendon to bone healing, other studies in our lab have shown that it can take up to 16 weeks of immobilization for increased mechanical properties to result.[8,28] While a longer time point was not included in this study, future studies will investigate compositional and organizational changes in these tendons which we found to precede changes in mechanical parameters in our tendon to bone healing studies.[8,28]

Detrimental changes in some whole tendon parameters (viscoelastic, structural fit) were found with decreased loading after 4 weeks but by 8 weeks there were no longer any differences between decreased loading and detachment alone. It is interesting to note that the detrimental changes seen in whole tendon structural fit parameters at 4 weeks

with decreased loading were only seen during the stress-relaxation test and not during the ramp to failure. Since detrimental changes in regional mechanical properties were only found in the intra-articular space, perhaps there is a link between this tendon location and changes in viscoelastic parameters which can only be determined for the tendon as a whole.

The rotator cuff tendon tears in this study were made acutely, which may be considered a limitation of this model. However, biceps tendon pathology occurs over time without surgical injury to the tendon itself. The actual amount of load that was added to or taken away from the tendon in our altered loading scenarios was not determined although we are confident from preliminary studies that loads on the tendon are truly increasing and decreasing. Future directions of this work include immunohistochemical staining in order to determine compositional changes that may be occurring in these tendons at these and earlier time points. Additionally, we will be evaluating the regional collagen organization and histological characteristics (cellularity, cell shape) of these tendons.

In summary, it was shown that increasing the load on the biceps tendon following a rotator cuff tear caused decreased mechanical properties along the entire tendon length and this begins to implicate altered loading as a possible mechanism for biceps tendon damage in the presence of a rotator cuff tear. Our results regarding the effect of decreased loading were less clear, but promising, as there were changes at 4 weeks but by 8 weeks there were no differences from detachment alone. Lastly, although it cannot be concluded at which location changes begin, it was shown that regional differences do exist and are important in biceps tendon studies.

E. References

1. **Adams, G. R.; Haddad, F.; and Baldwin, K. M.:** Time course of changes in markers of myogenesis in overloaded rat skeletal muscles. *J Appl Physiol,* 87(5): 1705-12, 1999.
2. **Baldwin, K. M.; Valdez, V.; Schrader, L. F.; and Herrick, R. E.:** Effect of functional overload on substrate oxidation capacity of skeletal muscle. *J Appl Physiol,* 50(6): 1272-6, 1981.
3. **Belkoff, S. M., and Haut, R. C.:** A structural model used to evaluate the changing microstructure of maturing rat skin. *J Biomech,* 24(8): 711-20, 1991.
4. **Carpenter, J. E.; Wening, J. D.; Mell, A. G.; Langenderfer, J. E.; Kuhn, J. E.; and Hughes, R. E.:** Changes in the long head of the biceps tendon in rotator cuff tear shoulders. *Clin Biomech (Bristol, Avon),* 20(2): 162-5, 2005.
5. **Chen, C. H.; Hsu, K. Y.; Chen, W. J.; and Shih, C. H.:** Incidence and severity of biceps long head tendon lesion in patients with complete rotator cuff tears. *J Trauma,* 58(6): 1189-93, 2005.
6. **Favata, M.:** Scarless healing in the fetus: Implications and strategies for postnatal tendon repair. In *PhD Thesis: Bioengineering*, pp. 216. Edited, 216, Philadelphia, University of Pennsylvania, 2006.
7. **Fung, Y. C.:** Stress-strain-history relations of soft tissues in simple elongation. In *Biomechanics: Its foundations and objectives*, pp. 181-208. Edited by Fung Y.C., P. N., and Anliker M., 181-208, San Diego, Prentice- Hall, 1970.

8. **Gimbel, J. A.; Van Kleunen, J. P.; Williams, G. R.; Thomopoulos, S.; and Soslowsky, L. J.:** Long durations of immobilization in the rat result in enhanced mechanical properties of the healing supraspinatus tendon insertion site. *J Biomech Eng,* 129(3): 400-4, 2007.

9. **Gomoll, A. H.; Katz, J. N.; Warner, J. J.; and Millett, P. J.:** Rotator cuff disorders: recognition and management among patients with shoulder pain. *Arthritis Rheum,* 50(12): 3751-61, 2004.

10. **Harwood, M. I., and Smith, C. T.:** Superior labrum, anterior-posterior lesions and biceps injuries: diagnostic and treatment considerations. *Prim Care,* 31(4): 831-55, 2004.

11. **Herbison, G. J.; Jaweed, M. M.; and Ditunno, J. F.:** Muscle fiber atrophy after cast immobilization in the rat. *Arch Phys Med Rehabil,* 59(7): 301-5, 1978.

12. **Hurschler, C.; Loitz-Ramage, B.; and Vanderby, R., Jr.:** A structurally based stress-stretch relationship for tendon and ligament. *J Biomech Eng,* 119(4): 392-9, 1997.

13. **Joseph, M.; Maresh, C. M.; McCarthy, M. B.; Kraemer, W. J.; Ledgard, F.; Arciero, C. L.; Anderson, J. M.; Nindl, B. C.; and Mazzocca, A. D.:** Histological and molecular analysis of the biceps tendon long head post-tenotomy. *J Orthop Res*, 2009.

14. **Kadi, F.:** Cellular and molecular mechanisms responsible for the action of testosterone on human skeletal muscle. A basis for illegal performance enhancement. *Br J Pharmacol,* 154(3): 522-8, 2008.

15. **Kido, T.; Itoi, E.; Konno, N.; Sano, A.; Urayama, M.; and Sato, K.:** The depressor function of biceps on the head of the humerus in shoulders with tears of the rotator cuff. *J Bone Joint Surg Br,* 82(3): 416-9, 2000.

16. **Maxwell, L. C., and Enwemeka, C. S.:** Immobilization-induced muscle atrophy is not reversed by lengthening the muscle. *Anat Rec,* 234(1): 55-61, 1992.

17. **Murthi, A. M.; Vosburgh, C. L.; and Neviaser, T. J.:** The incidence of pathologic changes of the long head of the biceps tendon. *J Shoulder Elbow Surg,* 9(5): 382-5, 2000.

18. **Necking, L. E.; Lundstrom, R.; Lundborg, G.; Thornell, L. E.; and Friden, J.:** Skeletal muscle changes after short term vibration. *Scand J Plast Reconstr Surg Hand Surg,* 30(2): 99-103, 1996.

19. **Neer, C. S., 2nd:** Anterior acromioplasty for the chronic impingement syndrome in the shoulder: a preliminary report. *J Bone Joint Surg Am,* 54(1): 41-50, 1972.

20. **Peltz, C. D.; Dourte, L. M.; Kuntz, A. F.; Sarver, J. J.; Kim, S. Y.; Williams, G. R.; and Soslowsky, L. J.:** The effect of postoperative passive motion on rotator cuff healing in a rat model. *J Bone Joint Surg Am,* 91(10): 2421-9, 2009.

21. **Peltz, C. D.; Perry, S. M.; Getz, C. L.; and Soslowsky, L. J.:** Mechanical properties of the long-head of the biceps tendon are altered in the presence of rotator cuff tears in a rat model. *J Orthop Res,* 27(3): 416-20, 2009.

22. **Peltz, C. D.; Sarver, J. J.; Dourte, L. M.; Wurgler-Hauri, C. C.; Williams, G. R.; and Soslowsky, L. J.:** Exercise following a short immobilization period is detrimental to tendon properties and joint mechanics in a rat rotator cuff injury model. *J Orthop Res*.

23. **Peltz, C. D.; Sarver, J. J.; Dourte, L. M.; Wurgler-Hauri, C. C.; Williams, G. R.; and Soslowsky, L. J.:** Shoulder joint mechanics remain altered following post-operative immobilization and exercise in a rat rotator cuff injury and repair model. In *Transactions of the Orthopaedic Research Society*, pp. 105. Edited, 105, 2007.

24. **Roy, R. R.; Meadows, I. D.; Baldwin, K. M.; and Edgerton, V. R.:** Functional significance of compensatory overloaded rat fast muscle. *J Appl Physiol,* 52(2): 473-8, 1982.

25. **Roy, R. R.; Monke, S. R.; Allen, D. L.; and Edgerton, V. R.:** Modulation of myonuclear number in functionally overloaded and exercised rat plantaris fibers. *J Appl Physiol,* 87(2): 634-42, 1999.

26. **Sarver, J. J.; Peltz, C. D.; Dourte, L.; Reddy, S.; Williams, G. R.; and Soslowsky, L. J.:** After rotator cuff repair, stiffness--but not the loss in range of motion--increased transiently for immobilized shoulders in a rat model. *J Shoulder Elbow Surg,* 17(1 Suppl): 108S-113S, 2008.

27. **Sverdlik, A., and Lanir, Y.:** Time-dependent mechanical behavior of sheep digital tendons, including the effects of preconditioning. *J Biomech Eng,* 124(1): 78-84, 2002.

28. **Thomopoulos, S.; Williams, G. R.; and Soslowsky, L. J.:** Tendon to bone healing: differences in biomechanical, structural, and compositional properties due to a range of activity levels. *J Biomech Eng,* 125(1): 106-13, 2003.

29. **Woo, S. L.; Gomez, M. A.; Woo, Y. K.; and Akeson, W. H.:** Mechanical properties of tendons and ligaments. II. The relationships of immobilization and exercise on tissue remodeling. *Biorheology,* 19(3): 397-408, 1982.

30. **Yamaguchi, K.; Riew, K. D.; Galatz, L. M.; Syme, J. A.; and Neviaser, R. J.:** Biceps activity during shoulder motion: an electromyographic analysis. *Clin Orthop Relat Res,* (336): 122-9, 1997.

Chapter 5: The effect of altered loading following rotator cuff tears on the histological, organizational and compositional properties of the long head of the biceps tendon

A. Introduction

This chapter will investigate the changes over time in histological, organizational and compositional properties of the long head of the biceps tendon in the presence of rotator cuff tears followed by altered loading in a rat model.

Damage to the long head of the biceps tendon is common clinically, although it is rarely isolated and often seen in conjunction with rotator cuff tears.[2,9] However, there is some debate over the role of the biceps tendon at the shoulder following rotator cuff tears.[7,17] The mechanism responsible for the associated pathology is unknown and its optimal treatment is somewhat controversial. There is evidence that the biceps tendon plays an increased role as a humeral head depressor when one or more of the rotator cuff tendons are torn.[7] Therefore, the pathology seen may be a direct result of the tendon experiencing loads not seen with an intact rotator cuff.

The histology, organization and composition along the entire length of the biceps tendon are not well-characterized. It has been shown that the proteoglycan content is much higher, and very similar to rotator cuff tendons, near the insertion than it is in the bicipital groove.[6,8] Both tensile and compressive loading is seen at this location and the insertion site of a biceps tendon in an uninjured shoulder is less organized and expresses different amounts of various collagens and proteoglycans than the rest of the tendon. Away from the insertion site, the composition is markedly different and the collagen fibers are organized along the long axis of the tendon as the tendon experiences primarily

tensile loading in this location. The tendon's vascularity has also been shown to be more dense away from the insertion site.[8] The variations in function and composition along the length of the biceps tendon may play a role in how and where pathology begins in the presence of rotator cuff tears.

Clinicians have noted the biceps tendon to be flattened, widened and/or frayed at the time of rotator cuff repair and the damage has also been seen to increase with increasing tear size.[2,6] However, it is often not clear whether the changes are truly degenerate or are due to inflammation alone. The location where pathologic changes begin is also somewhat controversial. Some believe that pathology occurs at the entrance to the bicipital groove, and suspect the tendon first becomes inflamed and then damaged when it is has trouble sliding when hypertrophied. Neer has long believed that the biceps tendon is susceptible to impingement under the acromion after a rotator cuff tear occurs and that changes begin near the tendon's attachment to the glenoid on its bursal side.[10] It is also possible that changes may occur in this location but on the articular side, as increased compressive loading against the humeral head is present. In Chapter 3, the effect of rotator cuff tears on the histological, compositional and organizational properties along the entire length of the biceps tendon was examined. It was shown that many compositional changes appeared at the insertion site as early as 1 week following rotator cuff tendon detachments and that the tendon was also more disorganized in the intra-articular space at this time point. By later time points, this increased disorganization had extended along the entire length of the tendon. It was therefore concluded that a truly degenerate process was occurring in the tendon and that increased loading near the

insertion site was a major contributor to biceps tendon pathology in the presence of cuff tears.

Subsequently in Chapter 4, this model was used to examine the effect of altered loading post rotator cuff tendon detachment on biceps tendon mechanics in order to begin to elucidate its role as a possible mechanism for this pathology. It was shown that increased loading resulted in detrimental changes along the entire tendon length as early as 4 weeks post detachments while there were no changes between detachment alone and decreased loading by 8 weeks. However, earlier time points were not examined and therefore the biological processes that result in the mechanical changes seen with increased loading are unknown. Additionally, it is possible that improved biological properties are present with decreased loading without yet having a mechanical effect. Therefore, the objective of this study was to determine the effect of altered loading following rotator cuff tears on the regional organizational, histological and compositional properties of the long head of the biceps tendon. Our hypotheses were that: 1) changes with altered loading will begin at the insertion site and progress along the tendon length at later time points, 2) increasing loading will result in further detrimental changes compared to detachment alone while 3) decreased loading will result in increased organization and more normal tendon composition by 8 weeks.

B. Methods

Forty-two Sprague-Dawley rats (Charles River, 400-450g) were used in this study approved by the University of Pennsylvania Institutional Animal Care and Use Committee. Rats were divided into 3 groups dependent on the amount of post surgical

loading and rats from each group were sacrificed at 1, 4 and 8 weeks after surgical tendon detachments: supraspinatus+infraspinatus detachment only, supraspinatus+infraspinatus tendon detachment followed by decreased loading, and supraspinatus+infraspinatus tendon detachment followed by increased loading. The animals from all time points in the detachment only group are the same as those previously reported in Chapter 3. In all groups, a unilateral surgery was performed to sharply detach the rotator cuff tendons from their bony insertion, as described in previous chapters but is repeated here for completeness.[13] Briefly, with the arm in external rotation, a 2 cm skin incision was made followed by blunt dissection down to the rotator cuff musculature. The rotator cuff was exposed and the tendons were visualized at their insertion on the humerus. The supraspinatus was first separated from the other rotator cuff tendons before sharp detachment at its insertion on the greater tuberosity using a scalpel blade before detaching the infraspinatus tendon in the same manner. Any remaining fibrocartilage at the insertion was left intact and detached tendons were allowed to freely retract without attempt at repair creating a gap ~4 mm from their insertion sites. The overlying muscle and skin were closed.

Post-surgical loading protocols are the same as those previously reported in Chapter 4 but are included here for completeness. Animals in the supraspinatus and infraspinatus detachment only group (SI Only) were then allowed unrestricted cage activity. Animals in the post-detachment decreased loading group (SI+DEC) were immediately immobilized post-operatively using Vetrap.[11,12] Animals in the post-detachment increased loading group (SI+INC) had an additional surgical detachment of the short-head of the biceps tendon immediately following rotator cuff detachments.

Additionally, these same animals were prescribed a moderate treadmill running protocol (10 m/min) beginning 3 days after surgery. This protocol began initially at 10 minutes on the first day and increased over a 2 week period to 1 hour/day and continued at this time until the end of the study.

All histological methods (grading, polarized light and immunohistochemistry) are the same as those described in Chapter 3, but are repeated here for completeness. Each tendon was analyzed in 4 locations: the insertion site (0-1.5mm), the intra-articular space (1.5-3.5mm), the proximal bicipital groove (3.5-6mm) and the distal bicipital groove (6-8.5mm). Sagittal sections (7μm) were collected serially and stained with hematoxylin and eosin. Quantitative polarized light microscopy was used to determine collagen fiber orientations on these H&E stained sections.[4] Briefly, a rotatable λ compensator was used and a set of grayscale images (100x mag.) were taken at each tendon location at 10º increments as the crossed analyzer and polarizer were simultaneously rotated through 90º. Next, a set of color images was taken at 10º increments as the compensator and crossed analyzer and polarizer were rotated through 90º. A custom MATLAB program was then used to analyze approximately 120 points for each set of pictures to determine the collagen organization. The grayscale images were used to calculate the extinction angle and the color images to determine the orientation of the collagen. The angular deviation (AD) of the collagen orientation, a measure of the fiber distribution spread, in each tendon location for each specimen was then calculated as used previously.[19]

H&E stained sections were also analyzed for changes in cell shape and cellularity. Histological grading standards for cellularity and cell shape were produced by first organizing images for each tendon location from either least to most cellular or most

elongated to more rounded cell shape. These images were then divided into four quadrants and the middle image from each quadrant was chosen as the representative image for that quadrant and assigned a grade of 0 (least cellular or most elongated), 1, 2 or 3 (most cellular or most rounded). Images were then assigned grades by 3 blinded graders who compared each image to these standards for each location. The median grade between the 3 blinded graders for each image was then assigned to that image.

Finally, the distribution of various extra-cellular matrix proteins was localized in the biceps tendon using immunohistochemistry. The same specimens were used as for histological and polarized light analyses and one section from each specimen was stained for collagens type I, II, III and XII as well as proteoglycans aggrecan, biglycan and decorin (Table 5.1). Briefly, standard 7μm sections were first dewaxed and rehydrated followed by blocking and antibody reactions.[18] Sections for aggrecan were pretreated with 10-mmol/L dithiothreitol-50mmol/L tris-hydrocholic acid and 200 mmol/L sodium chloride for 2 hours at 37ºC and then alkylated with 40 mmol/L iodoacetamide-1 mol/L PBS for 1 hour at 37ºC. Sections for collagen type III were pretreated for 4 minutes with Protease K at room temperature. For all antibodies, various enzyme incubations were carried out at 37ºC (Table 5.1). Endogenous peroxidase activity was blocked in all sections by treatment with 3% hydrogen peroxide in methanol for 10 minutes, and non-specific binding of the secondary antibody was blocked with both 5% skim milk-PBS for 30 minutes and appropriate serum for 20 minutes. Tissue sections were then incubated with primary antibodies for up to 38 hours (Table 5.1) at 4ºC. Negative control sections were incubated with nonimmune horse serum diluted to the same protein content. The sections were then exposed to biotin-conjugated secondary antibodies (1:100 rat anti-

Table 5.1: Primary antibodies used for immunohistochemical staining

Protein Target	Antibody	Host	Type	Enzyme pretreatment	Dilution	Incubation Period (h)	Source
Collagen I	AB755P	Rabbit	Polyclonal	Hyaluronidase	1:200	16	Chemicon (Temecula, CA)
Collagen II	II-116B3	Mouse	Monoclonal	Hyaluronidase	1:4	16	DSHB (Iowa City, IA)
Collagen III	c7805	Mouse	Monoclonal	Hyaluronidase	1:50	38	Sigma (St. Louis, MO)
Collagen XII	LB-1200	Rabbit	Polyclonal	Hyaluronidase	1:100	16	Cosmo-bio (Tokyo, Japan)
Aggrecan	LF-113	Rabbit	Polyclonal	Chondroitinase ABC	1:200	16	L. Fisher (Bethesda, MD)
Biglycan	LF-159	Rabbit	Polyclonal	Chondroitinase ABC	1:200	38	L. Fisher
Decorin	JSCATE	Rabbit	Polyclonal	Chondroitinase AC	1:300	38	J. Sandy (Chicago, IL)

mouse monoclonal antibody or 1:200 goat anti-rabbit polyclonal antibody) for 30 minutes, and then avidin-biotinylated peroxidase complex reagent was applied for 30 minutes at room temperature. Finally, sections were incubated with 3,3'-diaminobenzidine for 4 minutes.

The same 4 regions were analyzed for immunohistochemical staining as for polarized light analysis and histological grading. Images were taken at 100X and evaluated semi-quantitatively using a custom DAB intensity measurement program (MATLAB).[16,20] Briefly, quartiles were produced for each tendon location using the total target DAB intensity ranges for each protein target, which were determined as the difference between the most and least stained specimens in each group. Each quartile was assigned a value of undetectable (0), low (1), moderate (2) or high (3) and each image was assigned one of these grades.

Angular deviation data were compared across time points using a one-way ANOVA with Bonferroni post-hoc correction. This data is presented as average +/- standard deviation. For histological and immunohistochemical analyses, median grades were compared for each tendon location across time points using a non-parametric Kruskal-Wallis test followed by Mann-Whitney post-hoc tests and this data is presented

as median +/- interquartile ranges. Significance was set at p=0.17 (0.5/3) and trends at p=0.33 (0.1/3).

C. Results

After 1 week, there were no differences in angular deviation between groups at any location along the tendon (Figure 5.1). After 4 weeks, angular deviation was increased in the intra-articular space in the SI+INC group compared to SI only and SI+DEC (Figures 5.2 and 5.4). Following 8 weeks of altered loading, there was a decrease in angular deviation in the SI+DEC group compared to both SI only and SI+INC groups in the intra-articular space and proximal and distal bicipital groove (Figures 5.3 and 5.5). Angular deviation was increased in the SI+INC group compared to SI only in the intra-articular space and proximal bicipital groove (Figures 5.3 and 5.5).

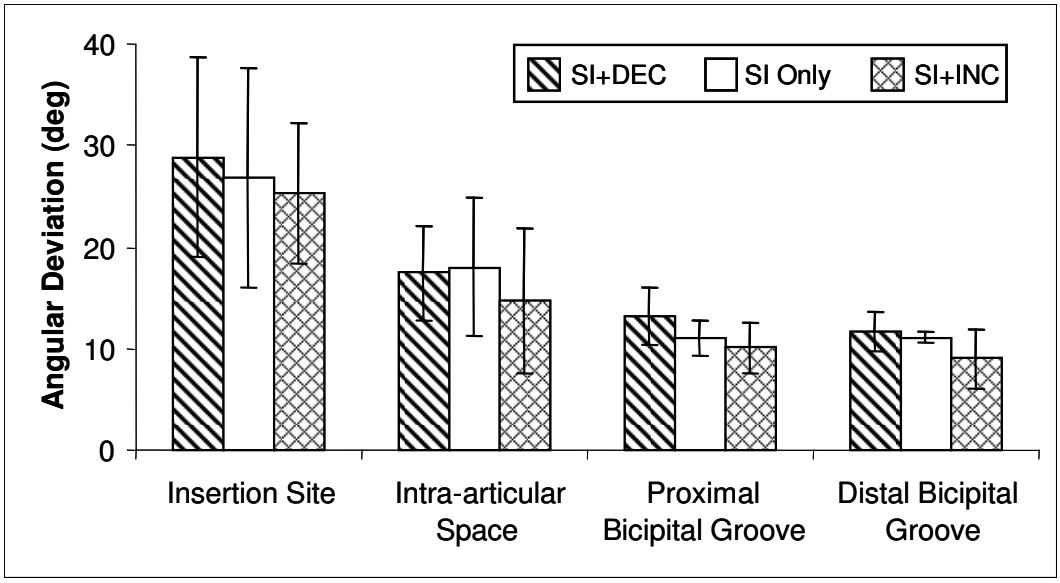

Figure 5.1: No differences were seen in angular deviation following 1 week of detachments and altered loading.

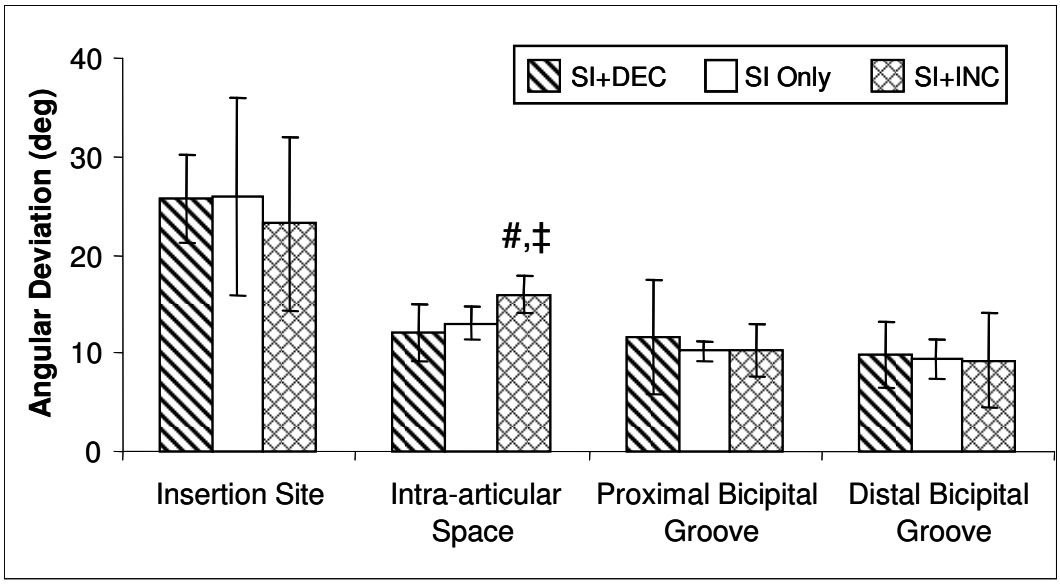

Figure 5.2: Angular deviation was increased with increased loading in the intra-articular space 4 weeks following detachments. (#trend from SI only, ‡trend from SI+DEC)

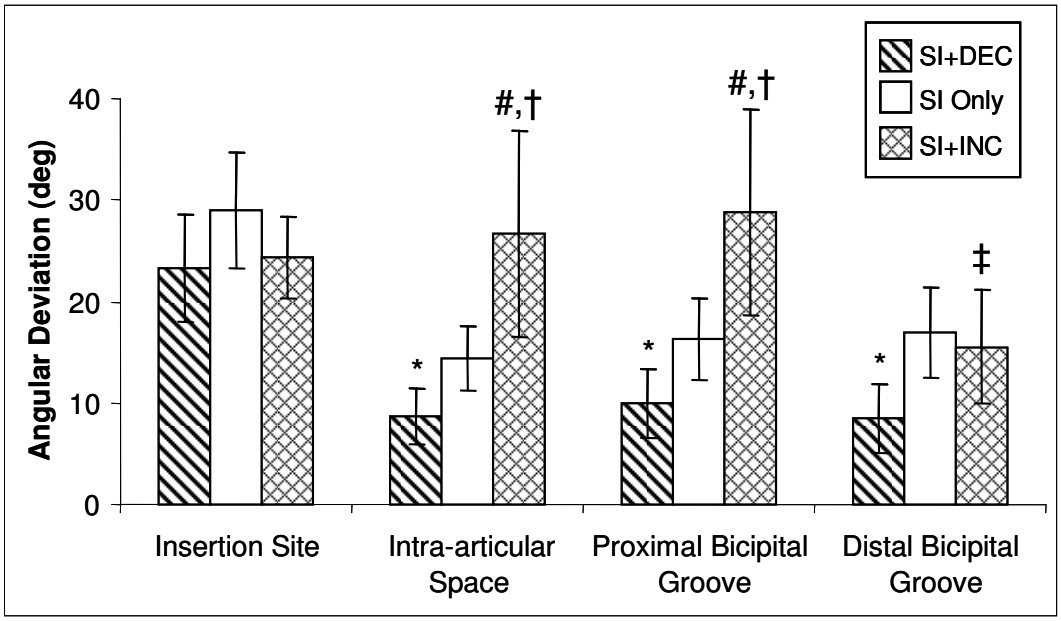

Figure 5.3: Eight weeks following detachments, angular deviation was increased with increased loading and decreased with decreased loading. (*sig from SI only, #trend from SI only, †sig from SI+DEC, ‡trend from SI+DEC)

There were no differences in cell shape or cellularity between groups at 1 or 4 weeks post detachments. After 8 weeks, cellularity decreased in the SI+DEC group in the intra-articular space and bicipital groove compared to SI only (Figure 5.6).

Figure 5.4: After 4 weeks, increased angular deviation in the intra-articular space was seen with SI+INC compared to SI only and SI+DEC.

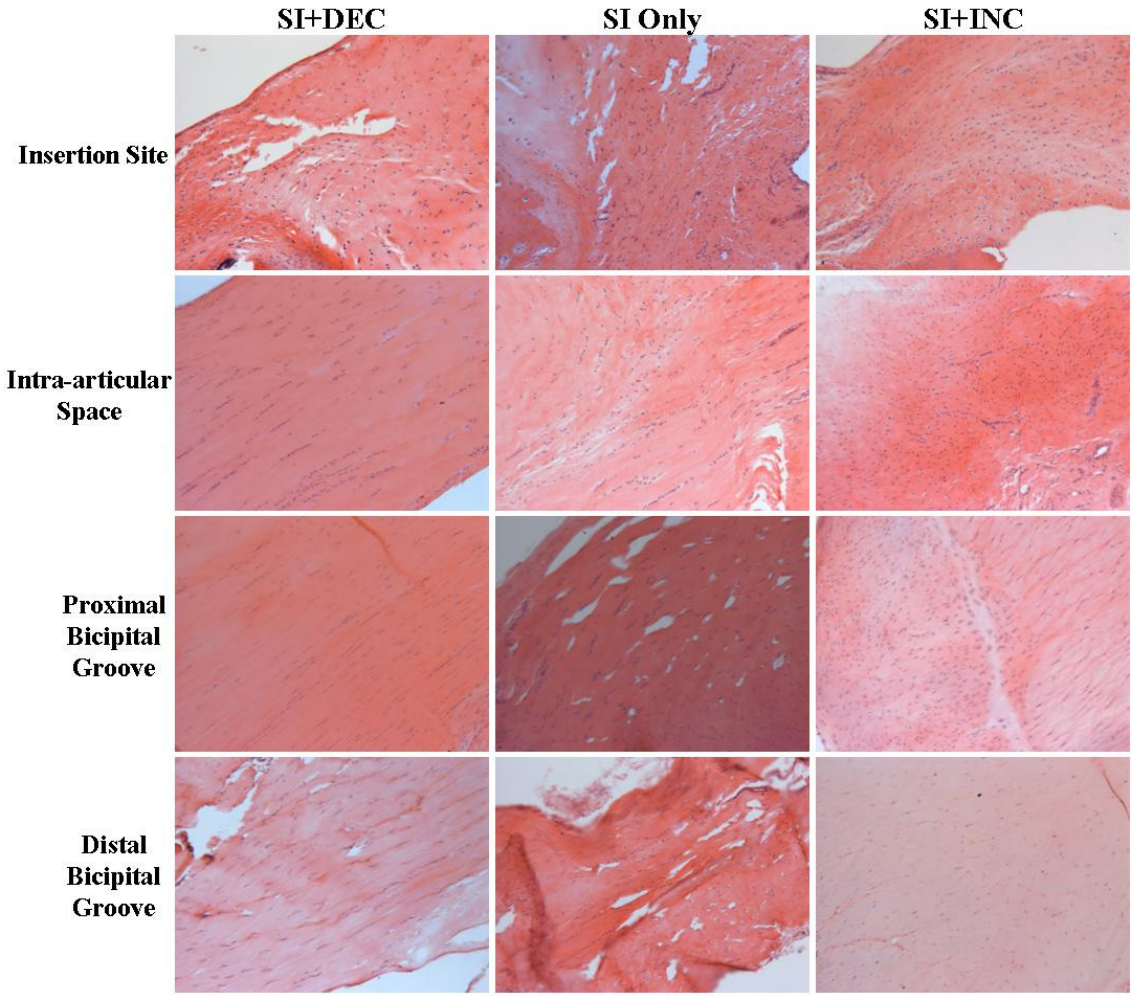

Figure 5.5: After 8 weeks of altered loading, angular deviation is decreased in the SI+DEC group compared to SI only and SI+INC in the intra-articular space and proximal and distal bicipital grooves. Additionally, angular deviation is increased with SI+INC compared to SI only in the intra-articular space and proximal bicipital groove.

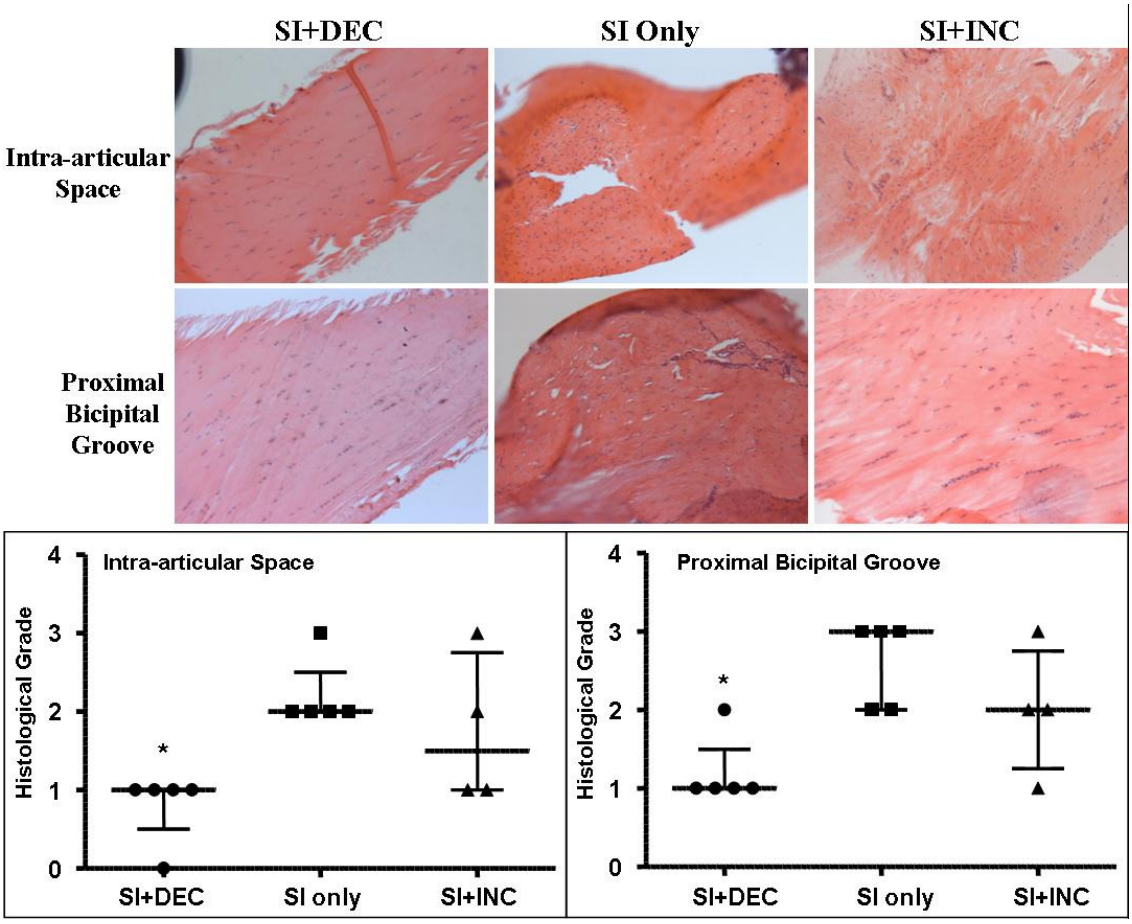

Figure 5.6: Cellularity was decreased with decreased loading in the intra-articular space and proximal bicipital groove 8 weeks following detachments. (*sig from SI only)

Cell shape also became more elongated in the SI+DEC group in the intra-articular space and proximal and distal bicipital groove compared to both SI only and SI+INC (Figures 5.5 and 5.7).

After 1 week, aggrecan expression increased in the SI only and SI+DEC groups compared to SI+INC in the intra-articular space and proximal bicipital groove (Figure 5.8). Collagen I increased with SI+DEC in the distal bicipital groove compared to SI+INC and collagen II increased in the intra-articular space with SI only compared to SI+INC. Collagen III increased at the insertion site and collagen XII increased in the

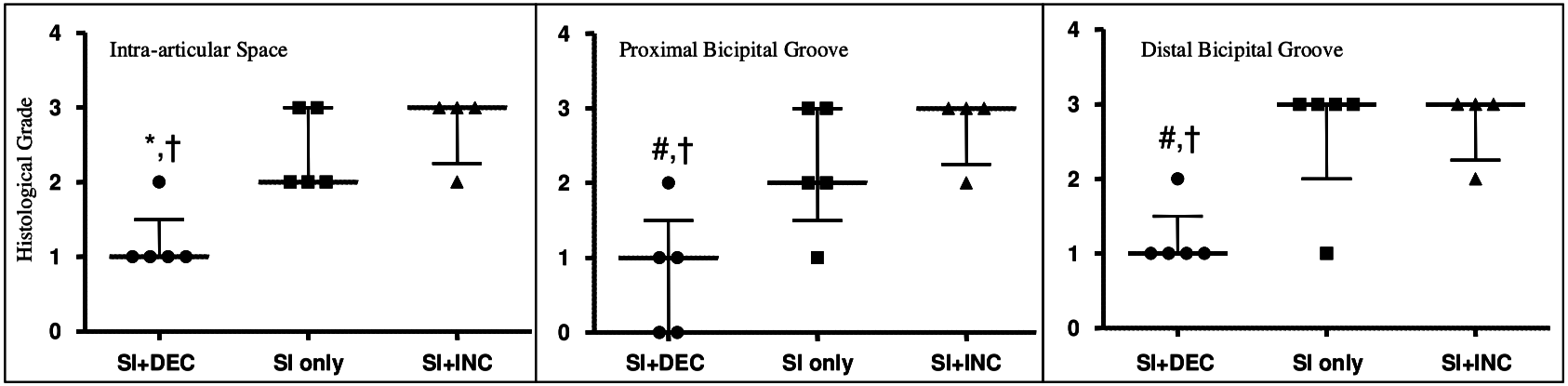

Figure 5.7: In this figure, an increase in histological grade indicates a more rounded cell, while a decrease indicates a more elongated cell. After 8 weeks, cell shape was more elongated with decreased loading in the intra-articular space and proximal and distal bicipital groove. (*sig from SI only, #trend from SI only, †sig from SI+INC)

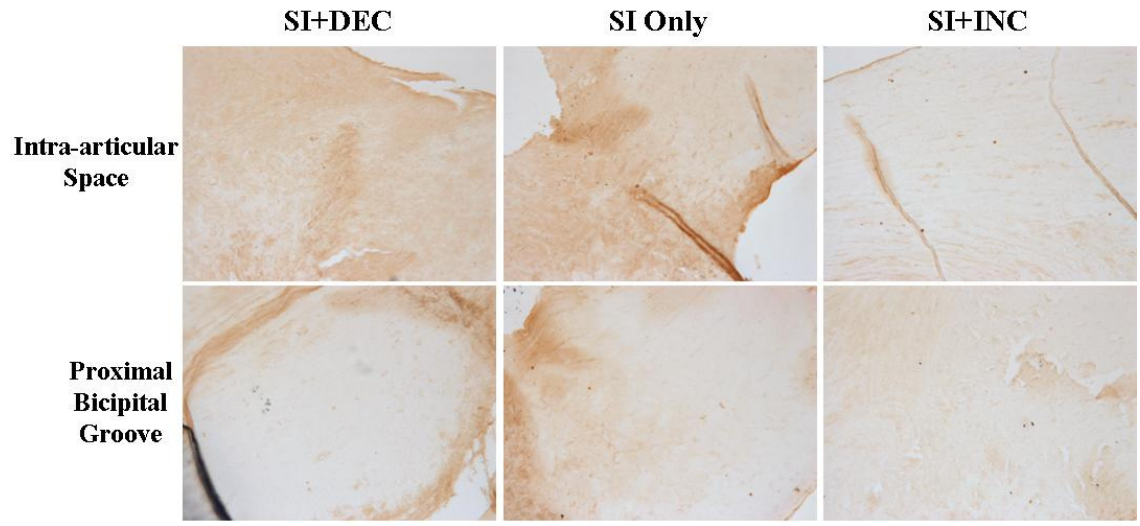

Figure 5.8: Aggrecan expression increased with SI+DEC and SI only compared to SI+INC in the intra-articular space and proximal bicipital groove 1 week following detachments.

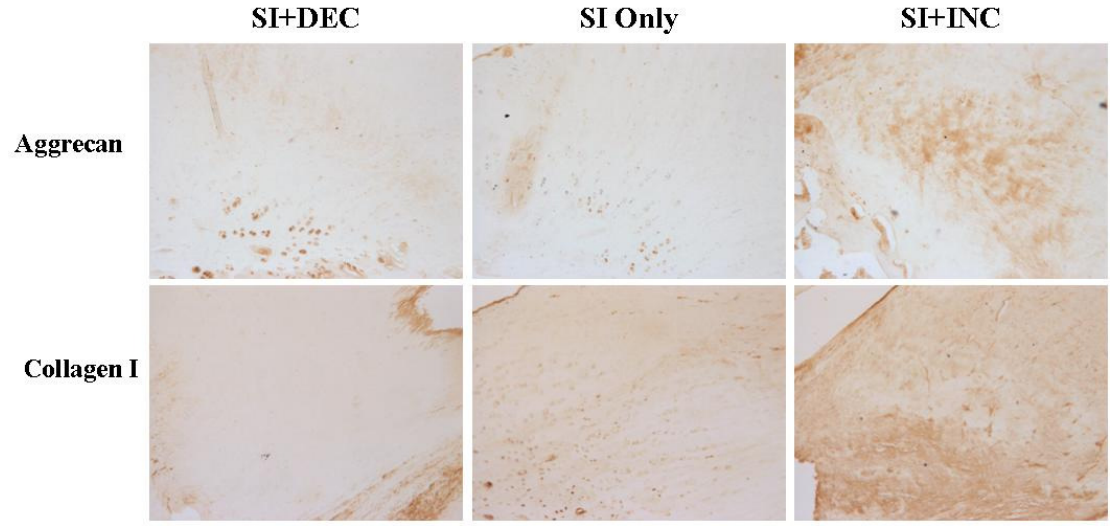

Figure 5.9: At the insertion site 4 weeks following detachments aggrecan expression increased with increased loading compared to SI only and collagen I increased with SI+INC compared to SI only and SI+DEC.

proximal and distal bicipital groove with SI+DEC compared to SI+INC. After 4 weeks, aggrecan and collagen I expression increased at the insertion site with SI+INC compared to SI only and SI+DEC (Figure 5.9). Finally, 8 weeks following detachments collagen I increased with SI only and SI+INC compared to SI+DEC in the distal bicipital groove. Aggrecan decreased in the intra-articular space with SI+DEC compared to SI+INC

(Figure 5.10). Biglycan decreased in the SI+DEC group compared to both SI only and SI+INC in the intra-articular space and distal bicipital groove (Figure 5.11).

D. Discussion

Results did not support our first hypothesis that changes with altered loading would begin at the insertion site and progress along the tendon length at later time points. After 1 week of altered loading, changes were seen in composition only and the changes found were seen at multiple locations along the tendon. However, after 4 weeks of increased loading, organizational changes were seen only in the intra-articular space, which then progressed to the proximal bicipital groove by 8 weeks. It is possible that organizational and histological parameters do not change at the insertion site due to its normal state being a disorganized one with a prevalent rounded cell phenotype already adapted to compressive loading. Changes therefore would be seen first next to this region, as was seen at 4 weeks with increased angular deviation in the intra-articular space with increased loading. The increased compressive loading in this region that normally sees primarily tensile loading resulted in collagen organization much more like the insertion site than the distal portion of the tendon. Additional analysis of the collagen organization data showed that with increased loading, organization was not different between the insertion site, intra-articular space and proximal bicipital groove. Organization did not increase in this group until the distal bicipital groove. Conversely, in both the SI only and SI+DEC groups, tendon organization improved significantly between the insertion site and intra-articular space and remained constant between in the intra-articular space and proximal and distal bicipital grooves.

Figure 5.10: Aggrecan was decreased with decreased loading compared to SI+INC in the intra-articular space 8 weeks following detachments.

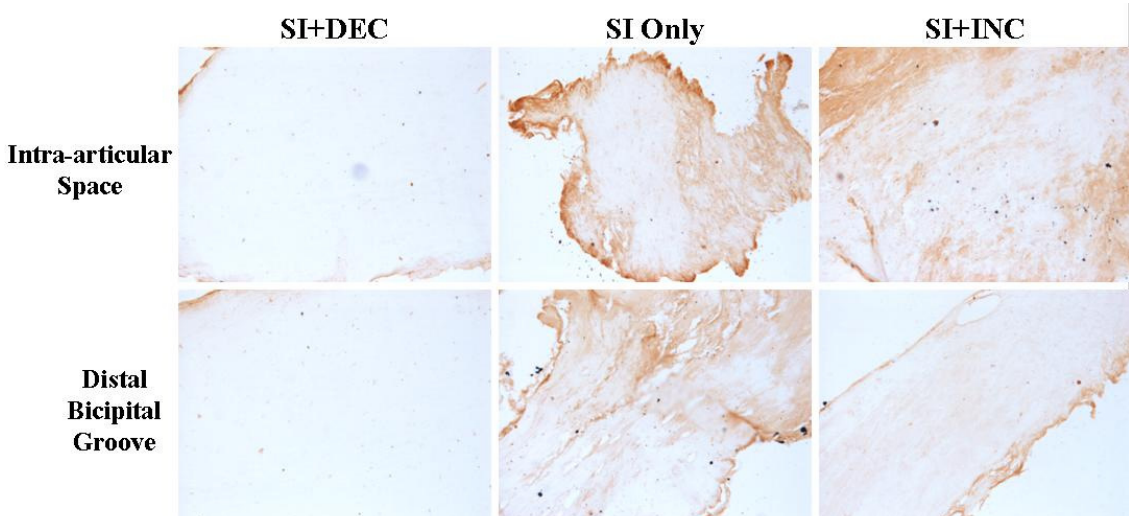

Figure 5.11: Biglycan expression decreased with decreased loading 8 weeks following detachments compared to both SI only and SI+INC.

Our second hypothesis that increased loading would result in further detrimental changes was supported as increased angular deviation was seen compared to detachment alone at both 4 and 8 weeks. However, there were no further detrimental changes seen at any time point in cellularity and cell shape. This may be due to the fact that both detachment alone and detachment followed by increased loading have altered pathology, and therefore, it was difficult to detect a difference in a parameter such as histological grading, in which the range is limited to between 0 and 3. For instance, both groups were a grade 2 or 3 in both parameters at all locations, and therefore statistical differences were

not seen between the two as were seen in a parameter such as angular deviation, in which the range and upper bound of the measurement is not limited. After 4 weeks, increased loading did result in increased aggrecan and collagen I production at the insertion site compared to detachment alone, but by 8 weeks there were no compositional differences between these groups.

Results also support our third hypothesis that decreased loading would result in improved tendon properties. After 1 week, changes with decreased loading were seen only in composition where increased production of several ECM components such as collagens I, III and XII were seen. However, 8 weeks following detachments, increased organization was found compared to both SI only and SI+INC in the intra-articular space and proximal and distal bicipital grooves. Decreased loading also resulted in decreased cellularity in the intra-articular space and proximal bicipital groove as well as a more elongated cell phenotype along the entire tendon away from the insertion site. Decreases in expression of aggrecan and biglycan were also seen at this time point. Aggrecan is an ECM component usually seen in cartilage or regions of compressive loading and biglycan is a proteoglycan indicative of an injury response. The decreased expression of these components with decreased loading in combination with the increased organization and more elongated cell shape indicates that with decreased loading, the tendon is able to remodel its structure to more closely resemble its normal structure and composition.

It is also interesting to note that changes were not seen in histological grading or organization with altered loading 1 week following detachments. Additionally, compositional changes seen at this time point were not consistent in location and often detrimental changes were seen with decreased loading, which is not supported at later

time points. Tendons in all groups were in the presence of rotator cuff tears, and these results indicate that after a short period of time, altered loading does not seem to have an effect. After 4 weeks, decreased loading did not yet show an improvement compared to detachment alone but did not exhibit detrimental compositional changes as seen after 1 week. These results were not surprising, as both improved and detrimental changes in mechanical parameters were seen with decreased loading at this time point in Chapter 4. It was not until 8 weeks following detachments that improved tendon properties were seen with decreased loading. However, improvements in tendon mechanics were not seen at this time point. It is possible that the improvements found in the current study may lead to improved tendon mechanics at later time points, as was seen in other studies investigating the effect of decreased loading by immobilization.[5,14]

In Chapter 3, organizational changes in the biceps tendon with a supraspinatus+infraspinatus detachment were seen first in the intra-articular space when compared to a sham surgery. In this study, organizational changes with increased loading were also seen first in the intra-articular space, further indicating that this may be the site where pathological changes originate. Results of this study also support the theory of increased loading as the mechanism responsible for biceps tendon pathology in the presence of rotator cuff tears. Additionally, further changes were seen in organization with increased loading at the same location changes were first seen with detachment alone. Decreasing the load on the tendon resulted in dramatically improved tendon organization and cell morphology, indicating that with removal of load, the tendon is able to remodel. The results regarding decreased loading indicate that with rotator cuff repair, biceps tendon pathology may be recoverable.

Several studies have examined the response of tendons to increased compressive loading. Specifically, a comprehensive review by Vogel and Koob details the ability of tendons to modify their structure in response to mechanical demands that differ from the tension usually experienced by tendon.[15] Tensional regions of tendon consist of collagen fibers aligned in the direction of tensile forces while collagen fibers in regions that experience compressive loading are arranged in a less-aligned matrix with a higher proteoglycan content.[15] Cells in this compressive region are often rounded in shape, which was seen in this study with detachment and increased loading, while cells in the decreased group were elongated as is found most commonly in regions experiencing tensional loading only. For example, the FDP tendon in rabbits wraps around bone in several areas, and studies were done in which the tendon was translocated so that the portion of the tendon that normally experiences compressive forces would no longer experience them.[15] This study found that the histological appearance of this region of the tendon subsequently adapted to a linear alignment of collagen fibers found in tendons normally subjected to tension, as was found with decreased loading in this study. Additionally, the translocation of the FDP tendon resulted in a compressive loading in a portion of the tendon that normally experienced tensile loading and this portion of the tendon began to exhibit rounded cells and a more-cartilage like matrix, as was seen with detachment and increased loading in the present study. It has also been shown that other tendons that wrap around bone have an increased presence of fibrocartilage in those regions adjacent to bone compared to regions where compressive loading is not experienced by the tendon. Further, it is speculated that this change in composition is an

adaptation that allows the tendon to resist compression and would result in decreased tensile mechanics.[1]

Additionally, the scope of histological analyses used in this study was extensive, including histological grading, immunohistochemical staining, and quantification of collagen organization. Blinded histological grading was done semi-quantitatively and those grades were subsequently analyzed using non-parametric statistics. Immunohistochemical staining images were also analyzed with non-parametric statistics after being assigned grades based on the pixel intensity of the stain. Changes in this study were often seen in more than one of these assays, giving further confidence in the conclusions drawn here that improvements in tendon properties were seen following decreased loading after rotator cuff repair.

Furthermore, there are clearly a variety of biological changes occurring in this model that could be investigated in the future. While we controlled for inflammation due to detachment as all groups had detached tendons, it is possible that inflammatory cells may participate at later time points due to continued increased loading and these cells may contribute to the decreased organization and mechanics. We also found decreased cellularity and more elongated cells with decreased loading, and it is possible that this decreased cellularity and alteration in cell phenotype are related to decreased inflammation. Although this study was designed to investigate the effects of alterations in loading, it is clear that biological processes are also affected and future studies could continue to examine the resulting biological changes. Specifically, these studies could determine the types of cells that are present before and after cellularity is decreased as well as investigate the presence of inflammatory factors such as FLAP and COX-2.

This study is not without limitation. Quantification of the amount of load added to or taken away from the biceps tendon in our increased and decreased loading scenarios was not possible. However, preliminary studies were conducted to confirm that the methods used to induce altered loading did indeed increase and decrease the load on the tendon. It is also possible that additional biological changes may be taking place that were not detected with the immunohistochemical staining performed in this study. A group of targets were selected that, according to previous studies, would be expected to show differences across both time and the length of the tendon and have been extensively used for rotator cuff tendons in the rat model. Future work with this model may include additional biological assays such as PCR or staining for targets involved in collagen turnover. We also did not evaluate the tendons for mineralization or calcium deposits, which are possible long-term effects of tendon pathologies. Specifically, calcifying tendinitis is often found in the rotator cuff and can lead to tendon tears. These deposits are thought to be secondary to impingement under the acromion.[3] In this chapter and in Chapter 3, we found that changes began in the intra-articular portion of the tendon first; suggesting that compression in this region (either by impingement under the acromion, compression against the humeral head, or both) plays a role in the development of biceps tendon pathology in the presence of rotator cuff tears. With the further detrimental changes seen in the biceps tendon with increased loading following rotator cuff tears in this model, it is possible that tendons in that group may develop calcifications and this could be examined in future studies.

In summary, as seen in studies examining the effect of rotator cuff detachment alone on the biceps tendon, organizational changes began at the intra-articular space

while compositional changes were not consistent in location. In both studies, changes were seen in the intra-articular portion of the tendon before progressing to the extra-articular portion of the tendon at later time points. Additionally, increased loading resulted in further detrimental changes in organization and composition compared to detachment alone. Combined with the findings in Chapter 4 of decreased mechanics with increased loading, these results indicate increased compressive loading away from the insertion site as a mechanism for biceps tendon pathology in the presence of rotator cuff tears. Finally, decreased loading resulted in striking improvements in tendon organization, cellularity and cell shape by 8 weeks, further supporting increased loading as a mechanism for biceps tendon pathology as removal of this load led to a more normal tendon appearance.

E. References

1. **Benjamin, M.; Qin, S.; and Ralphs, J. R.:** Fibrocartilage associated with human tendons and their pulleys. *J Anat,* 187 (Pt 3): 625-33, 1995.
2. **Chen, C. H.; Hsu, K. Y.; Chen, W. J.; and Shih, C. H.:** Incidence and severity of biceps long head tendon lesion in patients with complete rotator cuff tears. *J Trauma,* 58(6): 1189-93, 2005.
3. **Depalma, M. J., and Johnson, E. W.:** Detecting and treating shoulder impingement syndrome: the role of scapulothoracic dyskinesis. *Phys Sportsmed,* 31(7): 25-32, 2003.
4. **Gimbel, J. A.; Van Kleunen, J. P.; Mehta, S.; Perry, S. M.; Williams, G. R.; and Soslowsky, L. J.:** Supraspinatus tendon organizational and mechanical

properties in a chronic rotator cuff tear animal model. *J Biomech,* 37(5): 739-49, 2004.

5. **Gimbel, J. A.; Van Kleunen, J. P.; Williams, G. R.; Thomopoulos, S.; and Soslowsky, L. J.:** Long durations of immobilization in the rat result in enhanced mechanical properties of the healing supraspinatus tendon insertion site. *J Biomech Eng,* 129(3): 400-4, 2007.

6. **Itoi, E.; Hsu, H. C.; Carmichael, S. W.; Morrey, B. F.; and An, K. N.:** Morphology of the torn rotator cuff. *J Anat,* 186 (Pt 2): 429-34, 1995.

7. **Kido, T.; Itoi, E.; Konno, N.; Sano, A.; Urayama, M.; and Sato, K.:** The depressor function of biceps on the head of the humerus in shoulders with tears of the rotator cuff. *J Bone Joint Surg Br,* 82(3): 416-9, 2000.

8. **Kolts, I.; Tillmann, B.; and Lullmann-Rauch, R.:** The structure and vascularization of the biceps brachii long head tendon. *Ann Anat,* 176(1): 75-80, 1994.

9. **Murthi, A. M.; Vosburgh, C. L.; and Neviaser, T. J.:** The incidence of pathologic changes of the long head of the biceps tendon. *J Shoulder Elbow Surg,* 9(5): 382-5, 2000.

10. **Neer, C. S., 2nd:** Anterior acromioplasty for the chronic impingement syndrome in the shoulder: a preliminary report. *J Bone Joint Surg Am,* 54(1): 41-50, 1972.

11. **Peltz, C. D.; Dourte, L. M.; Kuntz, A. F.; Sarver, J. J.; Kim, S. Y.; Williams, G. R.; and Soslowsky, L. J.:** The effect of postoperative passive motion on rotator cuff healing in a rat model. *J Bone Joint Surg Am,* 91(10): 2421-9, 2009.

12. **Peltz, C. D.; Sarver, J. J.; Dourte, L. M.; Wurgler-Hauri, C. C.; Williams, G. R.; and Soslowsky, L. J.:** Exercise following a short immobilization period is detrimental to tendon properties and joint mechanics in a rat rotator cuff injury model. *J Orthop Res*.

13. **Perry, S. M.; Getz, C. L.; and Soslowsky, L. J.:** After rotator cuff tears, the remaining (intact) tendons are mechanically altered. *J Shoulder Elbow Surg,* 18(1): 52-7, 2009.

14. **Thomopoulos, S.; Williams, G. R.; and Soslowsky, L. J.:** Tendon to bone healing: differences in biomechanical, structural, and compositional properties due to a range of activity levels. *J Biomech Eng,* 125(1): 106-13, 2003.

15. **Vogel, K. G., and Koob, T. J.:** Structural specialization in tendons under compression. *Int Rev Cytol,* 115: 267-93, 1989.

16. **Wurgler-Hauri, C. C.; Dourte, L. M.; Baradet, T. C.; Williams, G. R.; and Soslowsky, L. J.:** Temporal expression of 8 growth factors in tendon-to-bone healing in a rat supraspinatus model. *J Shoulder Elbow Surg,* 16(5 Suppl): S198-203, 2007.

17. **Yamaguchi, K.; Riew, K. D.; Galatz, L. M.; Syme, J. A.; and Neviaser, R. J.:** Biceps activity during shoulder motion: an electromyographic analysis. *Clin Orthop Relat Res,* (336): 122-9, 1997.

18. **Yokota, A.; Gimbel, J. A.; Williams, G. R.; and Soslowsky, L. J.:** Supraspinatus tendon composition remains altered long after tendon detachment. *J Shoulder Elbow Surg,* 14(1 Suppl S): 72S-78S, 2005.

19. **Zar, J. H.:** Biostatistical Analysis. Edited, Princeton, Prentice Hall, 1984.

20. **Zgonis, M.; Wurgler-Hauri, C. C.; Perry, S. M.; and Soslowsky, L. J.:** The effect of rest after overuse on extracellular matrix proteins in rat supraspinatus tendon: An immunohistochemical analysis. In *Transactions of the Orthopaedic Research Society*, pp. 854. Edited, 854, San Diego, 2007.

Chapter 6: Pathological changes in the long head of the biceps tendon over time in the presence of a rotator cuff tear in a rat model

A. Introduction

This chapter will investigate the changes over time in histological, organizational, compositional and mechanical properties of the long head of the biceps tendon following rotator cuff tears in a rat model.

Pathological changes in the long head of the biceps tendon are common clinical issues that are often seen in conjunction with rotator cuff tears.[2,7,9] These changes include a flattened, widened and/or frayed biceps tendon when visualized at the time of rotator cuff repair surgery.[6] However, there is some debate over the role the biceps tendon plays at the shoulder following a rotator cuff tear. Some believe the biceps tendon plays no role at all[14] while others believe it plays a significant role as a humeral head depressor when the more significant humeral head depressors (supraspinatus and/or infraspinatus) are missing.[8]

Therefore, controversy exists regarding its optimal treatment. The biceps tendon is thought to be a significant source of pain and in some cases is treated with tenotomy (detachment) or tenodesis (detachment from the scapula and reattachment elsewhere) even when the cuff tear is too massive to be repaired. If the biceps tendon does play an important functional role at the shoulder, retaining this tendon may be important. It is also unknown if the pathological changes due to an existing rotator cuff tear are recoverable with repair of the rotator cuff.

In Chapter 2, the effect of rotator cuff tears on the mechanical properties

biceps tendon 4 and 8 weeks post detachment was investigated in a rat model.[10] It was determined that mechanical properties did worsen in this time period; however, the effect of a longer time point was not examined and it is not known if the changes in the biceps tendon in this model are truly chronic. It is possible that after long periods of time, biceps tendons in the presence of rotator cuff tears in this model may continue to worsen in properties or perhaps even rupture. An animal model of this condition would allow for evaluation of multiple treatment strategies for biceps tendon pathology. Therefore, the objective of this study was to determine the histological, organizational, compositional and mechanical changes in the long head of the biceps tendon in the presences of a multiple rotator cuff tendon tear over time. Our hypothesis was that histological, compositional, organizational and mechanical properties would worsen with time.

B. Methods

Forty-eight Sprague-Dawley rats were used in this IACUC approved study. In all animals, a unilateral surgery was performed on the animal's left shoulder.[11] The surgical procedure is the same as in previous chapters but will be repeated here for completeness. Briefly, with the arm in external rotation, a 2 cm skin incision was made followed by blunt dissection down to the rotator cuff musculature. The rotator cuff was exposed and the tendons were visualized at their insertion on the humerus. The supraspinatus tendon was then separated from the other rotator cuff tendons before sharp detachment at its insertion on the greater tuberosity using a scalpel blade. The infraspinatus tendon was then detached in the same manner. Any remaining fibrocartilage at the insertion was left

intact and detached tendons were allowed to freely retract without attempt at repair creating a gap ~4 mm from their insertion sites. The overlying muscle and skin were closed and the animals were allowed unrestricted cage activity. Animals were sacrificed at 1, 4, 8 and 16 weeks post-surgery for histological analysis (n=4 or 5 per group and time point) and at 4, 8 and 16 weeks post-surgery for mechanical testing (n=10 per group and time point). Animals for histological analysis at 1, 4 and 8 weeks were previously reported in Chapter 3 and animals for mechanical testing at 4 and 8 weeks were previously reported in Chapter 2. Animals at the 16 week time point are discussed only in this chapter. Our initial hypotheses did not include changes over time, and therefore in previous chapters, comparisons were made only between groups at each time point. The addition of a later time point of 16 weeks was made specifically to address the question of if pathological changes worsen over time and therefore all previous time points are included here.

The mechanical testing procedure is the same as in Chapters 2, 3 and 4 but will be repeated here for completeness. For mechanical testing, the scapula, long-head of the biceps tendon and associated muscle were dissected out. The associated muscle was removed and the tendons were fine dissected under a microscope. Five Verhoeff stain lines were then placed along the length of each tendon denoting the insertion site (0-1.5mm), the portion of the tendon in the intra-articular space (1.5-3.5mm), and the portion in the bicipital groove (3.5-8.5mm). A fifth stain line was placed at 11.5mm to identify grip placement and these stain lines were used to determine the distribution of strain along the length of the tendon. These positions were determined using histology to identify the length of the insertion site and gross dissections to determine the portion in

the bicipital groove.[10] Tendon geometry was measured in each tendon portion using a laser based system.[4]

The scapula was then embedded in a holding fixture using polymethylmethacrylate (PMMA) and inserted into a specially designed fixture. The proximal end of the tendon was then held at the fifth stain line (11.5mm) in a screw clamp lined with fine grit sandpaper. The specimen was then immersed in a 39°C PBS bath, preloaded to 0.1N, preconditioned for 10 cycles from 0.1N to 0.5N at a rate of 1%/sec, and held for 300sec. Immediately following, a stress relaxation experiment was performed by elongating the specimen to a strain of 4% at a rate of 5%/sec (0.575 mm/sec) followed by a 600sec relaxation period. Specimens were then returned to the initial preload displacement and held for 60 seconds and ramp to failure was then applied at a rate of 0.3%/sec. Using the applied stain lines, local tissue strain in each tendon portion was measured optically with a custom program (MATLAB). Elastic properties, such as stiffness and modulus were calculated using linear regression from the visually determined linear region of the load-displacement and stress-strain curves, respectively. Peak and equilibrium load were determined from the stress relaxation test and percent relaxation was then calculated from these values.

Animals were sacrificed for histological analyses 1, 4, 8 and 16 weeks following surgery. All histological analyses (grading, polarized light, immunohistochemistry) are the same as discussed in Chapters 3 and 5, but are included here for completeness. Cross-sectional area was also measured along the length of the tendon in the 1 week specimens. Each tendon was analyzed in 4 locations: the insertion site (0-1.5mm), the intra-articular space (1.5-3.5mm), the proximal bicipital groove (3.5-6mm) and the distal

bicipital groove (6-8.5mm). Sagittal sections (7μm) were collected serially and stained with hematoxylin and eosin. Quantitative polarized light microscopy was used to determine collagen fiber orientations on these H&E stained sections.[5] Briefly, a rotatable λ compensator was used and a set of grayscale images (100x mag.) were taken at each tendon location at 10º increments as the crossed analyzer and polarizer were simultaneously rotated through 90º. Next, a set of color images was taken at 10º increments as the compensator and crossed analyzer and polarizer were rotated through 90º. A custom MATLAB program was then used to analyze approximately 120 points for each set of pictures to determine the collagen organization. The grayscale images were used to calculate the extinction angle and the color images to determine the orientation of the collagen. The angular deviation (AD) of the collagen orientation, a measure of the fiber distribution spread, in each tendon location for each specimen was then calculated as used previously.[16]

H&E stained sections were also analyzed for changes in cell shape and cellularity. Histological grading standards for cellularity and cell shape were produced by first organizing images for each tendon location from either least to most cellular or most elongated to more rounded cell shape. These images were then divided into four quadrants and the middle image from each quadrant was chosen as the representative image for that quadrant and assigned a grade of 0, 1, 2 or 3. Images were then assigned grades by 3 blinded graders who compared each image to these standards for each location. The median grade between the 3 blinded graders for each image was then assigned to that image.

Finally, the distribution of various extra-cellular matrix proteins was localized in the biceps tendon using immunohistochemistry. The same specimens were used as for histological and polarized light analyses and one section from each specimen was stained for collagens type I, II, III and XII as well as proteoglycans aggrecan, biglycan and decorin (Table 6.1). Briefly, standard 7μm sections were first dewaxed and rehydrated followed by blocking and antibody reactions.[15] Sections for aggrecan were pretreated with 10-mmol/L dithiothreitol-50mmol/L tris-hydrocholic acid and 200 mmol/L sodium chloride for 2 hours at 37ºC and then alkylated with 40 mmol/L iodoacetamide-1 mol/L PBS for 1 hour at 37ºC. Sections for collagen type III were pretreated for 4 minutes with Protease K at room temperature. For all antibodies, various enzyme incubations were carried out at 37ºC (Table 6.1). Endogenous peroxidase activity was blocked in all sections by treatment with 3% hydrogen peroxide in methanol for 10 minutes, and non-specific binding of the secondary antibody was blocked with both 5% skim milk-PBS for 30 minutes and appropriate serum for 20 minutes. Tissue sections were then incubated with primary antibodies for up to 38 hours (Table 6.1) at 4ºC. Negative control sections were incubated with nonimmune horse serum diluted to the same protein content. The sections were then exposed to biotin-conjugated secondary antibodies (1:100 rat anti-mouse monoclonal antibody or 1:200 goat anti-rabbit polyclonal antibody) for 30 minutes, and then avidin-biotinylated peroxidase complex reagent was applied for 30 minutes at room temperature. Finally, sections were incubated with 3,3'-diaminobenzidine for 4 minutes.

Figure 6.1: Primary antibodies used for immunohistochemical staining

Protein Target	Antibody	Host	Type	Enzyme pretreatment	Dilution	Incubation Period (h)	Source
Collagen I	AB755P	Rabbit	Polyclonal	Hyaluronidase	1:200	16	Chemicon (Temecula, CA)
Collagen II	II-116B3	Mouse	Monoclonal	Hyaluronidase	1:4	16	DSHB (Iowa City, IA)
Collagen III	c7805	Mouse	Monoclonal	Hyaluronidase	1:50	38	Sigma (St. Louis, MO)
Collagen XII	LB-1200	Rabbit	Polyclonal	Hyaluronidase	1:100	16	Cosmo-bio (Tokyo, Japan)
Aggrecan	LF-113	Rabbit	Polyclonal	Chondroitinase ABC	1:200	16	L. Fisher (Bethesda, MD)
Biglycan	LF-159	Rabbit	Polyclonal	Chondroitinase ABC	1:200	38	L. Fisher
Decorin	JSCATE	Rabbit	Polyclonal	Chondroitinase AC	1:300	38	J. Sandy (Chicago, IL)

The same 4 regions were analyzed for immunohistochemical staining as for polarized light analysis and histological grading. Images were taken at 100x and evaluated semi-quantitatively using a custom DAB intensity measurement program (MATLAB).[13,17] Briefly, quartiles were produced for each tendon location using the total target DAB intensity ranges for each protein target, which were determined as the difference between the most and least stained specimens in each group. Each quartile was assigned a value of undetectable (0), low (1), moderate (2) or high (3) and each image was assigned one of these grades.

Mechanical testing parameters and angular deviation were compared across time points using a one-way ANOVA with Bonferroni post-hoc correction. This data is presented as average +/- standard deviation. For histological and immunohistochemical analyses, median grades were compared for each tendon location across time points using a non-parametric Kruskal-Wallis test followed by Mann-Whitney post-hoc tests and this data is presented as median and interquartile ranges. Properties were compared between adjacent time points, with 2 comparisons for mechanical testing (4 vs. 8 weeks and 8 vs. 16 weeks) and 3 comparisons for area, histological and immunohistochemical analyses (1 vs. 4, 4 vs. 8 and 8 vs. 16 weeks). For biomechanical parameters, significance was set at $p=0.25$ (0.5/2) and trends at $p=0.5$ (0.1/2). For area, histological and

immunohistochemical parameters, significance was set at p=0.17 (0.5/3) and trends at p=0.33 (0.1/3).

C. Results

Area increased in all tendon locations from 1 to 4 weeks and further increased from 4 to 8 weeks after detachments (Figure 6.1). However, between 8 and 16 weeks following detachments, area decreased in all locations (Figure 6.1). Stiffness decreased between 8 and 16 weeks in the insertion site, intra-articular space and bicipital groove (Figure 6.2). There were no changes in modulus (Figure 6.3) or viscoelastic parameters over time.

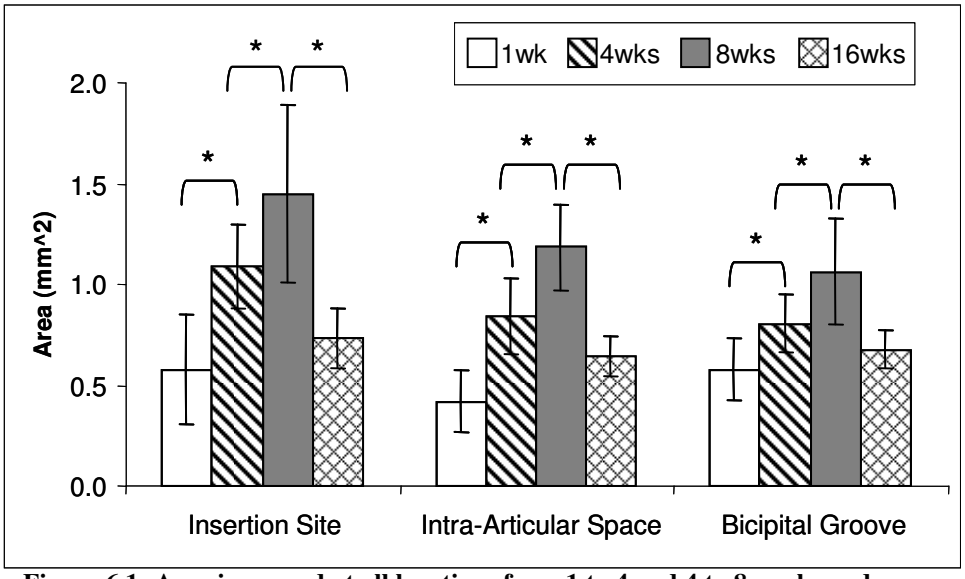

Figure 6.1: Area increased at all locations from 1 to 4 and 4 to 8 weeks and decreased in all locations from 8 to 16 weeks. (*sig between adjacent time points.

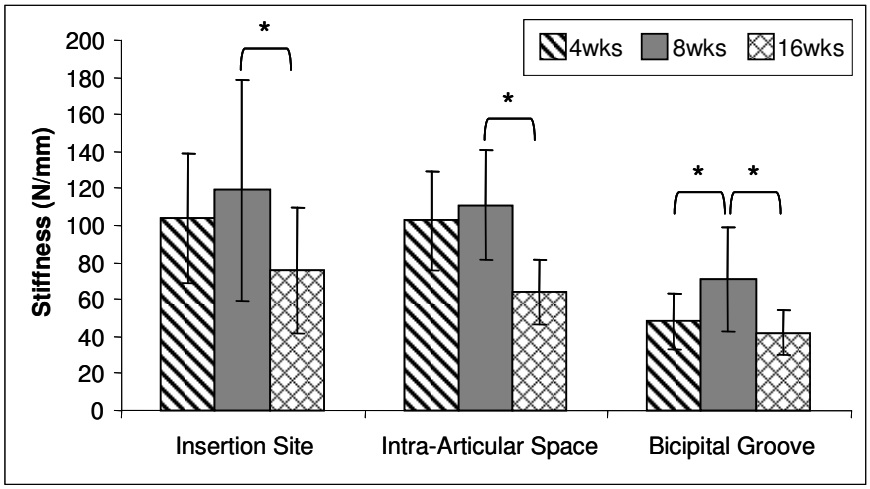

Figure 6.2: Stiffness decreased from 8 to 16 weeks in all locations. (*sig between adjacent time points.

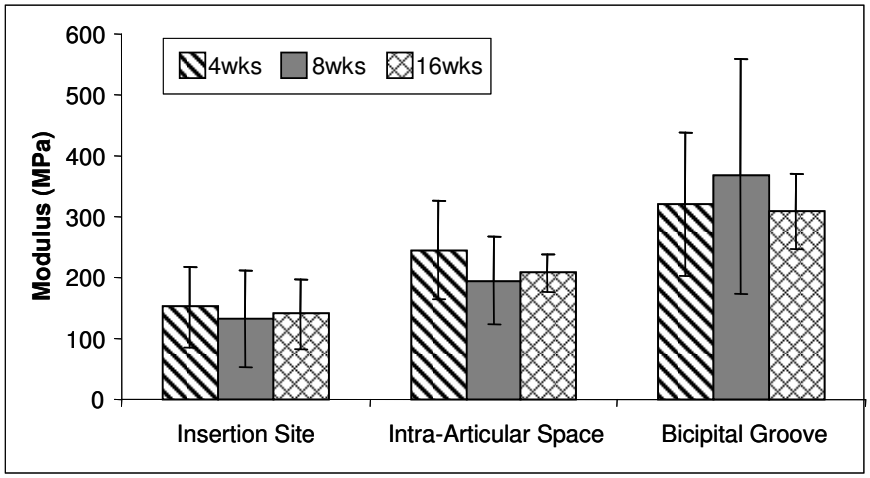

Figure 6.3: Modulus did not change over time in any location.

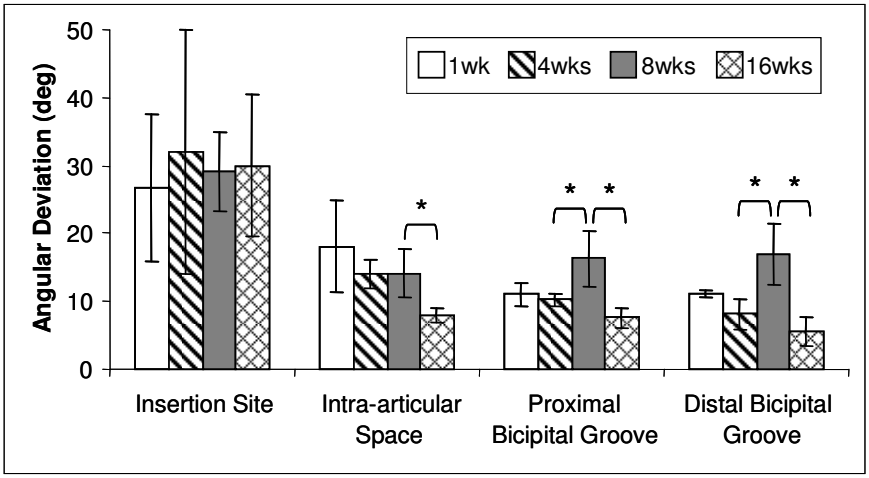

Figure 6.4: Angular deviation increased from 4 to 8 weeks in the proximal and distal bicipital groove and decreased from 8 to 16 weeks at all locations away from the insertion site. (*sig between adjacent time points)

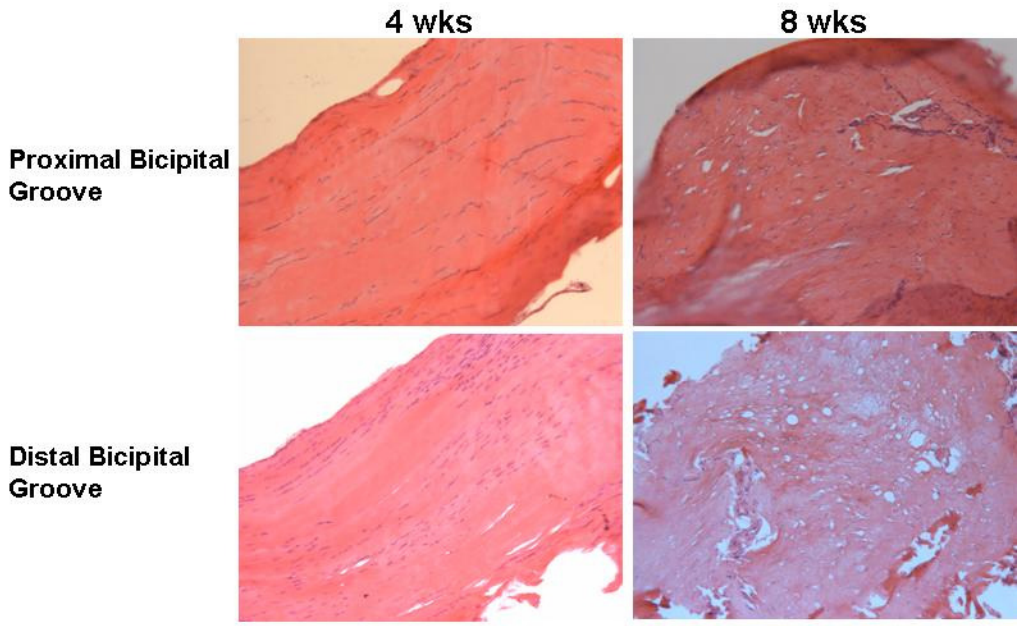

Figure 6.5: The biceps tendon in the proximal and distal bicipital groove became more disorganized from 4 to 8 weeks.

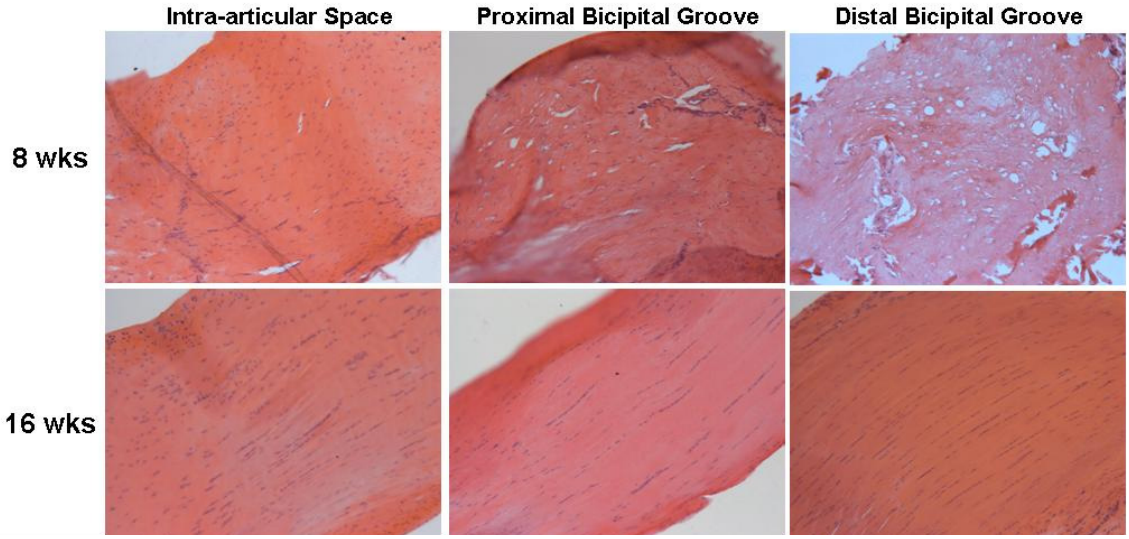

Figure 6.6: The biceps tendon became more organized from 8 to 16 weeks in the intra-articular space and proximal and distal bicipital groove. Also note the more elongated cell shape in these locations at 16 weeks.

There were no differences in angular deviation between 1 and 4 weeks (Figure 6.4). Angular deviation increased in the proximal and distal bicipital groove between 4 and 8 weeks post detachments (Figures 6.4 and 6.5). Between 8 and 16 weeks,

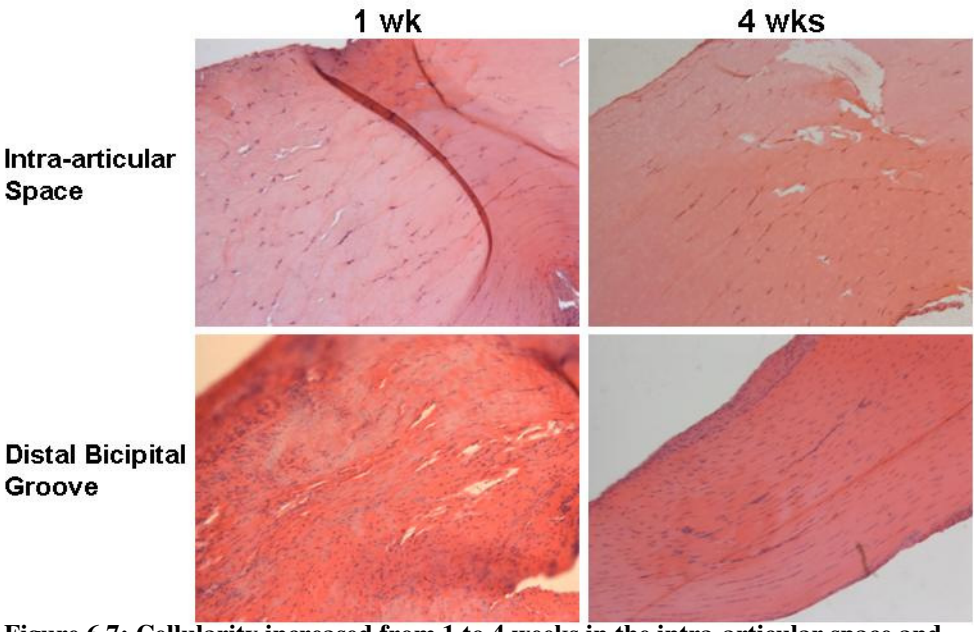

Figure 6.7: Cellularity increased from 1 to 4 weeks in the intra-articular space and distal bicipital groove.

angular deviation decreased in the intra-articular space and proximal and distal bicipital groove (Figure 6.4 and 6.6). There were no changes in angular deviation at the insertion site between any time points.

Between 1 and 4 weeks, cellularity increased in the intra-articular space and distal bicipital groove (Figure 6.7). There were no changes in cell shape at any location between these time points. Between 4 and 8 weeks, cellularity increased in the distal bicipital groove and there were again no differences in cell shape. Between 8 and 16

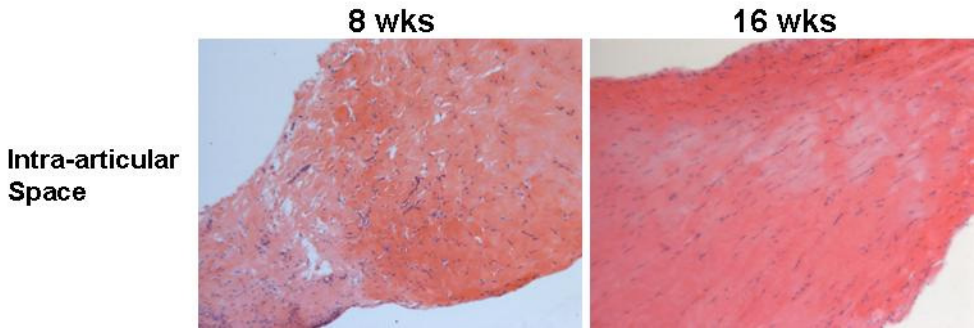

Figure 6.8: Cellularity in the intra-articular space decreased between 8 and 16 weeks.

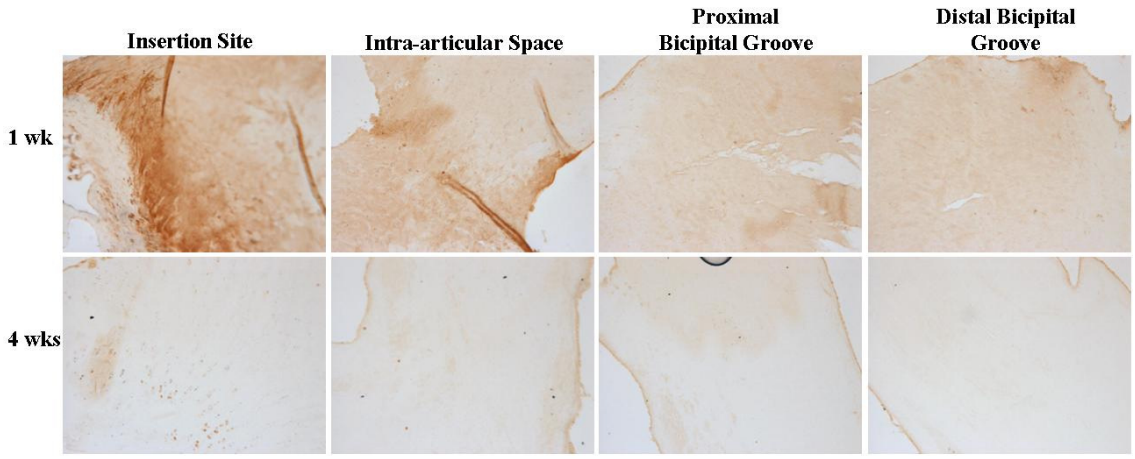

Figure 6.9: Aggrecan expression decreased from 1 to 4 weeks in the insertion site, intra-articular space and distal bicipital groove.

weeks, cellularity decreased in the intra-articular space (Figure 6.8) and cell shape became more elongated in the intra-articular space and proximal and distal bicipital groove (Figure 6.6).

Aggrecan expression decreased at the insertion site, in the intra-articular space and distal bicipital groove from 1 to 4 weeks (Figure 6.9). Also between these time

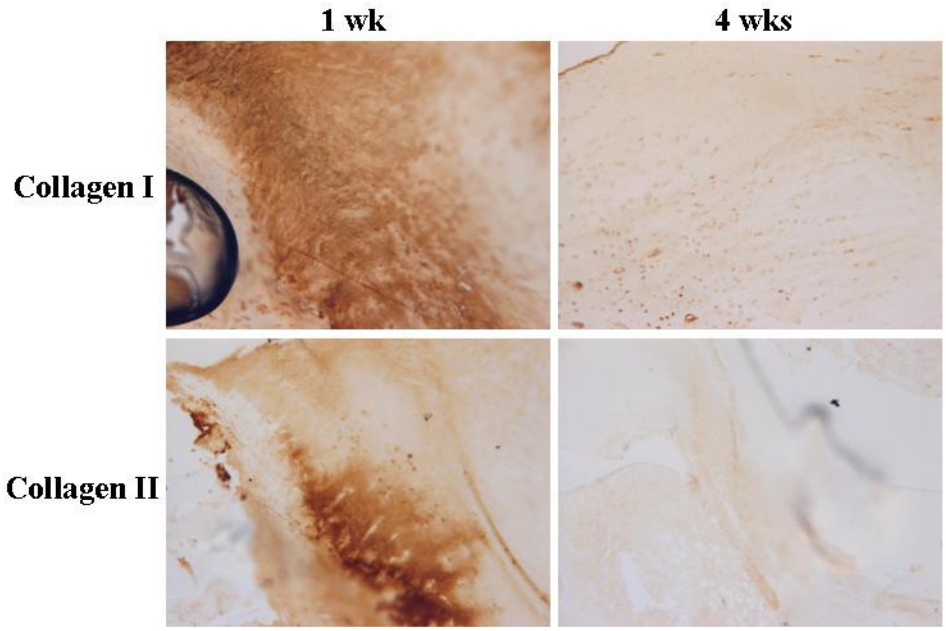

Figure 6.10: Expression of collagens I and II decreased at the insertion site between 1 and 4 weeks post detachment.

points, expression of collagens I and II decreased at the insertion site (Figure 6.10). Additionally, collagen III decreased in the intra-articular space and collagen II decreased in the proximal bicipital groove. Between 4 and 8 weeks, collagen I increased at the insertion site and in the distal bicipital groove (Figure 6.11). Finally, between 8 and 16 weeks, biglycan decreased at the insertion site (Figure 6.12) and collagen I decreased in the distal bicipital groove.

D. Discussion

Results support our hypothesis between several, but not all, of the time points examined in this study. There were changes in composition between 1 and 4 weeks, however decreased cellularity and expression of several ECM proteins was found. Area in all tendon locations also increased between these time points. It is interesting to note that in the compositional changes found between 1 and 4 weeks, the expression of proteins generally decreased between these time points while we expected proteins indicative of injury, such as biglycan and collagen III, to continue to increase over time. It is possible that expression of ECM proteins only needs to be increased initially in order to result in changes in cell shape, organization and mechanics at later time points.

Area continued to increase between 4 and 8 weeks, and collagen I expression also increased during this time period. This could be due to the tendon attempting to compensate for changes in tensile properties by producing more type I collagen, which is the collagen most associated with bearing tensile loads. Increased angular deviation was also found between 4 and 8 weeks in the proximal and distal bicipital groove. This increased angular deviation into the extra-articular portion of the tendon supports the

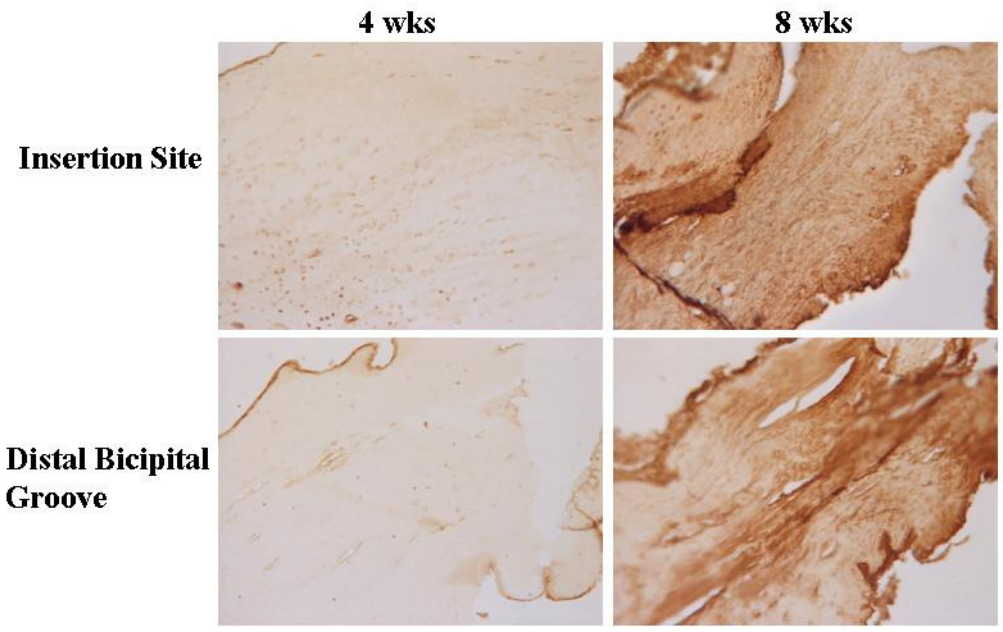

Figure 6.11: Collagen I expression increased from 4 to 8 weeks at the insertion site and in the distal bicipital groove.

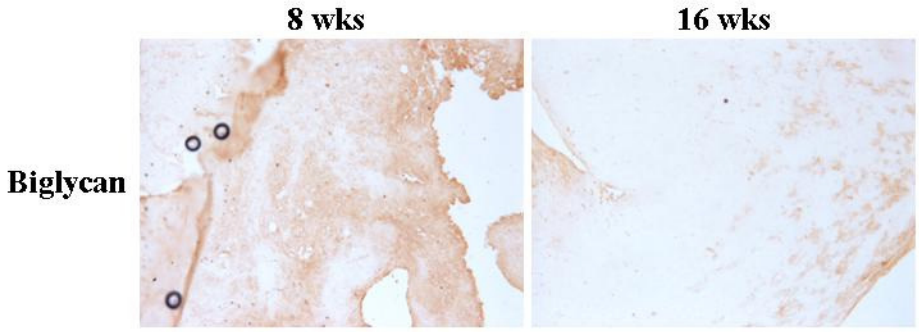

Figure 6.12: Biglycan expression decreased between 8 and 16 weeks at the insertion site.

theory that tendon properties first worsen near the tendon's insertion site and move along the tendon length with time.

Unexpectedly, there were many parameters improved from 8 to 16 weeks. Area decreased in all tendon locations during this time period. Increased organization was also found in the intra-articular space and proximal and distal bicipital groove. This increased organization may be explained by the additional finding of changes in cell shape from a rounded to more elongated phenotype in these same locations during this time period.

Additionally, there was a decrease in biglycan expression, generally thought to be present in injured tissue, at the insertion site between 8 and 16 weeks. Although we did find decreased stiffness at all tendon locations from 8 to 16 weeks, that result can be explained by the fact that area also decreased, and with less tissue present the tendon becomes less stiff.

Another recent study in our laboratory used this model of supraspinatus+infraspinatus detachment to determine the long term effects on the properties of the detached tendons.[3] After 16 weeks of detachment, it was found that while supraspinatus properties were still decreased from normal, infraspinatus properties had recovered to control values.[3] In an earlier study, it was concluded that biceps tendon pathology was worse in the presence of a supraspinatus+infraspinatus tear than in the presence of a supraspinatus tear alone.[10] It is possible that as the infraspinatus properties return toward normal as the infraspinatus tendon begins to bear load. As a result, the increased load on the biceps, thought to be a result of the torn rotator cuff tears, is lessened and approaches loads more normally seen by this tendon. The tendon would

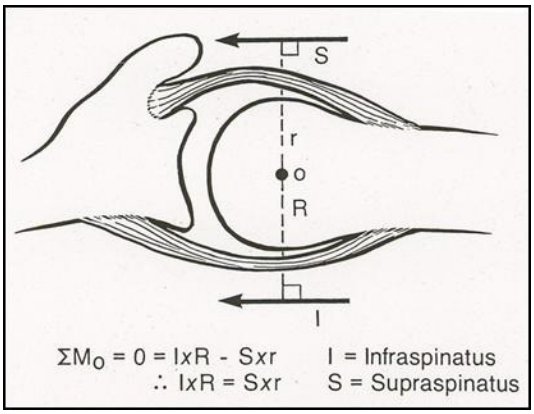

Figure 6.13: Transverse balance of forces between the infraspinatus and subscapularis.[1]

then be able to adapt to these more normal loads, resulting in decreased area and increased organization. This concept is supported by the theory of balanced forces in the transverse rotator cuff (Figure 6.13), in which a tear of the infraspinatus would disrupt the balance of forces[1], leading to drastic changes in load and joint kinematics, while a tear of the supraspinatus tendon alone would not disrupt these balanced forces, leading to minimal load changes on the intact tendons. However, the presence of inflammation was not examined in either study and therefore it is possible that inflammation decreased between 8 and 16 in addition to the return of infraspinatus properties to normal levels, and both biologic and mechanical factors contributed to the improved biceps tendon properties seen here. Cellularity in the intra-articular space was found to decrease from 8 to 16 weeks, though the type of cells present at either time point was not investigated. Future studies could evaluate the cells more carefully to determine if inflammatory cells are present at early time points and are no longer present at 16 weeks.

Clinically, little information is available regarding the time course of biceps tendon pathology in the presence of rotator cuff tears. Some of this is due to the difficulty in determining the time at which the rotator cuff tear initiated and therefore further difficulty establishing a relationship between extent of biceps tendon pathology and time post cuff tear Chen et al reported biceps tendon pathology as a function of time between rotator cuff injury or onset of symptoms and surgery and found that when surgery was delayed more than 3 months, all biceps tendons showed pathological changes.[2] While not directly relating time of injury to amount of pathology present, Murthi did note that abnormal histological findings were directly proportional to the patient's age[9], suggesting that they may worsen with time. However, information on

what type of change (compostional, organizational, etc) occurs first and where that change occurs is unknown. This study attempted to determine the time course of pathologic changes through evaluation of histological, organizational, compositional and mechanical properties. Specifically, organization was determined quantitatively along the entire length of the tendon using a polarized light system. Additionally, histological grading was done by 3 blinded graders and non-parametric statistics were used to determine significance while changes in immunohistochemical staining were determined based on grades assigned using a custom program measuring staining intensity, followed by statistical analysis.

This study is not without limitation. Earlier studies in this model also evaluated the associated functional deficits. However, those studies only evaluated these parameters after 4 and 8 weeks, during which time properties worsened.[12] It is unknown if the restoration in properties measured here is correlated with improvement in functional measures. The rotator cuff tears in this study were made acutely, and do not represent the most common clinical condition of chronic tears which occur slowly over time. However, biceps tendon pathology (the focus of this study) occurred without any direct manipulation to the tendon. Future studies will investigate the effect repairing either the infraspinatus tendon alone or the supraspinatus and infraspinatus tendons 4 weeks following detachment to determine if properties improve similarly to what was found in the current study. Lastly, due to the improvements in tendon properties found after 16 weeks here, this model would not be suitable for studies investigating long-term effects of rotator cuff tears on the biceps tendon. However, this model is appropriate for investigating biomechanical changes at early time points. Additionally, as discussed in

Chapter 3, several changes in the biceps tendon following rotator cuff tear are present as early as 1 week following detachments. Therefore, this model is useful for examining the early biological changes in the biceps tendon.

In summary, it was shown that biceps tendon properties in the presence of a rotator cuff tear worsened from 1 to 4 and 4 to 8 weeks after detachment, but greatly improved from 8 to 16 weeks. With the return of infraspinatus properties to control levels by the same time point, these results indicate that repair of one or more of the rotator cuff tendons may lead to resolved pathology of the long head of the biceps tendon.

E. References

1. **Burkhart, S. S.:** Arthroscopic treatment of massive rotator cuff tears. Clinical results and biomechanical rationale. *Clin Orthop Relat Res,* (267): 45-56, 1991.
2. **Chen, C. H.; Hsu, K. Y.; Chen, W. J.; and Shih, C. H.:** Incidence and severity of biceps long head tendon lesion in patients with complete rotator cuff tears. *J Trauma,* 58(6): 1189-93, 2005.
3. **Dourte, L. M.; Perry, S. M.; Getz, C. L.; and Soslowsky, L. J.:** Tendon Properties Remain Altered in a Chronic Rat Rotator Cuff Model. *Clin Orthop Relat Res*.
4. **Favata, M.:** Scarless healing in the fetus: Implications and strategies for postnatal tendon repair. In *PhD Thesis: Bioengineering*, pp. 216. Edited, 216, Philadelphia, University of Pennsylvania, 2006.
5. **Gimbel, J. A.; Van Kleunen, J. P.; Mehta, S.; Perry, S. M.; Williams, G. R.; and Soslowsky, L. J.:** Supraspinatus tendon organizational and mechanical

properties in a chronic rotator cuff tear animal model. *J Biomech,* 37(5): 739-49, 2004.

6. **Itoi, E.; Hsu, H. C.; Carmichael, S. W.; Morrey, B. F.; and An, K. N.:** Morphology of the torn rotator cuff. *J Anat,* 186 (Pt 2): 429-34, 1995.

7. **Joseph, M.; Maresh, C. M.; McCarthy, M. B.; Kraemer, W. J.; Ledgard, F.; Arciero, C. L.; Anderson, J. M.; Nindl, B. C.; and Mazzocca, A. D.:** Histological and molecular analysis of the biceps tendon long head post-tenotomy. *J Orthop Res*, 2009.

8. **Kido, T.; Itoi, E.; Konno, N.; Sano, A.; Urayama, M.; and Sato, K.:** The depressor function of biceps on the head of the humerus in shoulders with tears of the rotator cuff. *J Bone Joint Surg Br,* 82(3): 416-9, 2000.

9. **Murthi, A. M.; Vosburgh, C. L.; and Neviaser, T. J.:** The incidence of pathologic changes of the long head of the biceps tendon. *J Shoulder Elbow Surg,* 9(5): 382-5, 2000.

10. **Peltz, C. D.; Perry, S. M.; Getz, C. L.; and Soslowsky, L. J.:** Mechanical properties of the long-head of the biceps tendon are altered in the presence of rotator cuff tears in a rat model. *J Orthop Res,* 27(3): 416-20, 2009.

11. **Perry, S. M.; Getz, C. L.; and Soslowsky, L. J.:** After rotator cuff tears, the remaining (intact) tendons are mechanically altered. *J Shoulder Elbow Surg,* 18(1): 52-7, 2009.

12. **Perry, S. M.; Getz, C. L.; and Soslowsky, L. J.:** Alterations in function after rotator cuff tears in an animal model. *J Shoulder Elbow Surg,* 18(2): 296-304, 2009.

13. **Wurgler-Hauri, C. C.; Dourte, L. M.; Baradet, T. C.; Williams, G. R.; and Soslowsky, L. J.:** Temporal expression of 8 growth factors in tendon-to-bone healing in a rat supraspinatus model. *J Shoulder Elbow Surg,* 16(5 Suppl): S198-203, 2007.

14. **Yamaguchi, K.; Riew, K. D.; Galatz, L. M.; Syme, J. A.; and Neviaser, R. J.:** Biceps activity during shoulder motion: an electromyographic analysis. *Clin Orthop Relat Res,* (336): 122-9, 1997.

15. **Yokota, A.; Gimbel, J. A.; Williams, G. R.; and Soslowsky, L. J.:** Supraspinatus tendon composition remains altered long after tendon detachment. *J Shoulder Elbow Surg,* 14(1 Suppl S): 72S-78S, 2005.

16. **Zar, J. H.:** Biostatistical Analysis. Edited, Princeton, Prentice Hall, 1984.

17. **Zgonis, M.; Wurgler-Hauri, C. C.; Perry, S. M.; and Soslowsky, L. J.:** The effect of rest after overuse on extracellular matrix proteins in rat supraspinatus tendon: An immunohistochemical analysis. In *Transactions of the Orthopaedic Research Society*, pp. 854. Edited, 854, San Diego, 2007.

Chapter 7: Conclusions and future directions

A. Introduction

The established animal model of multiple rotator cuff tendon tears was used to develop an animal model of biceps tendon pathology in the presence of rotator cuff tears (Chapter 2). This model was then used to investigate the histological, compositional, organizational and mechanical changes in the biceps tendon in the presence of a supraspinatus+infraspinatus tear compared to a sham surgery (Chapter 3) and over time (Chapter 6). Additionally, this model was used to investigate the effect of altered loading following rotator cuff tears on the long head of the biceps tendon in mechanical (Chapter 4) as well as histological, compositional and organizational properties (Chapter 5). The essential findings and conclusions from these chapters, plus future directions, are included in this chapter.

B. Development of an animal model for biceps tendon pathology in the presence of a rotator cuff tear

Damage to the long head of the biceps tendon is a common clinical finding often found in conjunction with rotator cuff tears.[4,21] However, its etiology is not well understood. Clinical and cadaveric studies are useful in determining if certain pathologies are present, but are unable to rigorously characterize the changes that occur over time along the entire length of the tendon. Therefore, we sought to develop an animal model of this condition which could subsequently be used for studies to investigate the mechanisms responsible.

We utilized the existing rat model of multiple rotator cuff tear combinations[8,24,25] to investigate their effect on the long head of the biceps tendon. Our hypotheses were that an increased number of tendons torn would result in further decreased mechanical properties of the biceps tendon, that a 2 tendon tear involving the infraspinatus would be worse for the biceps tendon than a 2 tendon tear involving the subscapularis and finally that these properties would continue to decrease over time.

Consistent with these hypotheses, we found that 8 weeks following tendon detachments, biceps tendons in the presence of 2 tendon tears had a larger area along the entire length of the tendon than those in the presence of a 1 tendon (supraspinatus) tear. Additionally, biceps tendons in the presences of a supraspinatus+infraspinatus tear had increased area compared to those in the presence of a supraspinatus+subscapularis tear. Maximum stress and modulus were also further decreased with a 2 tendon tear compared to a 1 tendon tear, and also further decreased when involving the infraspinatus as opposed to the subscapularis.

When changes in properties were examined over time, it was found that all tendons in the 2 tendon tear groups had increased area and decreased modulus over time from 4 to 8 weeks post detachments. Additionally, biceps tendons in the presence of a supraspinatus+infraspinatus tear increased in area over time more than those in the presence of a supraspinatus+subscapularis tear.

This study also found that modulus increased along the length of the tendon. The modulus was lowest at the insertion site, increased in the intra-articular space and was highest in the bicipital groove. This could be due to the different functions and loading environments seen in each of these areas. This reiterates the general concept that the

material properties of tendon vary depending on location and that average whole tissue properties may not be an accurate representation of each portion of the tissue.

The results of this study are important because they define the rat rotator cuff injury model as consistent with the biceps tendon pathology seen clinically with rotator cuff tears. The results shown here clearly demonstrate that in this model, biceps tendon pathology in the presence of a rotator cuff tear exists, increases with increasing tear size and continues to worsen over time. The identification of an animal model of biceps tendon pathology with rotator cuff tears allows for controlled studies to investigate the etiology of this problem as well as potential treatment strategies.

C. Changes in mechanical, histological, compositional and organizational properties in the biceps tendon in the presence of a rotator cuff tear compared to sham surgery

Little is also known about the effect of rotator cuff tendon tears on the regional histological properties of the biceps tendon over time.[4,12,21] These questions are difficult to address in clinical studies due to both the inability to harvest the entire biceps tendon during surgery and the complexity of evaluating the effect of time post-repair when the precise history including the exact instance of tear initiation is often unknown. In addition, it would not be possible to obtain many specimens at time points soon after a rotator cuff tear occurs. Previously, we developed an animal model for biceps tendon pathology in the presence of rotator cuff tears (Chapter 2). This study looked at only biomechanical changes and found increased area after 4 weeks and increased area and decreased modulus after 8 weeks compared to uninjured control tendons.[23] Assays

focusing on biological changes at these and earlier time points were not performed and the mechanism responsible for these changes remained unknown. However, when looking at earlier time points, it is possible that there may be effects of the surgical exposure itself.

Therefore, we sought to determine the histological, organizational, compositional and mechanical changes in the biceps tendon following a rotator cuff tear compared to a sham surgery at early, intermediate and late time points. Our hypotheses were that: 1) histological and compositional changes will appear before organizational changes, and both will appear before mechanical changes and 2) changes in all properties will begin at the insertion site and proceed along the length of the tendon at later time points.

Consistent with our hypothesis, organizational changes were seen prior to changes in mechanics although compositional and organization changes were both seen at the earliest time point examined (1 week). However, more disorganized tissue was seen in the intra-articular space at 1 and 4 weeks followed by a decrease in modulus in the intra-articular space 8 weeks following detachment. It is also interesting to note that changes in histological grading support changes seen in organization. After 1 week, a more disorganized tendon was seen in the intra-articular space. Also at this time point, there was a trend toward a more rounded cell phenotype at this location. After 4 weeks, it seems that cell shape changes precede organizational changes as again the tendon was only disorganized in the intra-articular space but a more rounded cell shape was seen along the entire tendon length. Finally, after 8 weeks decreased organization and a more rounded cell phenotype were present along the entire tendon length.

While not all changes occur first at the insertion site, it was consistently shown that changes appear in the intra-articular portion of the tendon before the extra-articular portion. Immunohistochemical results support our hypothesis that changes begin at the insertion site as, other than aggrecan, all changes at 1 week were only at the insertion site. However, histological grading and organizational results indicate changes may begin in the intra-articular space. The lack of changes in organization seen at the insertion site may be due simply to the fact that a disorganized collagen matrix already exists at this location and further disorganization may be difficult to detect.

In summary, it was shown that organizational and compositional changes precede changes in area, which in turn precede changes in mechanical properties. In addition, it was shown that organizational and mechanical property changes begin in the intra-articular space while most immunohistochemical changes began at the insertion site. These results illustrate that changes in the biceps tendon occur gradually over time and represent true degenerative changes and not inflammation alone. This model can now be used to rigorously investigate the mechanism responsible for biceps tendon pathology in the presence of rotator cuff tears.

D. The effect of altered loading following rotator cuff tears on the mechanical, histological, compositional and organizational properties of the long head of the biceps tendon

The proposed role of the biceps tendon as a humeral head depressor is thought to be a significant contributor to changes seen in the biceps tendon with a rotator cuff tear, where one or more of the significant superior stabilizers (supraspinatus and/or

infraspinatus) would not be present.[15] This could lead to an overload situation on the biceps tendon, impingement of the tendon against the acromion, or a combination of the two. The location where pathologic changes begin is also somewhat controversial. Some believe that pathology occurs at the entrance to the bicipital groove, and suspect the tendon first becomes inflamed and then damaged when it is has trouble sliding when hypertrophied. Neer has long believed that the biceps tendon is susceptible to impingement under the acromion after a rotator cuff tear occurs and that changes begin near the tendon's attachment to the glenoid on its bursal side.[22] It is also possible that changes may occur in this location but on the articular side, as increased compressive loading against the humeral head is present.

Therefore, we used the established rat model to investigate the effect of altered loading on the biceps tendon following rotator cuff tears in order to begin to elucidate the mechanism by which these pathologies occur. Our hypotheses were that: 1) changes will begin near the insertion site and progress along the tendon length with time, 2) increased loading will result in further detrimental changes and 3) decreased loading will result in superior properties to those in the presence of a rotator cuff tear alone.

Similarly to our results regarding the effect of rotator cuff tears alone on the tendon, it was unclear as to where changes first began. However, we did find organization first changed with altered loading in the intra-articular space, where it was increased with increased loading after 4 weeks. Contrary to the detachment alone results, compositional changes were not isolated to the insertion site after 1 week. Results were mixed in regards to decreased loading as after 4 weeks improved properties were seen at the insertion site while detrimental changes were found in the intra-articular space.

Consistent with our hypothesis, increased loading resulted in further detrimental changes in mechanical properties than detachment alone along the entire length of the tendon at both 4 and 8 weeks. Further decreases in organization were found in the intra-articular space after 4 weeks and along the entire tendon length after 8 weeks. Also consistent with our hypothesis, decreased loading resulted in increased organization, decreased cellularity, more elongated cell phenotype and decreased expression of aggrecan and collagen III after 8 weeks.

In summary, as seen previously when examining the effect of rotator cuff detachment alone on the biceps tendon, organizational changes began at the intra-articular space while compositional changes were not consistent in location. In both studies, changes were seen in the intra-articular portion of the tendon before progressing to the extra-articular portion of the tendon at later time points. Additionally, increased loading resulted in further detrimental changes in mechanical, organizational and compositional properties compared to detachment alone. These results indicate increased compressive loading away from the insertion site as a mechanism for biceps tendon pathology in the presence of rotator cuff tears. Finally, decreased loading resulted in striking improvements in tendon organization, cellularity and cell shape by 8 weeks, further supporting increased loading as a mechanism for biceps tendon pathology as removal of this load led to a more normal tendon appearance.

E. The effect of rotator cuff tears on biceps tendon pathology over time

We previously investigated the effect of rotator cuff tears on the mechanical properties of biceps tendon 4 and 8 weeks post detachment in a rat model (Chapters 2 and

3). It was determined that mechanical properties did worsen in this time period; however, the effect of a longer time point was not examined and it is not known if the changes in the biceps tendon in this model are truly chronic. It is possible that after long periods of time, biceps tendons in the presence of rotator cuff tears in this model may continue to worsen in properties or perhaps even rupture. An animal model of this condition would allow for evaluation of multiple treatment strategies for biceps tendon pathology. Therefore, we sought to determine the histological, organizational, compositional and mechanical changes in the long head of the biceps tendon in the presences of a multiple rotator cuff tendon tear over time. Our hypothesis was that histological, compositional, organizational and mechanical properties would worsen with time.

Our hypothesis was supported between several, but not all, of the time points examined. There were changes in composition between 1 and 4 weeks, however decreased cellularity and expression of several ECM proteins was found. Area in all tendon locations also increased between these time points. It is interesting to note that in the compositional changes found between 1 and 4 weeks, the expression of proteins generally decreased between these time points while we expected proteins indicative of injury, such as biglycan and collagen III, to continue to increase over time. It is possible that expression of ECM proteins only needs to be increased initially in order to result in changes in cell shape, organization and mechanics at later time points. Area continued to increase along the entire tendon length between 4 and 8 weeks and angular deviation increased in the proximal and distal bicipital groove. This increased angular deviation into the extra-articular portion of the tendon supports the theory that tendon properties first worsen near the tendon's insertion site and move along the tendon length with time.

However, results were not consistent with our hypothesis between 8 and 16 weeks, as many parameters actually improved during this time. Area decreased in all tendon locations and increased organization was also seen in the intra-articular space and proximal and distal bicipital groove. Additionally, cell shape changed from a rounded to more elongated phenotype in these same locations during this time period. There was also a decrease in biglycan expression, generally thought to be present in injured tissue, at the insertion site between 8 and 16 weeks.

In summary, it was shown that biceps tendon properties in the presence of a rotator cuff tear worsened from 1 to 4 and 4 to 8 weeks after detachment, but greatly improved from 8 to 16 weeks. Previously, we found that biceps tendons were worse in the presence of tears involving the infraspinatus in addition to the supraspinatus compared to tears involving the infraspinatus alone. A recent study in our laboratory has further investigated the multiple rotator cuff tendon tear model and found that by 16 weeks, properties of the detached infraspinatus tendon were improved.[8] With the return of infraspinatus properties to control levels by the same time point, these results indicate that repair of one or more of the rotator cuff tendons, and therefore restoration of the rotator cuff balance of forces[1], may lead to resolved pathology of the long head of the biceps tendon.

F. Final conclusions

We developed a model of biceps tendon pathology in the presence of rotator cuff tears in the rat. We then utilized this model to investigate the early, intermediate and late histological, compositional, organizational and mechanical properties along the length of

the tendon in the presence of a supraspinatus and infraspinatus tear compared to a sham surgery. We found that histological, organizational and compositional properties changes prior to mechanical properties and those changes began in the intra-articular portion of the tendon (both insertion site and intra-articular space) before progressing to the extra-articular portion with time. Additionally, we utilized this model to investigate the effect of altered loading following rotator cuff tears on the biceps tendon. We found that increased loading resulted in further detrimental changes in histological, compositional, organizational and mechanical properties along the entire tendon length. Finally, we found that decreased loading after rotator cuff tears resulted in improved histological, compositional and organizational properties along the entire tendon length at the latest time point examined here. Therefore, increased loading plays an important role in the development of biceps tendon pathology following rotator cuff tears. Decreasing this load through immobilization or rotator cuff repair may lead to restoration of normal biceps tendon properties.

The results of this study provide significant information on the effect of rotator cuff tears on the mechanical, histological, organizational and compositional properties of the biceps tendon. Several theories regarding the reason behind and location of these changes exist. One such theory suggests that changes in the biceps tendon are inflammatory in nature alone and that damage to the tendon such as fraying or flattening occurs at the entrance to the bicipital groove when the tendon can no longer easily slide in it. In this study, we found changes in the biceps tendon indicative of structural damage as early as 1 week following rotator cuff tears. Changes were also seen first in the intra-articular portion of the tendon rather than in the bicipital groove, and these changes are

indicative of increased compressive loading. These results indicate that a true degenerative process is occurring in the biceps tendon and pathology is not due to pure inflammation. Rather, pathology is the result of increased loading against the humeral head. We can also conclude that altered loading plays an important role in the initiation of these changes. Increased loading resulted in further detrimental changes, again first in the intra-articular portion, while decreased loading resulted in improved properties. These results indicate that the biceps tendon plays an increased role as a load bearing structure in the presence of rotator cuff tears and that these changes may be recoverable with decreased loading. This information will be helpful to clinicians when deciding the optimal treatment for biceps tendon pathology in the presence of rotator cuff tears.

G. Future directions

There are many possible future areas of study based on the results of this work. These include: 1) further elucidating the role of altered loading as a mechanism of biceps tendon injury in the presence of rotator cuff tears, 2) alternative mechanical testing assays, 3) use this model to investigate the effect of subacromial impingement on the biceps tendon, 4) using this model to investigate the effect of these injuries on pain and function, 5) investigate treatment strategies such as rotator cuff repair, tenotomy or tenodesis, and 6) investigate the increased loading following rotator cuff repair model as a possible model of spontaneous tendon rupture.

a. Further elucidation of altered loading mechanism using biological assays

Although several biological assays were utilized in the current study, much more could be done to further investigate the changes happening in the biceps tendon as a result of rotator cuff tears with and without altered loading. Due to the fact that changes in organization and composition were seen as early as 1 week post detachment in this model, these studies should be focused on this first week and include a variety of assays to characterize the biological environment. These assays could include mircroarray analysis, expression of various cytokines and inflammatory markers, identification of infiltrating cells and determination of collagen turnover, content and fibril diameter.

The use of microarray analysis at early time points would help to identify other pathways involved in the degeneration following altered loading. These studies could also be followed up with PCR assays to quantify expression in tendon segments for each location to determine how the expression is related to the immunohistochemical staining investigated in this study. For example, the ratio of collagen III to collagen I is something that has often been reported in studies of tendinopathy, where an elevated ratio is seen. Additionally, expression of MMPs and TIMPs could be quantified. MMPs are proteins that are active in ECM development, degradation and remodeling while TIMPs are inhibitors of these proteins. In normal tissue, the expression of these 2 families of proteins is balanced and an unbalanced expression profile could lead to increased degradation of the tissue, such as increased MMP expression without the appropriate inhibition or conversely, increased inhibition of MMPs when they would be helpful in a remodeling role.

Although changes in cellularity were found in this study with detachment and altered loading at various time points and locations along the tendon length, the types of

cells present were not evaluated. Specifically, although an increase in cellularity and more rounded cell shape were seen here following cuff tears, the source of these cells was not determined and whether the rounded cell shape was the result of an infiltration of new rounded cells or a change in the phenotype of the elongated cells found in normal tendons is not known. While we controlled for inflammation due to surgery by comparing to a sham, it is possible that inflammatory cells may participate at later time points due to the injury and healing response following rotator cuff tendon detachments or in response to the altered loading environments. The role of pro-inflammatory cytokines and apoptotic genes such as caspases could be evaluated in this model. Interestingly, Millar et al evaluated torn human supraspinatus tendons as well as matched intact subscapularis tendons for such markers and found that while levels were highest in the torn supraspinatus tendons, the genes were also increased in the subscapularis tendons that were not thought to be degenerate based on imaging studies.[19] Therefore, it is possible that intact tendons may be affected by the same inflammatory process as their surrounding torn tendons and this model could be used to look at the time course of such interactions.

Future studies could also determine the types of cells that are present when cellularity is increased. For example, if inflammation is shown to play a role, staining could be done to determine if macrophages are present. Specifically, studies have shown macrophages to be present in the early phases of tendon to bone healing in the rat ACL[14], and it is possible that macrophages are present as a result of rotator cuff tendon detachments and may play a role in biceps tendon degeneration. Additionally, immobilization was shown to result in fewer ED1+ macrophages (thought to play a

phagocytic role following tissue injury) and more ED2+ macrophages (thought to have an anabolic role in tendon healing)[5], and it is possible immobilization may have a similar effect in this model. Studies can also be done to attempt to determine whether the source of increased cellularity is from within the tendon or from surrounding circulating cells. For instance, other studies have investigated this phenomenon in patellar tendon healing using rats that expressed GFP in either only circulating cells or only in the patellar tendon in order to determine the source of reparative cells in that model.[13] A similar study could be done investigating biceps tendon pathology in the presence of rotator cuff tears utilizing rats that express GFP in 3 different locations (in synovial cells, the detached rotator cuff tendons and the biceps tendon) in order to determine the source of the infiltrating cells seen here.

While changes were seen in collagen organization, it is unknown if these changes were a result of new collagen formation or alterations to the existing collagen network. Studies involving markers of collagen turnover would provide insight into whether new collagen is being produced as a result of altered loading or the existing collagen is altered as a result. Assays could also be used to quantify the amount of collagen present at various time points. Other studies have pointed to decreases in overall collagen content and increased water content as the etiology for decreased mechanical properties.[26] Additionally, changes in fibril diameter could be examined with the use of TEM. If new collagen is being produced, inferior tendon properties may be a result of collagen fibrils with smaller diameters than is normal.[29] Additionally, decreased loading may result in the formation of collagen fibrils of a larger diameter that would result in increased mechanics at later time points.

The objective of this study would be to examine early biological changes in the long head of the biceps tendon following rotator cuff tears. This could be achieved by focusing on the first week following detachment and evaluating timepoints as early as 1 and 3 days following rotator cuff detachments. Follow-up biological assay investigations could then be done at later time points, where data already exists regarding detrimental changes in organizational and mechanical properties, to determine the relationship between these changes, biological changes present at these time points, and early biological results. The associated hypotheses would be that at early time points, microarray analysis would show upregulation of genes involved in cartilage synthesis at the insertion site and intra-articular space and tendons would exhibit a non-balanced MMP/TIMP expression profile as well as expression of inflammatory markers, while at later time points, decreased fibril diameter and collagen content as well as an increased type III to type I collagen ratio would be present.

b. Alternative mechanical testing assays

The results of these studies indicate that the biceps tendon may be remodeling due to an increase in compressive loading seen at various locations along the tendon. This theory could be further tested by measuring the compressive properties of the tendon over time. Normally, we would expect that the tendon is very weak in compressive properties away from the insertion site.[29] However, due to the histological results seen here, we would expect that the tendon would become stronger in compression along the length of the tendon with time following rotator cuff detachments. Recently, work has been done in our laboratory to investigate the compressive properties of the mouse patellar tendon and adapting these protocols for testing of the regional compressive properties of the

biceps tendon is certainly feasible. The objective of this study would be to determine the regional compressive properties of the long head of the biceps tendon both before and after rotator cuff tears. The associated hypotheses would be: 1) in normal biceps tendons, the insertion site has increased compressive properties compared to the intra-articular space and bicipital groove, 2) in the presence of a rotator cuff tear, compressive properties increase and 3) compressive properties increase first in the intra-articular space and proceed along the tendon length with time.

In addition, it has been speculated that the biceps tendon changes would occur first on either the articular or bursal side of the tendon. However, some studies have noted that changes occurred throughout the tendon thickness.[17] Previous studies in our laboratory have investigated regional mechanical properties of the human supraspinatus tendon and found striking differences between the articular and bursal side of the tendon.[16] Although testing either side of the tendon separately would be difficult while still attached to the glenoid, it would be possible to section articular and bursal side samples for testing of purely tendon material both in tensile and compressive loading. These tests would give further insight into not only the normal function of the biceps tendon but as to how this function changes with rotator cuff tears and altered loading.

The objective of this study would be to compare the tensile and compressive mechanical properties of the articular and bursal sides of the biceps tendon. The associated hypotheses would be that: 1) normally, there is no difference between the mechanical properties of the articular and bursal sides of the tendon due to the fact that the biceps tendon does not experience contact with the acromion on the bursal side and plays a minimal role against the humeral head in a normal shoulder and 2) when in the

presence of a rotator cuff tear, tensile properties decrease and compressive properties increase on the articular side of the tendon first in response to increased compressive loading experienced by the tendon as its role as a humeral head depressor is increased and 3) changes first seen on the articular side would progress to the bursal side at later time points as the tendon is unable to adapt and the degeneration is no longer concentrated on the articular side.

c. Effect of subacromial impingement

Although the results of this study lead us to believe that increased compressive loading against the humeral head plays a large role as a mechanism for biceps tendon pathology, it is possible that impingement of the tendon between the humerus and the acromion is also present. Similarly to the studies performed here where loading was increased and decreased in order to determine its effect, studies can be done in this model to both decrease and increase the role of the acromion near the biceps tendon. An acromioplasty or subacromial decompression could be performed which would allow us to determine if pathology is not present when the acromion is missing or less thick. Conversely, an acromion allograft could be added underneath the existing acromion or a tendon allograft could be wrapped around the acromion, as previously described[2,28], to magnify any effect it might have, as in the increased loading scenario performed in the current study.

The objective of this study would be to determine the role of subacromial impingement in biceps tendon pathology following rotator cuff tears. The associated hypotheses would be that: 1) acromioplasty does not effect the existence of biceps tendon pathology following rotator cuff tears due to the theory that biceps tendon pathology is a

result of increased compressive loading against the humeral head and not impingement under the acromion and 2) acromion allografts would cause detrimental changes at earlier time points than with a rotator cuff tear alone since this would result in additional increased loading on both the articular and bursal sides of the tendon as the tendon is compressed between the acromion allograft and the humeral head.

d. Studies involving pain and functional assays

Clinically, biceps tendon pathology has been considered to be a significant source of shoulder pain. In humans, release of the long head of the biceps tendon has been shown to significantly reduce shoulder pain. Investigations into pain in this model have not been previously attempted. However, there are many assays used to examine pain in animal models. These assays range from biological markers of pain such as substance P[10] to more functional pain assays such as mechanical or thermal allodynia.[3,6,20,30] These studies would allow further insight into how well the rat model of biceps tendon pathology in the presence of rotator cuff tears represents the human clinical condition. The pathological biceps tendon is thought to be a significant source of pain in shoulders with rotator cuff tears. The objective of this study would be to investigate the effect of biceps tendon pathology in the presence of rotator cuff tears on pain in this model. The associated hypothesis would be that as biceps tendon pathology worsens, for example from 4 to 8 weeks or with increased loading, pain would also increase. Additionally, since we found that biceps tendon properties improved from 8 to 16 weeks or with decreased loading, our second hypothesis would be that these scenarios would result in decreased shoulder pain.

Additionally, functional parameters were not investigated in the current study. Our lab has the capability to measure alterations in gait parameters such as stride lengths and widths as well as ground reaction forces.[27] It would be interesting to examine the effect of altered loading on these parameters as well as additional functional assays such as grip strength in the injured limb, with the hypotheses that increased loading would cause further functional deficits while decreased loading would result in some restorations of functional properties. Functional assays could also be performed in conjunction with pain studies to determine the relationship between pain and functional limitations. In this study, the objective would be to determine the contribution of pain to functional deficits seen following rotator cuff repairs. This would be accomplished by measuring functional parameters, such as the existing gait analysis system or new assays such as grip strength, both with and without administration of pain medication. Our first hypothesis would be that at early time points, pain would play a large role in functional deficits. Specifically that when pain medication is given, there would be less functional changes than without pain relief indicating that early functional deficits are due to pain limitations. The second hypothesis would be that functional deficits at later time points would not be altered with administration of pain medication and therefore would be true functional deficits not due to pain limitations.

e. Possible treatment strategies

This animal model could also be used to determine the effect of rotator cuff repair on biceps tendon pathology. Delayed repair following supraspinatus tendon detachment has been performed previously in our laboratory[9] and this model could be expanded to include repair of the infraspinatus tendon as well. As discussed in regards to the

improvement in biceps tendon pathology after 16 weeks, it is possible that restoration of infraspinatus tendon properties alone may be sufficient to decrease the load and therefore restore the mechanics of the biceps tendon. Future studies could compare repair of the infraspinatus tendon alone and combined repair of the supraspinatus and infraspinatus tendons on the properties of the biceps tendon. Specifically, detachment of the supraspinatus and infraspinatus tendons would be performed and after 4 or 8 weeks, the tendons would be repaired, either separately or in combination. After an additional 4 or 8 weeks, biceps tendons could be analyzed to determine if rotator cuff repair in this model leads to restoration of normal biceps tendon properties. These studies have already begun and will allow insight into the role of the restoration of the rotator cuff balance of forces on biceps tendon pathology. Based on the results seen after 16 weeks in the current study, we hypothesize that restoration of the balance of forces by repair of the infraspinatus tendon alone will result in improved biceps tendon properties.

Additionally, this model could be used to evaluate the clinical practices of biceps tendon tenotomy (detachment) or tenodesis (detachment from its insertion on the glenoid and reattachment to a different site) on various shoulder properties. For example, these procedures could be performed and shoulder function evaluated to determine their effect when compared to retention of the pathologic biceps tendon. Clinically, studies have reported that performing tenotomy or tenodesis procedures does not result in functional deficits, even when performed in the presence of non-repairable rotator cuff tears. However, the long term outcome of these procedures has not been studied. It is possible that while macroscopic functional deficits do not occur, altered kinematics at the joint level are present that lead to increased degeneration in the remaining rotator cuff tendons

or glenoid cartilage. The objective of this study would be to determine the effects of biceps tendon tenotomy and tenodesis, both alone and in the presence of rotator cuff tears, on whole joint properties such as gait, cartilage and surrounding tendon properties. The first associated hypothesis is that tenotomy or tenodesis alone will not result in functional deficits or alterations in cartilage or surrounding tendon properties. Secondly, in the presence of rotator cuff tears, tenotomy and tenodesis will result in further functional deficits, cartilage and surrounding tendon degeneration as the biceps tendon will no longer be present to function as a humeral head depressor.

These studies could also be combined with the studies discussed above using assays to measure pain, as clinically biceps tendon tenotomy and tenodesis are thought to relieve shoulder pain. If pain is indeed decreased following these procedures, follow-up studies could investigate the mechanism involved. In addition to these clinical and functional assays above, once the model has been further characterized biologically, it is possible to target biological treatments. For instance, if we find that large changes in MMP expression are present, perhaps treatments inhibiting this expression could be targeted. We also propose future studies to further examine the effect and presence of inflammation in this model. If we find that inflammation is a key factor in these changes, anti-inflammatory treatments could be explored.

f. Investigations in other model systems

Other model systems, both in the rotator cuff and not, could also be used to investigate further into some of the mechanisms proposed here. Since this is the first animal model to examine the biceps tendon in the presence of rotator cuff tears, it is not known if the anatomy of the biceps tendon is similar to the human in other rotator cuff

animal models, or if the biceps tendon is even present. However, if the biceps tendon is present, large animal models could be used to further elucidate the source of initiation of biceps tendon pathology following rotator cuff tears. In this study, we found that changes in the biceps tendon began in its intra-articular portion before extending into the extra-articular portion. We concluded that this was due to increased compressive loading of the tendon in this location; however, it is possible that the intra-articular synovial environment also contributed to these changes. In large animal models such as the dog and sheep, the rotator cuff tendons are extra-articular, not intra-articular.[7] If similar studies were carried out in either of these models and biceps tendon changes still occur intra-articularly first, we could conclude that the intra-articular environment is not responsible. However, in these animals the bony anatomy is not as similar to the human as in the rat, and it is not clear if the biceps tendon would pass underneath the acromion as it does in the rat and human. If biceps tendon pathology does not occur in the same way in these animals as it does in the rat, it could be due to the absence of an intra-articular environment or the altered bony anatomy. However, in the dog model particularly, a portion of the joint capsule is often resected when a rotator cuff injury is made in order to recreate the intra-articular environment seen in the human.[7] Studies investigating biceps tendon pathology in this model could be done both with and without resection of the joint capsule in order to determine the contribution of the intra-articular environment.

Additionally, Chapter 6 discussed that biceps tendon properties improved by 16 weeks in the rat supraspinatus+infraspinatus detachment model. Rotator cuff tear models without spontaneous tendon healing or scar formation between the tendon end and bone

would allow for studies to investigate the effects of long-term biceps tendon pathology both on the tendon itself as well as the surrounding joint. While rotator cuff tears in large animal models result in a higher degree of tendon retraction than in the rat[7], scar still forms between the tendon end and bone. However, if the biceps tendon anatomy is found to be similar, it would be interesting to see if the pathology in large animal models such as the dog or sheep persists over long periods of time.

A model of changes in type of loading in the rabbit FDP was discussed in Chapter 5.[29] In this model, a long tendon sees areas of both compressive and tensile loading resulting in very different composition and properties. When the tendon is translocated from its normal position, areas that normally experience compression begin to experience tension and vice versa. Since our results lead us to believe that this is what is happening in the rat biceps tendon in our model, the rabbit FDP model could be used to further investigate the biological response of tendon to a change from tensile to compressive loading. No tendon detachments are required, and therefore if inflammation is present it will be due to the change in loading demands on the tendon and not the tendon detachment environment.

While still in the rat, there are several other models of increased and decreased loading on the tendon that could be used in order to investigate more levels of loading than the increased and decreased loading scenarios used in this study. For instance, instead of increased loading by short head detachment and treadmill running, increased loading could be achieved by muscle stimulation. This system would allow for a variety of different levels of additional loading and it may be possible to determine if a correlation exists between extent of tendon damage and level of increased load.

Additionally, decreased loading could be achieved by botox injection or detachment of the biceps tendon at its muscle-tendon junction. Using those models would allow us to evaluate if complete absence of load has the same effect as decreased loading through immobilization. The ACL could also be examined in the rat or other animal models, as it can be immobilized using an external fixator. Using this model, it would be possible to fix the tendon in various levels of slacked position, again to tease out the relationship between no load and a low level static load.

g. Future uses of this model

i. Spontaneous tendon rupture

Increased loading following rotator cuff detachments resulted in universally decreased tendon properties as early as 4 weeks post detachments that persisted at 8 weeks, the latest time point examined with altered loading in this study. The continued striking detrimental tendon properties found with this combination may perhaps be useful in developing a model of spontaneous tendon rupture. Although biceps tendon properties improved at a later time point with detachment alone, it is possible that with the additional of increased loading, the tendon is not able to adapt and therefore properties continue to decrease. This could lead to fraying, calcifications or even partial or complete tendon ruptures in the biceps tendon. While models of tendon degeneration using methods such as overuse by treadmill running or collagenase injection have been widely used, an animal model of spontaneous tendon rupture has not been identified. The limitation of many animal studies regarding tendon injuries is that these injuries are made acutely and do not reflect the clinical condition of progressive degeneration that leads to eventual tendon rupture. An animal model of such a condition would allow for a

multitude of studies involving both elucidations of the mechanism responsible as well as possible treatment strategies to prevent eventual rupture. The objective of this study would be to create an animal model of spontaneous tendon rupture. In order to achieve this objective, we would investigate longer time points following supraspinatus, infraspinatus and short-head of the biceps tendon detachments combined with post-operative treadmill running. The associated hypothesis would be that after 16 weeks of post-surgical treadmill running, fraying and tears would be observed in the long-head of the biceps tendon. Due to the increased loading, the tendon would be unable to remodel and would further degenerate. A further degenerated tendon would then be susceptible to fraying and eventually tearing in the presence of rotator cuff tears and daily treadmill running.

ii. Instability

Since this model was found to correlate well with the clinical condition of biceps pathology following rotator cuff tears, it is possible that the rat may be a good model for other shoulder conditions involving the biceps tendon. Specifically, this model could be used to investigate instability in two ways. First, clinically the biceps itself can be unstable due to a variety of disorders including massive tears of the subscapularis tendon. In such a condition, the biceps tendon would continually dislocate from its position in the bicipital groove, which could lead to pathologies in this location. Since we demonstrated the ability to determine regional changes in the biceps tendon, the rat could be investigated as a possible model for this condition.

Secondly, tears of the biceps tendon have been shown to contribute to glenohumeral instability.[11,18] However, clinical studies are unable to determine an

interaction between extent of instability and changes in shoulder function or articular cartilage properties. In this study, it was shown that the rat biceps tendon is very similar to the human and therefore this model could be investigated to see if the same relationship exists between biceps tendon tears and glenohumeral instability in the rat and human. Surgical detachments of the biceps tendon could be made and glenohumeral instability measured ex-vivo. If instability exists, these studies could then be combined with assays such as range of motion and rat gait analysis as well as characterization of changes in articular cartilage to determine the relationship between these measures and instability. If these studies are successful, they could be expanded to include an in vivo measurement of instability of the rat as well as possible treatment options.

The results presented here allow us to identify many future areas of research. Studies can be done, both in the rat model established here as well as other model systems, to further elucidate the mechanisms associated with biceps tendon pathology in the presence of rotator cuff tears and associated possible treatment strategies. In addition, due to the similarity of the rat biceps tendon to the human, future studies can also be done to determine if the rat is an appropriate animal model for other clinical scenarios involving the biceps tendon.

H. References

1. **Burkhart, S. S.:** Arthroscopic treatment of massive rotator cuff tears. Clinical results and biomechanical rationale. *Clin Orthop Relat Res,* (267): 45-56, 1991.
2. **Carpenter, J. E.; Flanagan, C. L.; Thomopoulos, S.; Yian, E. H.; and Soslowsky, L. J.:** The effects of overuse combined with intrinsic or extrinsic

alterations in an animal model of rotator cuff tendinosis. *Am J Sports Med,* 26(6): 801-7, 1998.

3. **Chaplan, S. R.; Bach, F. W.; Pogrel, J. W.; Chung, J. M.; and Yaksh, T. L.:** Quantitative assessment of tactile allodynia in the rat paw. *J Neurosci Methods,* 53(1): 55-63, 1994.

4. **Chen, C. H.; Hsu, K. Y.; Chen, W. J.; and Shih, C. H.:** Incidence and severity of biceps long head tendon lesion in patients with complete rotator cuff tears. *J Trauma,* 58(6): 1189-93, 2005.

5. **Dagher, E.; Hays, P. L.; Kawamura, S.; Godin, J.; Deng, X. H.; and Rodeo, S. A.:** Immobilization modulates macrophage accumulation in tendon-bone healing. *Clin Orthop Relat Res,* 467(1): 281-7, 2009.

6. **DeLeo, J. A., and Winkelstein, B. A.:** Physiology of chronic spinal pain syndromes: from animal models to biomechanics. *Spine,* 27(22): 2526-37, 2002.

7. **Derwin, K. A.; Baker, A. R.; Iannotti, J. P.; and McCarron, J. A.:** Preclinical models for translating regenerative medicine therapies for rotator cuff repair. *Tissue Eng Part B Rev,* 16(1): 21-30.

8. **Dourte, L. M.; Perry, S. M.; Getz, C. L.; and Soslowsky, L. J.:** Tendon Properties Remain Altered in a Chronic Rat Rotator Cuff Model. *Clin Orthop Relat Res*.

9. **Gimbel, J. A.; Van Kleunen, J. P.; Lake, S. P.; Williams, G. R.; and Soslowsky, L. J.:** The role of repair tension on tendon to bone healing in an animal model of chronic rotator cuff tears. *J Biomech,* 40(3): 561-8, 2007.

10. **Gotoh, M.; Hamada, K.; Yamakawa, H.; Inoue, A.; and Fukuda, H.:** Increased substance P in subacromial bursa and shoulder pain in rotator cuff diseases. *J Orthop Res,* 16(5): 618-21, 1998.

11. **Harryman, D. T., 2nd; Sidles, J. A.; Harris, S. L.; and Matsen, F. A., 3rd:** The role of the rotator interval capsule in passive motion and stability of the shoulder. *J Bone Joint Surg Am,* 74(1): 53-66, 1992.

12. **Joseph, M.; Maresh, C. M.; McCarthy, M. B.; Kraemer, W. J.; Ledgard, F.; Arciero, C. L.; Anderson, J. M.; Nindl, B. C.; and Mazzocca, A. D.:** Histological and molecular analysis of the biceps tendon long head post-tenotomy. *J Orthop Res*, 2009.

13. **Kajikawa, Y. et al.:** GFP chimeric models exhibited a biphasic pattern of mesenchymal cell invasion in tendon healing. *J Cell Physiol,* 210(3): 684-91, 2007.

14. **Kawamura, S.; Ying, L.; Kim, H. J.; Dynybil, C.; and Rodeo, S. A.:** Macrophages accumulate in the early phase of tendon-bone healing. *J Orthop Res,* 23(6): 1425-32, 2005.

15. **Kido, T.; Itoi, E.; Konno, N.; Sano, A.; Urayama, M.; and Sato, K.:** The depressor function of biceps on the head of the humerus in shoulders with tears of the rotator cuff. *J Bone Joint Surg Br,* 82(3): 416-9, 2000.

16. **Lake, S. P.; Miller, K. S.; Elliott, D. M.; and Soslowsky, L. J.:** Tensile properties and fiber alignment of human supraspinatus tendon in the transverse direction demonstrate inhomogeneity, nonlinearity, and regional isotropy. *J Biomech,* 43(4): 727-32.

17. **Luo, Z. P.; Hsu, H. C.; Grabowski, J. J.; Morrey, B. F.; and An, K. N.:** Mechanical environment associated with rotator cuff tears. *J Shoulder Elbow Surg,* 7(6): 616-20, 1998.

18. **Malicky, D. M.; Soslowsky, L. J.; Blasier, R. B.; and Shyr, Y.:** Anterior glenohumeral stabilization factors: progressive effects in a biomechanical model. *J Orthop Res,* 14(2): 282-8, 1996.

19. **Millar, N. L.; Wei, A. Q.; Molloy, T. J.; Bonar, F.; and Murrell, G. A.:** Cytokines and apoptosis in supraspinatus tendinopathy. *J Bone Joint Surg Br,* 91(3): 417-24, 2009.

20. **Min, S. S.; Han, J. S.; Kim, Y. I.; Na, H. S.; Yoon, Y. W.; Hong, S. K.; and Han, H. C.:** A novel method for convenient assessment of arthritic pain in voluntarily walking rats. *Neurosci Lett,* 308(2): 95-8, 2001.

21. **Murthi, A. M.; Vosburgh, C. L.; and Neviaser, T. J.:** The incidence of pathologic changes of the long head of the biceps tendon. *J Shoulder Elbow Surg,* 9(5): 382-5, 2000.

22. **Neer, C. S., 2nd:** Anterior acromioplasty for the chronic impingement syndrome in the shoulder: a preliminary report. *J Bone Joint Surg Am,* 54(1): 41-50, 1972.

23. **Peltz, C. D.; Perry, S. M.; Getz, C. L.; and Soslowsky, L. J.:** Mechanical properties of the long-head of the biceps tendon are altered in the presence of rotator cuff tears in a rat model. *J Orthop Res,* 27(3): 416-20, 2009.

24. **Perry, S. M.; Getz, C. L.; and Soslowsky, L. J.:** After rotator cuff tears, the remaining (intact) tendons are mechanically altered. *J Shoulder Elbow Surg,* 18(1): 52-7, 2009.

25. **Perry, S. M.; Getz, C. L.; and Soslowsky, L. J.:** Alterations in function after rotator cuff tears in an animal model. *J Shoulder Elbow Surg,* 18(2): 296-304, 2009.

26. **Riley, G. P.; Harrall, R. L.; Constant, C. R.; Chard, M. D.; Cawston, T. E.; and Hazleman, B. L.:** Tendon degeneration and chronic shoulder pain: changes in the collagen composition of the human rotator cuff tendons in rotator cuff tendinitis. *Ann Rheum Dis,* 53(6): 359-66, 1994.

27. **Sarver, J. J.; Dishowitz, M. I.; Kim, S. Y.; and Soslowsky, L. J.:** Transient decreases in forelimb gait and ground reaction forces following rotator cuff injury and repair in a rat model. *J Biomech,* 43(4): 778-82.

28. **Soslowsky, L. J.; Thomopoulos, S.; Esmail, A.; Flanagan, C. L.; Iannotti, J. P.; Williamson, J. D., 3rd; and Carpenter, J. E.:** Rotator cuff tendinosis in an animal model: role of extrinsic and overuse factors. *Ann Biomed Eng,* 30(8): 1057-63, 2002.

29. **Vogel, K. G., and Koob, T. J.:** Structural specialization in tendons under compression. *Int Rev Cytol,* 115: 267-93, 1989.

30. **Yu, Y. C.; Koo, S. T.; Kim, C. H.; Lyu, Y.; Grady, J. J.; and Chung, J. M.:** Two variables that can be used as pain indices in experimental animal models of arthritis. *J Neurosci Methods,* 115(1): 107-13, 2002.

Appendix A: Experimental protocols

A1. Surgical protocol: sham, supraspinatus+infraspinatus detachment, short-head of the biceps detachment

Two people, not including the surgeon, are needed to operate on the rats. One person is needed for anesthesia and prep and one is needed to be scrubbed in as an assistant to the surgeon. Typically twelve rats are done per surgery. This takes approximately 2-3 hours.

The surgical room on the fifth floor of Stemmler needs to be reserved ahead of time by emailing George Wisor (wisor@pobox.upenn.edu). He needs the date of the surgery and the protocol number of the project. Also, the following materials need to be sterilized before the surgery. They should be sterilized using steam sterilization. A back-up pack with the same instruments should also be sterilized in case any instruments are dropped during surgery. A list of other non-sterilized materials is also listed below.

Instruments to be sterilized for surgery:

2 regular pick-ups (1 with teeth and 1 without teeth)
Fine pick-up with teeth
Fine pick-up without teet
Curved pick-up without teeth
2 curved hemostats
2 Castoviegos
Needle holders
Small scissors
Microscissors
Large scissors
2 blade holders

Other sterilized materials needed for surgery:

single armed 5-0 proline suture
Size-eleven blades
Size-fifteen blades
4-0 vicryl suture (Supplied by surgical room staff)
3-0 vicryl suture (Supplied by surgical room staff)
Staple gun (Supplied by the surgical room staff)
Fire stick (Supplied by the surgical room staff)
Metal container (Supplied by surgical room staff)
sodium chloride (Supplied by surgical room staff)
Surgical drape (Supplied by surgical room staff)
Surgical gowns (Supplied by surgical room staff)
Steralized gloves (Supplied by surgical room staff)

Materials needed for anesthesia and prep (not sterilized):

Scale
Clippers
Permanent Marker
Tissue scissors
Tupperware container with two holes in side
Lab notebook
2 metal containers (1 filled with alcohol and 1 filled with betadine)
Spray bottle filled with betadine/alcohol solution
Anesthesia machine w/ oxygen tank and isofluorane
Heat lamp
Cages filled with white alpha-chips
Rat surgical holder
Masks

On the day of surgery the following things need to be done to set-up the anesthesia area and surgical room before the surgeon arrives.

Anesthesia area

1. Turn on anesthesia machine. To do this, loosen the oxygen tank valve (directly above the green oxygen tank) with a wrench. Then, turn the green knob on the front of the anesthesia machine (dictates the amount of flow from the oxygen tank) until the floater is at 1. Do not turn on the isofluorane until the rat is needed to be anesthetized.
2. Place cages filled with white alpha-chips on the floor.
3. Put heat lamp near cages.
4. Plug in clippers and place on prep table.
5. Place the metal container filled with alcohol and the one filled with betadine on the prep table.
6. Place Tupperware container on the prep table.
7. Place scale and lab notebook on countertop nearest anesthesia table.

Surgical Area

1. Remove the protective wrap from the wound pack.
2. Open the package for the surgical drape.
3. Put on sterile gloves. Make sure you do not contaminate the gloves.
4. Place the surgical drape over the surgical table. This should now be a sterilized field.
5. Have another person place the rat surgical holder onto the far end of the field. Cover the rat holder and that end of the field with the drape in the wound pack that contains the hole for the rats shoulder.

6. Have another person open the primary pack of surgical instruments. Lay the instruments out on the table.
7. Have another person open up the 4-0 vicryl suture, 3-0 vicryl suture, eleven blades, fifteen blades, staple gun, and fire stick. Organize them on the table.
8. Take the metal container in the wound pack and have another person fill it with the sodium chloride solution supplied in the surgical room.

Just before the surgeon arrives, anesthetize and prep the rat by doing the following:

1. Place the rat in the Tupperware container.
2. Remove the oxygen and isofluorane tubes from the nose-cone and insert them into the holes in the side of the Tupperware container.
3. Turn the isofluorane on to flow level 5 until the rat falls asleep/does not respond to pinch test.
4. Quickly remove the tubes from the Tupperware container and place them back onto the nose-cone.
5. Quickly take the rat out of the Tupperware container and insert his nose in the nose-cone.
6. Decrease the isofluorane to flow level 3.
7. Shave the rats upper torso using the clippers.
8. Weigh the rat.
9. If it is an odd numbered rat, cut a notch in its ear with the tissue scissors.
10. Clean the rats upper torso with alcohol then betadyne.

Once the surgeon arrives and has put on his/her surgical gown and gloves, the rat should be:

1. Fastened onto the rat surgical holder using the Velcro straps
2. Then sprayed with the betadyne/alcohol solution.

The surgery to create an acute injury/detachment is done by following the below protocol.

A 2cm skin incision will be made over the craniolateral aspect of the scapulohumeral joint, followed by blunt and sharp dissection down to the rotator cuff musculature. The rotator cuff will be exposed and the tendons will be visualized to their insertion on the humerus. **The sham surgery ends here.** A 3.0 vicryl suture will then be passed underneath and around the acromion in order to apply an upward traction for further exposure. The supraspinatus tendon is then separated from other rotator cuff tendons by making a longitudinal incision using a scalpel, parallel to the long axis of the supraspinatus tendon through the rotator interval, or the anterior border, and through interdigitation fibers of the infraspinatus, or the posterior border. The tendon will be detached sharply at its insertion on the greater tuberosity using a scalpel blade. The tendon is allowed to freely retract without attempt at repair creating a gap approximately 4mm from its insertion. The infraspinatus tendon will then be detached in the same manner as the supraspinatus, with a sharp dissection from the insertion site. Any

remaining fibrocartilage at the tendon's insertion will be left intact. In groups designated for increased loading, following detachment of the supraspinatus and infraspinatus tendons, a retention suture is then passed under the distal clavicle. The distal clavicle is then gently retracted, exposing the coracoid process. A #11 blade is then used to release the short head of the biceps off its insertion point. The overlying deltoid muscle is then closed with 4-0 Vicryl and skin will then be closed with staples. The rats are then placed in cages with alpha-dry chips under a heat lamp to wake up.

A2. Decreased loading protocol - Immobilization

1. Immediately after surgery, keep rat under anesthesia in prep area
2. Prepare supplies needed for each rat:
    a. 2 large pieces of Webril for 'vest'
    b. One 'stomach roll' slightly overlapping the vest
    c. 2 thin webril pieces on the immobilized (left) arm
    d. 2 large pieces of Vetrap similar to large webril 'vest'
    e. 2 pieces of thin Vetrap on immobilized arm
    f. 1 thin piece of Vetrap cut in half to finish immobilized arm
3. Lay rat on back
4. Use 1 large piece of Webril to wrap from stomach, around uninjured shoulder and back to stomach.
5. Repeat step 4 for injured arm
6. Use 'stomach roll' to slightly overlap below existing Webril
7. Use 2 thin Webril pieces to cover injured arm
8. Repeat steps 4 and 5 with Vetrap.
9. Repeat step 7 with Vetrap.
10. Add final layer of Vetrap over injured arm to cover all exposed Webril.
11. Make sure the wrap is not too tight on the armpit of the unimmobilized arm
12. Place rat on stomach in cage and watch to make sure he 1) wakes up and 2) arm is not swollen badly

A3. Increased loading protocol – Treadmill running

Week Post Surgery	Mon, Tues, Wed, Thurs, Fri (treadmill minutes per day)	Sat, Sun
1	10, 15, 20, 25, 30	rest, rest
2	30, 40, 45, 50, 60	rest, rest
≥3	60, 60, 60, 60, 60	rest, rest

These rats **ALWAYS** run at **10 m/min** and **NO INCLINE**!!

A4. Dissection protocol for long-head of the biceps tendons to be used for mechanical testing or histology

• Equipment

- Triple Beam Balance Scale
- #3 Scalpel blade holders
- PBS solution
- curved hemostat
- small fine toothed forceps
- small dissection scissors
- bone cutters (or large dissection scissors)
- #11 and #15 scalpel blades
- labeled scintillation vials filled with PBS for specimen storage

• Dissection Procedure

1. Take out rats to thaw and place in the dissection room sink (following proper dissection room protocols). It takes approximately 6 hours for a rat to thaw at room temperature and approximately 1 hour for a rat to thaw in a lukewarm water bath, so plan accordingly for your timing needs. Keep rats dry (i.e. use double plastic bags) if using a water bath.

2. After thawing, weigh each rat, if this has not been done at time of sacrifice. Record weight of each rat in the notebook.

General Comments on Dissection:

It is generally difficult to describe the complete dissection technique because the technique seems to vary between individuals. The key to successful dissection is to try and apply the smallest possible load history to the tissue and to not damage the tissue during the dissection. This is achieved by being patient and careful.

The following steps may be helpful to you in the dissection.

3. First, externally rotate the arm using a curved hemostat to weigh it down and keep it in this position.

4. Remove the skin from the shoulder using a #11 blade. This should be similar to opening the skin for surgery. Take care not to cut into the muscle and damage the underlying tendons.

5. Next, using a #15 blade and the small toothed forceps, carefully cut away the deltoid from the greater tuberosity of the humerus and the top of the acromion. Cut away the superficial muscle on the top of the scapula.

6. Now that the acromion and the deeper muscles of the scapula are exposed, you should be able to visualize the supraspinatus tendon which lies beneath the acromion. Carefully cut the CA capsule and break off the acromion using a curved forceps. Clear the clavicle by cutting away all muscles attaching it to structures near the shoulder.

7. Identify the rotator cuff tendons and the long-head of the biceps tendon. Be careful, do not cut these. For many studies involving dissection of the biceps tendon, the rotator cuff tendons will also need to be saved. Even if you are not saving the rotator cuff tendons for future testing, the cleanest and easiest way to dissect the long head of the biceps tendon is to first remove the rotator cuff tendons.

8. Make a cut along the edge of the scapular spine to free the supraspinatus muscle. With forceps or scalpel, scrape the supraspinatus muscle off the scapula.

9. Next, make a cut along the other edge of the scapular spine to free the infraspinatus muscle. Again with forceps scrape the muscle off the scapula.

10. Using the #15 blade, scrape the subscapularis muscle off the anterior portion of the scapula. The muscle may get caught on the coradoid, carefully scrape around it with a #11 blade.

11. With the scapula free of rotator cuff tendons, cut the origin of the triceps and other muscles located on the scapula.

12. Using a #11 blade, carefully cut the sheath holding the biceps tendon in the bicipital groove of the humerus. **(If dissecting for histological analysis, skip to step #16)**

13. Remove the scapula with the long-head of the biceps tendon still attached. Tuck muscle belly next to scapular spine. Wrap scapula-biceps tendon complex in diaphragm, skin, saline soaked gauze, and finally dry gauze. Place each individual biceps tendon in a small bag labeled with the specimen number. Put these small bags in a biohazard bag labeled with the specimen numbers and the date. Freeze.

14. On morning of mechanical testing day, remove biceps tendons in bags from freezer and run under warm water for approximately 20 minutes to thaw.

15. Once thawed, scrape away biceps muscle and then clean fascia from tendon under stereomicroscope before measuring area and applying stain lines.

16. For histological analysis, remove the scapula and long-head of the biceps tendon. Cut the tendon at the muscle tendon junction and use bone cutters to remove all scapula except for the glenoid.

17. Using pins (or syringe needles), secure the bone-tendon complex to a small piece of Styrofoam or cork in a flattened and straight position before placing in tissue cartridge. Place cartridge in Calex.

18. Change Calex after 24 hours and remove from Calex after 7 days.

19. Place in 70% EtOH and give to Bob Caron for processing.

A5. Stain line protocol for long-head of the biceps tendons

• Equipment

- 6-0 silk suture
- Verhoff's stain
- Ruler
- small curved forceps

• Application

1. Place a small amount of verhoff's stain in a weighing boat. Allow a piece of suture to rest in the stain for about 10 min or until small bubble appear on the suture.

2. Fan the tendon out next to the ruler.

3. Blot the tendon with a paper towel to prevent the stain from running.

4. Use 6.0 silk suture to apply stain lines on the tendon at the tendon insertion and then 1.5, 3.5, 8.5, and 11.5 mm from the insertion.

5. Wait about 60 sec and blot the tendon to ensure the stain does not run.

6. Place the specimens back in the vials with PBS.

A6. Area data collection and analysis protocol for long-head of the biceps tendon

Data Capture:

1. Allow the laser to warm up for 20 minutes prior to use. Do this by turning on the switch on the box next to GisMO. Make sure that both averaging LEDs on the controller box are lit; if not, press the "avg" key until they are.
2. When ready to begin taking measurements, run Labview and open the Mogware program located in \\medfiles\Departments\Orthopedic Research\Shared\Common\McKay Software\Tendon Area (GisMO)\Mogware (data collection)\current.
3. Ensure that the stage area you intend to use is within the measuring range of the LVDTs; you can do this by performing a "mock" measurement sequence with the custom-designed fixture on the stage and running Mogware (step i below) with the oval Capture button inactivated.
4. Remove the tendon from the PBS and dab briefly on both sides with Kimwipe.
5. Place the tendon on a rubber pad bursal side down. Prop up the scapula in order to get the tendon flat.
6. Using forceps, ensure that the tendon is lying flat on top of the black surface. Ensure that the scapula will not be too close to the laser beam as this will cause spikes in your data.
7. If any standing PBS remains around the tendon, gently dab this off with a Kimwipe, taking care not to dab the tendon itself.
8. Place the rubber on the stage.
    a. For Area 1, place it so that the laser is just barely touching the scapula/glenoid. Go 2 turns (~0.5 mm), taking you to position **1** in Figure 1. This will coincide with the stain line at the insertion site.
9. Press the Run (➔) button in Mogware and ensure that the oval Capture button beneath the Start button is activated (lit) so that your data will be captured. Press the Start button to begin recording data.
10. Zero the laser and both LVDTs.
11. With the coarse adjust knob, move the stage in *x*-direction so that the laser beam crosses the entire width of the tendon (position **2)**.
12. With the fine adjust knob, move the stage in the *y*-direction to position **3**, 2 turns (~0.5 mm).
13. With the coarse adjust knob, move the stage in *x*-direction back across the entire width of the tendon.

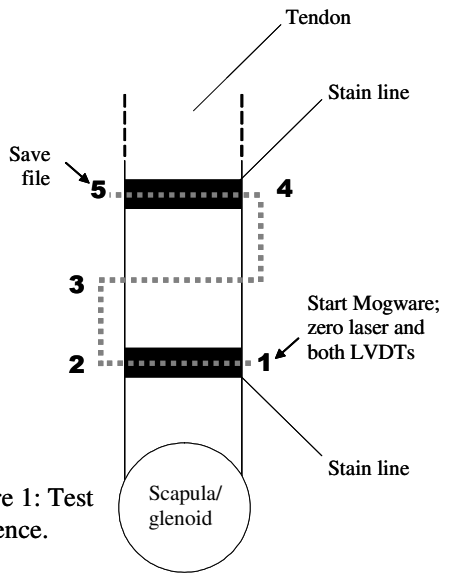

Figure 1: Test sequence.

14. With the fine adjust knob, move the stage in the *y*-direction to position **4**, 2 turns (~0.5 mm).
15. With the coarse adjust knob, move the stage in *x*-direction back across the entire width of the tendon, stopping at position **5**.
16. Press Stop button and save file.
17. Proceed to the "Thickness Selection" section of the protocol and ensure that your data is acceptable (i.e., not usable due to spikes or being out of the LVDT measuring ranges).
18. You can either proceed to "Area Selection" at this point or leave that part of the analysis until later if desired (note that area selection should take less than a minute).
19. Perform steps **i** through **r** again with the following differences:
20. For Area 2: start at the second stain line, perform 1 pass, move 4 turns in the y-direction, perform a second pass, move 4 turns in the y-direction and perform the third pass (ending at stain line 3)
21. For Area 3: start at the third stain line, perform 1 pass, move 10 turns in the y-direction, perform a second pass, move 10 turns in the y-direction and perform the third pass (ending at stain line 4).

Data Analysis:

Thickness Selection:

1. Run the Matlab file named "select_thickness" in \\medfiles\Departments\Orthopedic Research\Shared\Common\Rat Multi Tendon Detach\Matlab\Area. Do this by ensuring that this directory is in your path and then typing "select_thickness;" at the Matlab prompt.
2. When prompted, choose your data file.
3. A figure showing the thickness data will open and a dialog box will ask you to select the first thickness range. Using the cursor, draw a box that includes all of the thickness data for the first pass across the tendon (**A** in Figure 2). Note that you can maximize the window if this is helpful.
4. After you do this, another dialog box will prompt you to select the second range. Using the cursor, draw a box that includes all of the thickness data for the second pass across the tendon (**B** in Figure 2).
5. Repeat this for as many passes as you have done (Typically 3, but 5 in this example).
6. The program will then prompt you to save a figure file for this data; do this.

Area Calculation:

1. Run the Matlab file named "specimen_area_multi" in \\medfiles\Departments\Orthopedic Research\Shared\Common\ Rat Multi Tendon Detach\Matlab\Area. Do this by ensuring that this directory is in your path and then typing "specimen_area_multi;" at the Matlab prompt.
2. When prompted, select your figure file saved above.
3. The program will prompt you to save a Matlab file for this specimen; do this.

4. The program will then open a figure with a graphical representation of your specimen data and will compute an average cross sectional area, which is returned in the main Command Window. Save the figure and record the area.

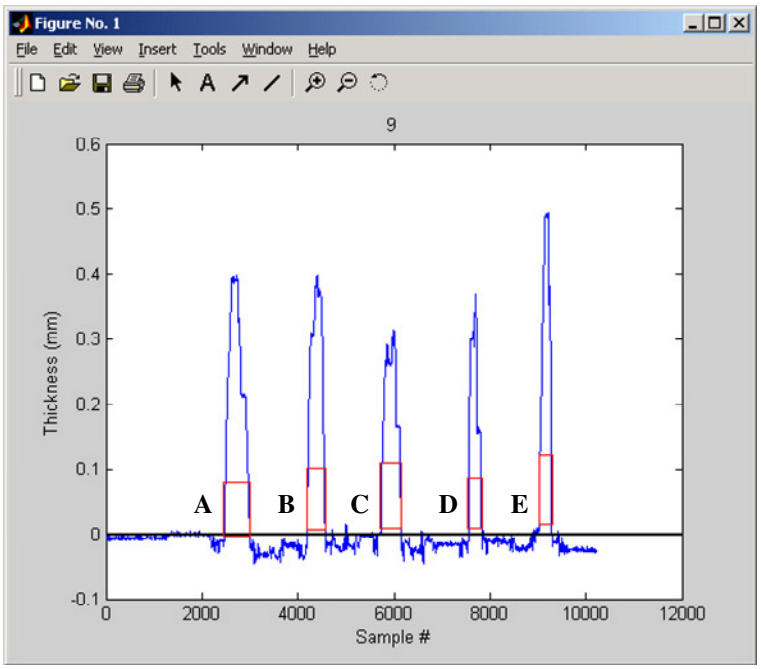

Figure 2: Sample thickness selection.

A7. Mechanical testing protocol for long-head of the biceps tendons

Note: Make sure all equipment is on for at least 30min before calibration or testing. The tank must be filled with 1X PBS and heated to 37°C. The heating process takes approximately 2 hours.

• Set-up of Instron

1. Load Merlin and choose the testing protocol name 'Biceps'.
2. Click on the 'specimen/sample' button on the right of the screen. Under 'specimen', enter the name of the first specimen to be tested. Before running each test, be sure to enter the specimen name in this field. If you do not enter the new sample name before each test, subsequent tests will be labeled with the last specimen typed into this field.
3. Click on the 'load cell' button and then on 'calibrate'. This only needs to be done once, at the beginning of the testing day.
4. Make sure Load is enabled every 15 mN and Time is enabled every 10000ms and that the instron will stop at 100 N.
5. Check the testing protocol:
   Intact tendons – 'biceps'
   - 1st block – absolute ramp to 0.1 N at 0.115 mm/sec
   - 2nd block – triangle – 10 cycles between 0.1 and 0.5 N at 0.115 mm/sec
   - 3rd block – hold 300 s
   - 4th block – relative ramp with a delta of 0.46 mm at a rate of 0.575 mm/sec (therefore 4% strain)
   - 5th block – hold 600 s
   - 6th block – relative ramp with a delta of 0.46 mm at a rate of -0.575 mm/sec (return to zero)
   - 7th block – hold 60 s
   - 8th block – relative ramp with a delta of 50 mm at a rate of 0.0345 mm/sec (therefore 0.3%/sec)

6. Set up the camera and check VLEPO settings
   - The camera should be positioned to see from the insertion site, up to the upper grip. Remember the specimen will move, so make sure you'll be able to see the correct stain line at the end too.
   - Choose ICP to choose an image capture protocol from the left menu. On the pop-up menu choose Load – choose REMO VLEPO block control
   - Check Blocks:
     1. Block 1 -no pictures for 1200 sec
     2. Block 2 – no pictures for 285 sec
     3. Block 3 – pictures every 0.5 sec for 15 sec
     4. Block 4 – no pictures for 585 sec
     5. Block 5 – pictures every 1.5 sec for 1200 sec

• Mounting

1. Place a small amount of paper towel in the bottom of each pot. Label the pots with the specimen numbers. Make PMMA (orthojet) following the manufacturer's directions. Place the scapula of each sample in their respective pots and wait for PMMA to cure. PMMA gets hot while curing, so once the cement is hard enough to hold the scapula upright but before it gets hot, place the samples in a cup of PBS. Allow this to harden.
2. Place the tendon between a small piece of fine sandpaper with superglue, lining up the edge of the sandpaper with the fifth stain line (11.5 mm from insertion). Mount the tendon end in the large screw clamp, careful not to put loads on the tendon. Place the potted humerus in the fixture for mouse patellar tendon testing.
3. Mount fixture to testing device by lowering the stage until the clamp can be attached without loading the tendon (i.e. make sure the tendon is slack when you slide the clamp in).
4. Make sure the tendon is aligned correctly; straight up and down.
5. Apply a little less than a 0.1N load to the tendon by SLOWLY raising the stage (use the 'fine position' knob).

• **Running the test**

1. Start the test on Merlin and VLEPO at the same time.

2. At the top of the 9th preconditioning cycle, hit "NEXT" on VLEPO

3. Make sure VLEPO is taking pictures at the time of stress-relaxation and during the ramp to failure.

4. When the specimen breaks, stop the test and the image capture. Wrap the specimens in gauze, dip in PBS, and place in bag to be frozen and saved.

5. Choose End&Save under the DATA menu of Merlin. Save each test as the specimen number, side and tendon type. Record the location of failure.

6. Save the VLEPO images. You should have a folder for each day of testing, and inside that folder have a folder for each specimen. Label the specimens by their number, side, and tendon type (ex. 13-126Lbiceps).

A8. Mechanical testing analysis protocol

General analysis:

1. Remove raw data files from Merlin computer to common drive or local computer
2. Open Matlab and set path to folder that includes Matlab data in 3 columns
3. Run readMerlin – when prompted choose the raw data file you would like converted into a text file. Depending on the version of Merlin you used, the data may be reported in N or kg (old version). Review the files before continuing to determine this. If the data is in kg, you must multiply the load by 9.81.
4. First type "data=readdata(1);". When prompted select the text file you have created.
5. To find the grip stiffness, type "[stiffness, r_squared] = fitdata(data);"
    a. Click once at the beginning of the linear region of the ramp-to-failure curve
    b. Click a second time at the end of the linear region of the curve
    c. You will have to click one more time to either move on to the next test in the file or to end the program
    d. Type "stiffness" to have the results appear and copy them to excel
6. To find the maximum load, type "[max_load] = findmaxload(data);"
    a. Click once prior to and once immediately after the quick ramp for stress-relaxation
    b. Click once prior to the peak of the ramp-to-failure test and once immediately after
    c. Again you will have to click to move on to the next test or to end
    d. Type "max_load" to have the results appear and copy them to excel.
7. To find the peak load, equilibrium load, and load ratio from the stress-relaxation test, type "[peak_loads, eq_loads, load_ratios] = qlvdata(data);"
    a. Click once prior to the peak of the stress-relaxation test and once immediately after the peak of the S-R test
    b. Click once to acknowledge you are finished
    c. Click once prior to the end of the S-R test, and click once more just after the ramp-to-failure has begun
    d. Click to move on to the next test or to end
    e. Type "peak_loads" to get the peak of the S-R test
    f. Type "eq_loads" to get the equilibrium of the S-R test
    g. Type "load_ratios" to get eq_load/peak_load
    h. Copy data to 'results' spreadsheet

Other basic parameters:

1. Grip Modulus is calculated by: Grip Stiffness * 11.5 mm (our theoretical initial specimen length) / Area. E(grip) = k(grip)*11.5 / A
2. Maximum Stress is calculated by : Maximum Load / Area.
3. Peak Stress is calculated by: Peak Load / Area.
4. Equilibrium Stress is calculated by: Equilibrium Load / Area

5. Percent relaxation is calculated by: (Peak Load – Equilibrium Load) / (Peak Load)

Optical parameters:

1. Run the optical strain program to get optical modulus and stiffness for each biceps tendon location (see Optical Strain protocol)
2. The protocol is for an area of 1.
3. Optical Modulus is calculated by: Optical Modulus of 1 / Area

Optical Stiffness is calculated by: Optical Modulus of 1 / 1.5 mm (the Length between stain lines for the insertion site, this number is 2 mm for the intra-articular space and 5 mm for the bicipital groove)

Optical Strain Protocol

Pick out pictures:

1. Make a new folder in each specimen/tendon combo folder titled 'whole curve'
2. In excel, open the text files created by the 'readMerlin' program and graph load vs displacement.
3. Identify the time before stress relaxation, at the end of stress relaxation, and 10 seconds past the maximum load.
4. Using the time stamp in the picture name, select and copy to 'whole curve' one picture correlating to the time before the SR ramp.
5. Select and copy to 'whole curve' evenly time-distributed pictures from the end of the stress relaxation test until 10 seconds past the maximum load.

Run matlab program:

6. Start Matlab.
7. Set the path to Y:\Software\optical strain\unstable-Steph
8. Type "[Timg, imgfiles] = getimagetimes;"
9. When the textbox appears, choose the folder with the pictures you would like to analyze. Open any picture, which in turns opens all of them.
10. Type "mckoptistrain(imgfiles)"
11. A textbox appears asking you to choose a reference picture. Choose the image from before stress-relaxation. (generally this is the picture the program has as default)
12. A textbox appears asking if the program should equalize the image – choose 'NO'
13. The program uses texture correlation to "track" the stainlines, so texture is always a good thing when choosing locations for analysis. Also be consistent as each part of the tendon has different strain.
14. A textbox appears telling you to draw a rectangle around the bottom stainline
    a. For intact tendons, draw the first "stainline" box around a stable portion of the insertion site (stainline1), one that does not move very much.
    b. For detached tendons, draw the box around the first "stainline"
15. A textbox appears telling you to draw a rectangle around the top stainline
    c. For intact tendons, draw the second "stainline" box around the 4^{th} stainline. Be sure that the box is only on tendon and does not include background.

d. For detached tendons, draw the box around the top stainline

16. A textbox appears asking where to save the reference figure. Make a new folder inside the 'whole curve' folder titled 'automated results'. Save the reference image here. Create a separate folder for each tendon location.
17. A textbox appears asking if the program should analyze incrementally – choose 'YES'
18. A textbox appears asking where to save the figures to. Save them to 'automated results', the same folder you saved the reference image to. (This should be the default)
19. The program will track the stainlines on the screen.
20. After it is finished, a textbox appears asking where to save the roip file. Save it to the 'automated results' folder, like the other files. (Again, this should be the default)
21. The program will then play a video of the test, while showing the stainline tracking. This will play twice.
22. A textbox will appear asking where to save the dY file to. Again, save it to 'automated results'. (Should be the default)
23. Do not close anything yet!
24. Type 'roip_summary;'
25. A textbox appears, prompting you for an excel file – choose 'SAVE'
26. A textbox appears asking you to load data – choose 'YES'
27. A textbox appears asking for a matlab data file – choose 'CANCEL'
28. A textbox appears telling you "No data given! Please choose Instron *.raw file" – hit 'OK'
29. A textbox appears asking you to select the data file. Open the instron raw file for the specimen you are working on.
30. A textbox appears asking for a specimen name, hit 'OK'
31. A textbox appears asking you to select a specimen. If you followed the mechanical testing protocol and saved each specimen independently, there will only be one specimen here. If you did not, you must figure out which specimen is the correct one.
32. A textbox appears asking you to save the raw file in matlab format. You should do this, so it can be opened with future programs.
33. Finally, the program finishes writing the excel file.
34. You can now close all the matlab windows.

Calculate modulus in excel:

35. Open the data in excel. Discard any points where the stainline was not found correctly.
36. Plot e21-L (column L) vs Load (column M) for the 2nd to the final picture.
37. Remove points from the graph that are not in the linear region of the curve.
38. Add a linear trendline to the remaining points. The slope of this line is the optical modulus using an area of 1.
39. Save the file and record the results in the 'results' spreadsheet.

A9. Histology protocols – Embedding and Sectioning

Embedding

1. After processing, place cassette in wax bath for approximately 10-15 minutes.
2. Remove samples from cartridge, straighten and flatten as much as possible.
3. Using a #11 scalpel blade, cut a sagittal slice down the length of the specimen, creating a flat edge.
4. Cut off as much bone as possible while leaving the insertion site into the glenoid intact.
5. Place the new flat edge face down on the bottom plastic embedding tray (from Bob).
6. Fill tray with paraffin and place cassette on top. Allow to cool.

Sectioning

1. Turn on water bath prior to start of sectioning. Wait for temperature of bath to equilibrate to 37-40ºC.
2. Place cassette in microtome and face off the sample until tissue appears.
3. Once you see tissue, place cassette face down in ImmunoCal bath for approximately 15 minutes in the freezer before sectioning again. This will give you about 15-20 good sections, after this return to the freezer for 10-15 minute intervals before returning to sectioning.
4. Set microtome to 7µm and begin sectioning.
5. Place individual sections in water bath to remove wrinkles in paraffin.
6. Place slides perpendicular to sections to remove from water bath.

***NOTE: If the specimen is perfectly straight, you will be able to get good sections of the entire length of the tendon. If not, you may need to gather multiple sections for each specimen as the tissue appears. For example, if the distal portion of the tendon appears first, take sections here in case you run out of tissue in this location before approaching tendon at the insertion site.**

7. Bake slides overnight at 50ºC or for 1 hour at 55 ºC.

A10. Histology protocols – H&E staining

1. This protocol was used on Bob's staining set in histology
2. Xylene 4 min
3. Xylene 4 min
4. Xylene 4 min
5. 100% EtOH 1 min
6. 100% EtOH 1 min
7. 100% EtOH 1 min
8. 95% EtOH 1 min
9. 95% EtOH 1 min
10. 70% EtOH 1 min
11. DI H_2O 1 min
12. Hematoxylin 1 min
13. Running DI H_2O Until clear
14. 3 dips in clarifier
15. Running DI H_2O 30 seconds
16. 3 dips in bluing solution
17. Running DI H_2O 30 seconds
18. 95% EtOH 2 min
19. Eosin 30 seconds
20. 95% EtOH 3 min
21. 95% EtOH 3 min
22. 100% EtOH 3 min
23. 100% EtOH 3 min
24. Xylene 3 min
25. Xylene 3 min
26. Xylene 3 min
27. Coverslip immediately using cytoseal

A11. Histology protocols – Histological grading

1. Before you begin, you must mark all H&E stained pictures with its appropriate specimen name. Be sure to also keep original unmarked images as that is what the graders will use.
2. Open a blank Powerpoint presentation
3. Place each H&E stained image into the powerpoint file, arranging from most elongated to most rounded cell shape (or least to most cellular).
4. After all images have been placed in the file, break the images into 4 equal sections.
5. Choose the middle image in each section to represent that grade (for example 0, 1, 2 or 3).
6. Create a separate powerpoint slide with each representative image and its associated grade to be used for blinded grading, such as seen below.
7. Instruct each blinded grader to set this image as their desktop, and then open each image to be graded against it.
8. Have them record their grade for each image.
9. After all 3 blinded graders are finished; assign the median grade among them to each sample.
10. Repeat for each tendon location.
11. Repeat for cellularity.

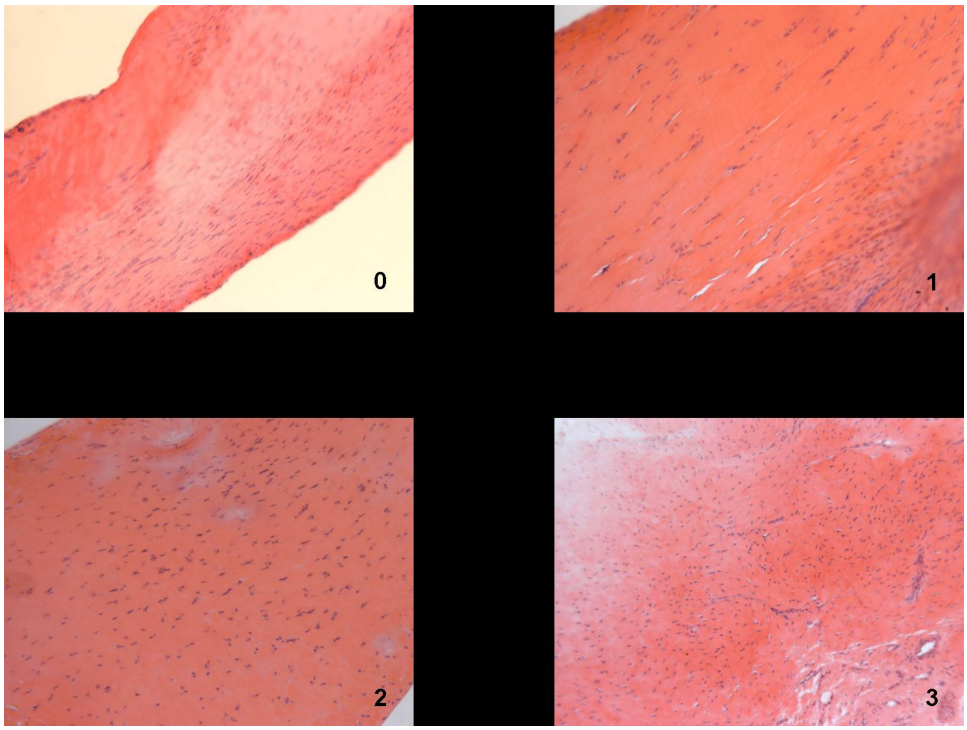

A12. Histology protocols – Polarized light analysis

This protocol is divided into three sections:

- Taking images at the polarizing microscope
- Analyzing these images using PolarWare program written in Matlab
- Importing results from this analysis into Oriana to obtain angular deviation values

---

Taking polarized light images

The setup on the microscope from top to bottom should be: eyepiece, rotating analyzer, objective, slide, stage, condenser, compensator (only for compensated images as described below), rotating polarizer

1. Turn on the microscope and the camera (plug firewire cable into either input on side of camera).
2. Using the 5X objective, focus the condenser so that the edges of the hexagon are sharp. (Dial at bottom left of microscope, on the base, changes the size of the hexagon. Condenser is focused using black knobs under stage).
3. Find the region of interest (e.g., injury) and focus the specimen.
4. As you change objectives from 5X to 10X, ensure that the edges of the hexagon are still in focus and that the specimen is still in focus.
5. Upon reaching the desired magnification, move the condenser hexagon out of view.
6. On the computer connected to the microscope, load QCapture Pro software. Click on the camera icon to bring up the capture menu. Click Preview to view the image.
7. Rotate the stage until the tendon is at a ~45 degree angle (bottom left to top right) and then lightly tighten the stage.
8. Set the analyzer to 180 degrees and the polarizer to 270 degrees. This position will be considered 45 degrees when saving the images.
9. Turn the light all the way up and ensure that all light is directed toward the camera.
10. Take the noncompensated images first. With the 10X objective in place, load the PLuncomp profile. Adjust exposure as needed. This can be done by checking that the image is not too bright (with the analyzer at 180 and the polarizer at 270) or too dark (with the analyzer at 135 and the polarizer rotated 45 clockwise to the blue line).
11. Rotate both the analyzer and polarizer in a clockwise direction by 10° increments. For both noncompensated and compensated images, pictures need to be taken across a 90° range in 10° increments.
12. Press Snap and save each picture as a tiff file. For each specimen, create a folder with the specimen number. Within this, create separate folders for compensated and noncompensated images. Save pictures using a 3 digit filename format. For example, a picture taken at 45° should be saved as 045. Repeat until a span of 90° (image named 135) has been reached.
13. Insert the compensator in its slot above the polarizer with the nail pointing down. The compensator must be oriented 45° counterclockwise from analyzer and polarizer (i.e., compensator nail should be pointing at 225 degrees – the blue line – on the polarizer).

14. Load the PLcomp profile and adjust exposure as needed.
15. Repeat steps 11 and 12; however, this time rotate the compensator in a clockwise direction with the analyzer and polarizer (make sure that compensator is always oriented 45° from the analyzer and polarizer while you are rotating). Instead of going from light to dark (or vice-versa) as you rotate analyzer compensator and polarizer, the images should go from blue to red (or vice versa).
16. Turn off camera by unplugging firewire cable and turn off microscope lamp.

Using PolarWare

1. Open MATLAB.
2. Set the correct path (Y:\Software\New Polarized Light Program\intensity_prog).
3. Type in "pl_PolarWare9v_fig".
4. Press button "Analyze images".
5. Put in the correct directories where the noncompensated and compensated images are saved.
6. Change parameters to desired values (values used for this data bolded below):
7. Bundle spacing determines the pixel distance between adjacent bundles (left, right, top, bottom)
    i. **Bundle spacing = 75**
8. Bundle size determines the size of each bundle. This value must be odd.
    i. **Bundle size = 3**
9. Angular increment determines the degree increment in which the pictures were taken.
    i. **Angular increment = 10**
10. Box width (% image) determines the total width of the grid of pixel bundles
    i. **Box width = 75**
11. Box height (% image) determines the total height of the grid of pixel bundles
    i. **Box width = 75**
12. Press button "Analyze images".
13. Click on the center of the region you are interested in.
14. Check compensated pictures 045 and 135 to see if color changes from blue to red or vice versa.
15. Go through each pixel bundle and ensure that the noncompensated and compensated light intensity graphs look good and that the correct extinction angle has been chosen. If the specimen was oriented at 45 degrees as described above, the bottom (i.e., compensated) graph should start high (red) and end low (blue). The extinction angle chosen by the program ("Min. Angle") should be 90 degrees off from the minimum (trough) of the top right (i.e., noncompensated) graph. If it is not (i.e., it matches) and the compensated graph still goes red to blue, then "move angle 90 degrees."
16. If the noncompensated or compensated light intensity graphs do not look good (i.e., very noisy) and/or are on a section of the slide that is not tendon, delete the bundle using the "delete" button.

17. After this is completed, move the mean orientation angle to 90 degrees by entering in the movement amount in the move angle by ___ degrees text box and then pressing the "move angles" button.
18. You can plot the histogram by pressing the histogram button and save if desired.
19. Export the data (COV, entropy, 2nd moment of inertia, and orientation angles for all the pixel buttons) by pressing the "export data" button. Data will be exported to folder where noncompensated images are stored (note: there is no feedback from program to indicate that data were exported).

Oriana Analysis

1. Open the exported output file in Excel.
2. Look through extinction angle data (first column). If there are any negative values, then add 180 to these; for values greater than 180, subtract 180.
3. In another column, multiply all extinction angle values by a factor of 2 (this is to make the analysis a complete circle).
4. Change column format to General (i.e., not scientific notation).
5. Open Oriana. From the File menu, select New and choose defaults (angles, circular data only) and click Next until Finish.
6. Copy and paste the newly created Excel column into the blank Oriana sheet.
7. From the Analyses menu, click on Stats. On the Main tab, make sure that Mean Angle, Length of Vector (r), and Standard Deviation are checked.
8. "Circular Standard Deviation" is the two times the angular deviation. Divide this value by 2.

A13. Immunohistochemical staining protocol – Collagen I

DAY 1

1.	CitriSolv®	5min×3 times
2.	100% EtOH	5min
3.	95% EtOH	5min
4.	70% EtOH	5min
5.	50% EtOH	5min
6.	DI H_2O	5min

7. Mark around samples using water-proof pen. **Be careful not to dry the slides out when immunostaining many slides at one time.**
8. Incubate samples in 100µl of 0.5mg/ml Hyalronidase-PBS (aliquots stored at -20°C) for 60 min at 37°C.
9. Rinse 2X with PBS for at least 5 min each.
10. Incubate samples in 0.5 N Acetic acid- DI H_2O for 4 hours at 4°C. Just before 4 hours is up, prepare H_2O_2-Methanol solution.
11. Rinse 2X with PBS for at least 5 min each.
12. Incubate samples in 3% H_2O_2-Methanol for 10 min at room temperature. During this time, thaw (or prepare) goat serum-PBS mixture.
13. Rinse with PBS for at least 5 min.
14. Apply Goat serum-PBS for 20 minutes for eliminating the background staining. To prepare: Three drops of goat serum (yellow label in VECTASTAIN ® ABC kit) in 10 ml PBS
15. Apply primary antibody AB755P (diluted 1:200 in 10% horse serum-PBS) to cover samples. For negative control apply the same amount of 10% horse serum-PBS.
16. Place several PBS-soaked kimwipes on tray with slides. Seal the lid of the moist chamber securely using Parafilm®.
17. Incubate overnight (approximately 16 hours) at 4°C. Turn off vacuum.

DAY 2

18. Rinse **3X** with PBS for at least 5 min each. Mix up secondary antibody.
19. Apply secondary antibody 550338 (diluted 1:200 10% horse serum-PBS) to cover samples and incubate for 30 min at room temp. **Be careful not to contaminate a negative control slide with the primary antibody.** While incubating: Make VECTASTAIN ABC reagent: 1 drop Reagent A in 2.5ml PBS vortex and 1 drop of Reagent B vortex and allow to stand in fridge for 30 min prior to use
20. Rinse 2X with PBS for at least 5 min each.
21. Apply VECTASTAIN ABC reagent to cover samples and incubate for 30 min at room temp.
22. Rinse with PBS for at least 5 min.
23. **Move to Hood.** Apply DAB substance solution to cover samples around 4 minutes or until suitable sraining is observed. **Immediately** remove DAB when ready and rinse with tap water. **DO NOT USE VACUUM.** To prepare: in 2.5 ml

DI H_2O add 1 drop Buffer and vortex. Then add two drops DAB solution and vortex. Then add 1 drop Hydrogen Peroxide and vortex. **Use DAB neutralizer for waste solution.**

24. Wipe the water outside of the circle. Add eight drops of crystal mounting medium and dry slides overnight at 37°C. (When using a coverglass, finish taking pictures **soon** otherwise a lot of bubble should appear all around the samples).

Preparing solutions for Collagen type I:

3% H_2O_2-Methanol – Make up fresh because hydrogen peroxide is sensitive to light. Both H_2O_2 and methanol are stored in the fridge. Prepare approximately 100 µL/slide. Example - 120 µL H_2O_2 and 1080 µL of methanol for 12 slides. Dispose of any extra H_2O_2-Methanol in the sink in the fume hood and rinse down.

Goat serum-PBS – Stored in blue-capped centrifuge tubes in the freezer. If you need more, mix 3 drops of goat serum (from old Vectastain container in the fridge) to 10 mL of PBS. Store in freezer when finished.

Col I Primary Antibody – The antibody AB755P is diluted 1:200 in **10%** horse serum-PBS. Prepare 100 µL (or less) per slide. The horse serum-PBS mix is stored in the freezer and the primary antibody (for collagen I) is stored in the freezer in 1 µL aliquots. Thaw each 1 µL aliquot, centrifuge and then add 200 µL of 10% horse serum-PBS. Try to use as little antibody as possible; just enough to cover the samples. Pure serum vials are also stored in the freezer if more horse serum-PBS mix is needed.

Col I Secondary Antibody – The antibody 550338 is diluted 1:200 in **10**% horse serum-PBS. Prepare 100 µL per slide. Example – 10 µL antibody and 1990 µL horse serum-PBS for 20 slides. The antibody is stored in the fridge and the serum is in the freezer. Parafilm seal the antibody container and immediately return the fridge after using.

Vectastain ABC – Prepare 30 minutes prior to use. Mix 1 drop Reagent A in 2.5 mL PBS and vortex. Add 1 drop Reagent B and vortex. Store in fridge until ready to use.

DAB – Prepare immediately before using. In 2.5 mL DI (or distilled) H_2O add 1 drop Buffer and vortex. Add two drops DAB solution and vortex. Add 1 drop hydrogen peroxide and vortex.

A14. Immunohistochemical staining protocol – Collagen II

DAY 1

1. CitriSolv® 5min×3 times
2. 100% EtOH 5min
3. 95% EtOH 5min
4. 70% EtOH 5min
5. 50% EtOH 5min
6. DI H_2O 5min
7. Mark around samples using water-proof pen. **Be careful not to dry the slides out when immunostaining many slides at one time.**
8. Incubate samples in 100µl of 0.5mg/ml Hyalronidase-PBS (aliquots stored at -20°C) for 60 min at 37°C.
9. Rinse 3X with PBS for at least 5 min each.
10. Incubate samples in 0.5 N Acetic acid- DI H_2O for 4 hours at 4°C. Just before 4 hours is up, prepare H_2O_2-Methanol solution.
11. Rinse 2X with PBS for at least 5 min each.
12. Incubate samples in 3% H_2O_2-Methanol for 10 min at room temperature. Prepare skimmilk solution during this 10 minute break.
13. Rinse with PBS for at least 5 min.
14. Apply 5% skimmilk-PBS for 30 minutes for eliminating the background staining. Prepare primary antibody solution during this 30 minutes.
15. Rinse with PBS for at least 5 min.
16. Apply primary antibody II-II6B3 (diluted 1:4 in 1% horse serum-PBS) to cover samples. For negative control apply the same amount of 1% horse serum-PBS.
17. Place several PBS-soaked kimwipes on tray with slides. Seal the lid of the moist chamber securely using Parafilm®.
18. Incubate overnight (approximately 16 hours) at 4°C. Turn off vacuum.

DAY 2

19. Prepare secondary antibody solution. Then rinse **3X** with PBS for at least 5 min each.
20. Apply secondary antibody 550331 (diluted 1:100 in 1% horse serum-PBS) to cover samples and incubate for 30 min at room temp. **Be careful not to contaminate a negative control slide with the primary antibody.** While incubating: Make VECTASTAIN ABC reagent: 1 drop Reagent A in 2.5ml PBS vortex and 1 drop of Reagent B vortex and allow to stand for 30 min prior to use
21. Rinse 2X with PBS for at least 5 min each.
22. Apply VECTASTAIN ABC reagent to cover samples and incubate for 30 min at room temp.
23. Rinse with PBS for at least 5 min.
24. **Move to Hood.** Apply DAB substance solution to cover samples around 4 minutes or until suitable sraining is observed. **Immediately** remove DAB when ready and rinse with tap water. **DO NOT USE VACUUM.** To prepare: in 2.5 ml

DI H_2O add 1 drop Buffer and vortex. Then add two drops DAB solution and vortex. Then add 1 drop Hydrogen Peroxide and vortex. **Use DAB neutralizer for waste solution.**

25. Can counter-stain cell nuclei with hematoxylin here, if desired.
26. Wipe the water outside of the circle. Add eight drops of crystal mounting medium and dry slides overnight at 37°C. (When using a coverglass, finish taking pictures **soon** otherwise a lot of bubble should appear all around the samples).

Preparing solutions for Collagen type II:

3% H_2O_2-Methanol – Make up fresh because hydrogen peroxide is sensitive to light. Both H_2O_2 and methanol are stored in the fridge. Prepare approximately 100 µL/slide. Example - 120 µL H_2O_2 and 1080 µL of methanol for 12 slides. Dispose of any extra H_2O_2-Methanol in the sink in the fume hood and rinse down.

5% Skimmilk-PBS – Make up fresh to avoid particles. Mix 0.5 g powdered milk with 10 mL PBS in a blue-cap centrifuge tube. Dispose extra solution in sink drain.

Col II Primary Antibody – The antibody II-II6B3 is diluted 1:4 in 1% horse serum-PBS. Prepare 100 µL per slide. Example – 500 µL antibody and 2000 µL horse serum-PBS for 25 slides. The horse serum-PBS mix is stored in the freezer and the primary antibody (for collagen II) is stored in the fridge. Pure serum vials are also stored in the freezer. When drawing fluid from the primary antibody container, use a sterilized pipette tip to avoid getting mold in the antibody container.

Col II Secondary Antibody – The antibody 550331 is diluted 1:100 in 1% horse serum-PBS. Prepare 100 µL per slide. Example – 20 µL antibody and 1980 µL horse serum-PBS for 20 slides. The antibody is stored in the fridge and the serum is in the freezer. Parafilm seal the antibody container and immediately return the fridge after using.

Vectastain ABC – Prepare 30 minutes prior to use. Mix 1 drop Reagent A in 2.5 mL PBS and vortex. Add 1 drop Reagent B and vortex. Store in fridge until ready to use.

DAB – Prepare immediately before using. In 2.5 mL DI (or distilled) H_2O add 1 drop Buffer and vortex. Add two drops DAB solution and vortex. Add 1 drop hydrogen peroxide and vortex.

A15. Immunohistochemical staining protocol – Collagen III

DAY 1

1. CitriSolv® 5min×3 times
2. 100% EtOH 5min
3. 95% EtOH 5min
4. 70% EtOH 5min
5. 50% EtOH 5min
6. DI H_2O 5min
7. Mark around samples using water-proof pen. **Be careful not to dry the slides out when immunostaining many slides at one time.**
8. Incubate samples in 100µl Protease K (0.4 mg/mL diluted in 30mM Tris HCL) for 4 min at room temperature.
9. Rinse 2X with PBS for at least 5 min each.
10. Incubate samples in 100µl of 0.5mg/ml Hyalronidase-PBS (aliquots stored at -20°C) for 60 min at 37°C.
11. Rinse 2X with PBS for at least 5 min each.
12. Incubate samples in 0.5 N Acetic acid- DI H_2O for 4 hours at 4°C.
13. Rinse 2X with PBS for at least 5 min each.
14. Incubate samples in 3% H_2O_2-Methanol for 10 min at room temperature.
15. Rinse with PBS for at least 5 min.
16. Apply 10% Horse serum-PBS to cover samples and incubate for 20 min to eliminate the background staining.
17. Apply primary antibody C7805 (diluted 1:50 in 10% horse serum-PBS) to cover samples. For negative control apply the same amount of 10% horse serum-PBS.
18. Seal the lid of the moist chamber **securely** using Parafilm®.
19. Incubate two nights and three days (approximately 34-38 hours) at 4°C.

DAY 3

20. Rinse **3X** with PBS for at least 5 min each.
21. Apply secondary antibody 550331 (diluted 1:100 10% horse serum-PBS) to cover samples and incubate for 30 min at room temp. **Be careful not to contaminate a negative control slide with the primary antibody.** While incubating: Make VECTASTAIN ABC reagent: 1 drop Reagent A in 2.5ml PBS vortex and 1 drop of Reagent B vortex and allow to stand for 30 min prior to use
22. Rinse 2X with PBS for at least 5 min each.
23. Apply VECTASTAIN ABC reagent to cover samples and incubate for 30 min at room temp.
24. Rinse with PBS for at least 5 min.
25. **Move to Hood.** Apply DAB substance solution to cover samples around 4 minutes or until suitable sraining is observed. **Immediately** remove DAB when ready and rinse with tap water. **DO NOT USE VACUUM.** To prepare: in 2.5 ml DI H_2O add 1 drop Buffer and vortex. Then add two drops DAB solution and

vortex. Then add 1 drop Hydrogen Peroxide and vortex. **Use DAB neutralizer for waste solution.**

26. Wipe the water outside of the circle. Add eight drops of crystal mounting medium and dry slides overnight at 37°C. (When using a coverglass, finish taking pictures **soon** otherwise a lot of bubble should appear all around the samples).

Preparing solutions for collagen III staining:

3% H_2O_2-Methanol – Make up fresh because hydrogen peroxide is sensitive to light. Both H_2O_2 and methanol are stored in the fridge. Prepare approximately 100 µL/slide. Example - 120 µL H_2O_2 and 1080 µL of methanol for 12 slides. Dispose of any extra H_2O_2-Methanol in the sink in the fume hood and rinse down.

Col III Primary Antibody – The antibody C7805 is diluted 1:50 in 10% horse serum-PBS. Prepare 100 µL per slide. Example – 80 µL antibody and 3920 µL horse serum-PBS for 40 slides. The horse serum-PBS mix is stored in the freezer and the primary antibody (for collagen III) is stored in the freezer. Pure serum vials are also stored in the freezer. When drawing fluid from the primary antibody container, use a sterilized pipette tip to avoid getting mold in the antibody container.

Col III Secondary Antibody – The antibody 550331 is diluted 1:100 in 1% horse serum-PBS. Prepare 200 µL per slide. Example – 40 µL antibody and 3960 µL horse serum-PBS for 40 slides. The antibody is stored in the fridge and the serum is in the freezer. Parafilm seal the antibody container and immediately return the fridge after using.

Vectastain ABC – Prepare 30 minutes prior to use. Mix 1 drop Reagent A in 2.5 mL PBS and vortex. Add 1 drop Reagent B and vortex. Store in fridge until ready to use.

DAB – Prepare immediately before using. In 2.5 mL DI (or distilled) H_2O add 1 drop Buffer and vortex. Add two drops DAB solution and vortex. Add 1 drop hydrogen peroxide and vortex.

A16. Immunohistochemical staining protocol – Collagen XII

DAY 1

1.	CitriSolv®	5min×3 times
2.	100% EtOH	5min
3.	95% EtOH	5min
4.	70% EtOH	5min
5.	50% EtOH	5min
6.	DI H_2O	5min

7. Mark around samples using water-proof pen. **Be careful not to dry the slides out when immunostaining many slides at one time.**
8. Incubate samples in 100µl of 0.5mg/ml Hyalronidase-PBS (aliquots stored at -20°C) for 60 min at 37°C.
9. Rinse 2X with PBS for at least 5 min each.
10. Incubate samples in 0.5 N Acetic acid- DI H_2O for 4 hours at 4°C.
11. Rinse 2X with PBS for at least 5 min each.
12. Incubate samples in 3% H_2O_2-Methanol for 10 min at room temperature.
13. Rinse with PBS for at least 5 min.
14. Apply 5% skimmilk-PBS for 30 minutes for eliminating the background staining
15. Rinse with PBS for at least 5 min.
16. Apply Goat serum-PBS for 20 minutes for eliminating the background staining. To prepare: Three drops of goat serum (yellow label in VECTASTAIN ® ABC kit) in 10 ml PBS
17. Apply primary antibody LB-1200 (diluted 1:100 in 10% horse serum-PBS) to cover samples. For negative control apply the same amount of 10% horse serum-PBS.
18. Seal the lid of the moist chamber securely using Parafilm®.
19. Incubate overnight (approximately 16 hours) at 4°C.

DAY 2

20. Rinse **3X** with PBS for at least 5 min each.
21. Apply secondary antibody 550338 (diluted 1:200 10% horse serum-PBS) to cover samples and incubate for 30 min at room temp. **Be careful not to contaminate a negative control slide with the primary antibody.** While incubating: Make VECTASTAIN ABC reagent: 1 drop Reagent A in 2.5ml PBS vortex and 1 drop of Reagent B vortex and allow to stand for 30 min prior to use
22. Rinse 2X with PBS for at least 5 min each.
23. Apply VECTASTAIN ABC reagent to cover samples and incubate for 30 min at room temp.
24. Rinse with PBS for at least 5 min.
25. **Move to Hood.** Apply DAB substance solution to cover samples around 4 minutes or until suitable sraining is observed. **Immediately** remove DAB when ready and rinse with tap water. **DO NOT USE VACUUM.** To prepare: in 2.5 ml DI H_2O add 1 drop Buffer and vortex. Then add two drops DAB solution and

vortex. Then add 1 drop Hydrogen Peroxide and vortex. **Use DAB neutralizer for waste solution.**

26. Wipe the water outside of the circle. Add eight drops of crystal mounting medium and dry slides overnight at 37°C. (When using a coverglass, finish taking pictures **soon** otherwise a lot of bubble should appear all around the samples).

Preparing solutions for collagen XII staining:

3% H_2O_2-Methanol – Make up fresh because hydrogen peroxide is sensitive to light. Both H_2O_2 and methanol are stored in the fridge. Prepare approximately 100 µL/slide. Example - 120 µL H_2O_2 and 1080 µL of methanol for 12 slides. Dispose of any extra H_2O_2-Methanol in the sink in the fume hood and rinse down.

5% Skimmilk-PBS – Make up fresh to avoid particles. Mix 0.5 g powdered milk with 10 mL PBS in a blue-cap centrifuge tube. Dispose extra solution in sink drain.

Col XII Primary Antibody – The antibody LB-1200 is diluted 1:100 in 10% horse serum-PBS. Prepare 100 µL per slide. Example – 40 µL antibody and 3960 µL horse serum-PBS for 40 slides. The horse serum-PBS mix is stored in the freezer and the primary antibody (for collagen XII) is stored in the freezer. Pure serum vials are also stored in the freezer. When drawing fluid from the primary antibody container, use a sterilized pipette tip to avoid getting mold in the antibody container.

Col XII Secondary Antibody – The antibody 550338 is diluted 1:200 in 10% horse serum-PBS. Prepare 100 µL per slide. Example – 20 µL antibody and 3980 µL horse serum-PBS for 40 slides. The antibody is stored in the fridge and the serum is in the freezer. Parafilm seal the antibody container and immediately return the fridge after using.

Vectastain ABC – Prepare 30 minutes prior to use. Mix 1 drop Reagent A in 2.5 mL PBS and vortex. Add 1 drop Reagent B and vortex. Store in fridge until ready to use.

DAB – Prepare immediately before using. In 2.5 mL DI (or distilled) H_2O add 1 drop Buffer and vortex. Add two drops DAB solution and vortex. Add 1 drop hydrogen peroxide and vortex.

A17. Immunohistochemical staining protocol – Aggrecan

DAY 1

1.	CitriSolv®	5min×3 times
2.	100% EtOH	5min
3.	95% EtOH	5min
4.	70% EtOH	5min
5.	50% EtOH	5min
6.	DI H_2O	5min

7. Mark around samples using water-proof pen. **Be careful not to dry the slides out when immunostaining many slides at one time.**
8. **Move to Hood since DTT smells bad.** Incubate samples in 10 mM dithiothreitol (DTT) in 50mM Tris-Hcl, 200mM sodium chloride, pH 7.4 (aliquots stored at -20°C) for 2 hours at 37°C. While incubating: Make 40mM iodoacetamide-PBS. **DO NOT USE VACUUM.**
9. Rinse with PBS for at least 5 min.
10. Alkylate samples in 40mM iodoacetamide (powder stored in the refrigerator)-PBS for 1 hour at 37°C. **NOT USE VACUUM.**
11. Rinse with PBS for at least 5 min. **Move back to desk.**
12. Incubate samples in 100µl of 0.25U/ml Chondroitinase-AC-0.02M phosphate Buffer, 1mg/ml BSA, pH 7.0 (aliquots stored at -20°C) for 60 min at 37°C.
13. Rinse 2X with PBS for at least 5 min each.
14. Incubate samples in 3% H_2O_2-Methanol for 10 min at room temperature.
15. Rinse with PBS for at least 5 min.
16. Apply 5% skimmilk-PBS for 30 minutes for eliminating the background staining
17. Rinse with PBS for at least 5 min.
18. Apply Goat serum-PBS for 20 minutes for eliminating the background staining. To prepare: Three drops of goat serum (yellow label in VECTASTAIN ® ABC kit) in 10 ml PBS
19. Apply primary antibody JSCATE (diluted 1:200 in 10% horse serum-PBS) to cover samples. For negative control apply the same amount of 10% horse serum-PBS.
20. Seal the lid of the moist chamber securely using Parafilm®.
21. Incubate overnight (approximately 16 hours) at 4°C.

DAY 2

22. Rinse **3X** with PBS for at least 5 min each.
23. Apply secondary antibody 550338 (diluted 1:200 10% horse serum-PBS) to cover samples and incubate for 30 min at room temp. **Be careful not to contaminate a negative control slide with the primary antibody.** While incubating: Make VECTASTAIN ABC reagent: 1 drop Reagent A in 2.5ml PBS vortex and 1 drop of Reagent B vortex and allow to stand for 30 min prior to use
24. Rinse 2X with PBS for at least 5 min each.

25. Apply VECTASTAIN ABC reagent to cover samples and incubate for 30 min at room temp.
26. Rinse with PBS for at least 5 min.
27. **Move to Hood.** Apply DAB substance solution to cover samples around 4 minutes or until suitable staining is observed. **Immediately** remove DAB when ready and rinse with tap water. **DO NOT USE VACUUM.** To prepare: in 2.5 ml DI H_2O add 1 drop Buffer and vortex. Then add two drops DAB solution and vortex. Then add 1 drop Hydrogen Peroxide and vortex.
28. Wipe the water outside of the circle. Add eight drops of crystal mounting medium and dry slides overnight at 37°C (when using a coverglass, finish taking pictures **soon** otherwise a lot of bubble should appear all around the samples).

Preparing solutions for aggrecan staining:

3% H_2O_2-Methanol – Make up fresh because hydrogen peroxide is sensitive to light. Both H_2O_2 and methanol are stored in the fridge. Prepare approximately 100 µL/slide. Example - 120 µL H_2O_2 and 1080 µL of methanol for 12 slides. Dispose of any extra H_2O_2-Methanol in the sink in the fume hood and rinse down.

5% Skimmilk-PBS – Make up fresh to avoid particles. Mix 0.5 g powdered milk with 10 mL PBS in a blue-cap centrifuge tube. Dispose extra solution in sink drain.

Aggrecan Primary Antibody – The antibody JSCATE (final concentration of 10µg/mL) is diluted 1:200 in 10% horse serum-PBS. Prepare 100 µL per slide. Example – 20 µL antibody and 3980 µL horse serum-PBS for 40 slides. The horse serum-PBS mix is stored in the freezer and the primary antibody (for aggrecan) is stored in the freezer. Pure serum vials are also stored in the freezer. When drawing fluid from the primary antibody container, use a sterilized pipette tip to avoid getting mold in the antibody container.

Aggrecan Secondary Antibody – The antibody 550338 is diluted 1:200 in 10% horse serum-PBS. Prepare 100 µL per slide. Example – 20 µL antibody and 3980 µL horse serum-PBS for 40 slides. The antibody is stored in the fridge and the serum is in the freezer. Parafilm seal the antibody container and immediately return the fridge after using.

Vectastain ABC – Prepare 30 minutes prior to use. Mix 1 drop Reagent A in 2.5 mL PBS and vortex. Add 1 drop Reagent B and vortex. Store in fridge until ready to use.

DAB – Prepare immediately before using. In 2.5 mL DI (or distilled) H_2O add 1 drop Buffer and vortex. Add two drops DAB solution and vortex. Add 1 drop hydrogen peroxide and vortex.

A18. Immunohistochemical staining protocol – Biglycan

DAY 1

1.	CitriSolv®	5min×3 times
2.	100% EtOH	5min
3.	95% EtOH	5min
4.	70% EtOH	5min
5.	50% EtOH	5min
6.	DI H_2O	5min

7. Mark around samples using water-proof pen. **Be careful not to dry the slides out when immunostaining many slides at one time.**
8. Incubate samples in 100µl of 0.2U/ml Chondroitinase-ABC-0.1M Tris-Acetate, 1mg/ml BSA (aliquots stored at -20°C) for 60 min at 37°C.
9. Rinse 2X with PBS for at least 5 min each.
10. Incubate samples in 0.5 N Acetic acid- DI H_2O for 4 hours at 4°C.
11. Rinse 2X with PBS for at least 5 min each.
12. Incubate samples in 3% H_2O_2-Methanol for 10 min at room temperature.
13. Rinse with PBS for at least 5 min.
14. Apply 5% skimmilk-PBS for 30 minutes for eliminating the background staining
15. Rinse with PBS for at least 5 min.
16. Apply Goat serum-PBS for 20 minutes for eliminating the background staining. To prepare: Three drops of goat serum (yellow label in VECTASTAIN ® ABC kit) in 10 ml PBS
17. Apply primary antibody LF-159 (diluted 1:200 in 10% horse serum-PBS) to cover samples. For negative control apply the same amount of 10% horse serum-PBS.
18. Seal the lid of the moist chamber securely using Parafilm®.
19. Incubate two night and three days (approximately 34-38 hours) at 4°C.

DAY 3

20. Rinse **3X** with PBS – 5 min wash, 30 min wash (in fridge), 5 min wash
21. Apply secondary antibody 550338 (diluted 1:200 10% horse serum-PBS) to cover samples and incubate for 30 min at room temp. **Be careful not to contaminate a negative control slide with the primary antibody.** While incubating: Make VECTASTAIN ABC reagent: 1 drop Reagent A in 2.5ml PBS vortex and 1 drop of Reagent B vortex and allow to stand for 30 min prior to use
22. Rinse 2X with PBS for at least 5 min each.
23. Apply VECTASTAIN ABC reagent to cover samples and incubate for 30 min at room temp.
24. Rinse with PBS for at least 5 min.
25. **Move to Hood.** Apply DAB substance solution to cover samples around 4 minutes or until suitable sraining is observed. **Immediately** remove DAB when ready and rinse with tap water. **DO NOT USE VACUUM.** To prepare: in 2.5 ml DI H_2O add 1 drop Buffer and vortex. Then add two drops DAB solution and

vortex. Then add 1 drop Hydrogen Peroxide and vortex. **Use DAB neutralizer for waste solution.**

26. Wipe the water outside of the circle. Add eight drops of crystal mounting medium and dry slides overnight at 37°C. (When using a coverglass, finish taking pictures **soon** otherwise a lot of bubble should appear all around the samples).

Preparing solutions for biglycan staining:

3% H_2O_2-Methanol – Make up fresh because hydrogen peroxide is sensitive to light. Both H_2O_2 and methanol are stored in the fridge. Prepare approximately 100 µL/slide. Example - 120 µL H_2O_2 and 1080 µL of methanol for 12 slides. Dispose of any extra H_2O_2-Methanol in the sink in the fume hood and rinse down.

5% Skimmilk-PBS – Make up fresh to avoid particles. Mix 0.5 g powdered milk with 10 mL PBS in a blue-cap centrifuge tube. Dispose extra solution in sink drain.

Biglycan Primary Antibody – The antibody LF-159 is diluted 1:200 in 10% horse serum-PBS. Prepare 100 µL per slide. Example – 20 µL antibody and 3980 µL horse serum-PBS for 40 slides. The horse serum-PBS mix is stored in the freezer and the primary antibody (for aggrecan) is stored in the freezer. Pure serum vials are also stored in the freezer. When drawing fluid from the primary antibody container, use a sterilized pipette tip to avoid getting mold in the antibody container.

Aggrecan Secondary Antibody – The antibody 550338 is diluted 1:200 in 10% horse serum-PBS. Prepare 100 µL per slide. Example – 20 µL antibody and 3980 µL horse serum-PBS for 40 slides. The antibody is stored in the fridge and the serum is in the freezer. Parafilm seal the antibody container and immediately return the fridge after using.

Vectastain ABC – Prepare 30 minutes prior to use. Mix 1 drop Reagent A in 2.5 mL PBS and vortex. Add 1 drop Reagent B and vortex. Store in fridge until ready to use.

DAB – Prepare immediately before using. In 2.5 mL DI (or distilled) H_2O add 1 drop Buffer and vortex. Add two drops DAB solution and vortex. Add 1 drop hydrogen peroxide and vortex.

A19. Immunohistochemical staining protocol – Decorin

DAY 1

1.	CitriSolv®	5min×3 times
2.	100% EtOH	5min
3.	95% EtOH	5min
4.	70% EtOH	5min
5.	50% EtOH	5min
6.	DI H_2O	5min

7. Mark around samples using water-proof pen. **Be careful not to dry the slides out when immunostaining many slides at one time.**
8. Incubate samples in 100µl of 0.2U/ml Chondroitinase-ABC-0.1M Tris-Acetate, 1mg/ml BSA (aliquots stored at -20°C) for 60 min at 37°C.
9. Rinse 2X with PBS for at least 5 min each.
10. Incubate samples in 0.5 N Acetic acid- DI H_2O for 4 hours at 4°C.
11. Rinse 2X with PBS for at least 5 min each.
12. Incubate samples in 3% H_2O_2-Methanol for 10 min at room temperature.
13. Rinse with PBS for at least 5 min.
14. Apply 5% skimmilk-PBS for 30 minutes for eliminating the background staining
15. Rinse with PBS for at least 5 min.
16. Apply Goat serum-PBS for 20 minutes for eliminating the background staining. To prepare: Three drops of goat serum (yellow label in VECTASTAIN ® ABC kit) in 10 ml PBS
17. Apply primary antibody LF-113 (diluted 1:300 in 10% horse serum-PBS) to cover samples. For negative control apply the same amount of 10% horse serum-PBS.
18. Create humid tray by placing PBS-soaked Kimwipes underneath parafilm on slide trays.
19. Seal the lid of the moist chamber securely using Parafilm®.
20. Incubate two nights and three days (approximately 34-38 hours) at 4°C.

DAY 3

21. Rinse **3X** with PBS for at least 5 min each.
22. Apply secondary antibody 550338 (diluted 1:200 10% horse serum-PBS) to cover samples and incubate for 30 min at room temp. **DO NOT contaminate a negative control slide with the primary antibody.** While incubating: Make VECTASTAIN ABC reagent: 1 drop Reagent A in 2.5ml PBS vortex and 1 drop of Reagent B vortex and allow to stand for 30 min prior to use
23. Rinse 2X with PBS for at least 5 min each.
24. Apply VECTASTAIN ABC reagent to cover samples and incubate for 30 min at room temp.
25. Rinse with PBS for at least 5 min.
26. Apply DAB substance solution to cover samples around 4 minutes or until suitable sraining is observed. **Immediately** remove DAB when ready and rinse with tap water. **DO NOT USE VACUUM.** To prepare: in 2.5 ml DI H_2O add 1

drop Buffer and vortex. Then add two drops DAB solution and vortex. Then add 1 drop Hydrogen Peroxide and vortex.

27. Wipe the water outside of the circle. Add eight drops of crystal mounting medium and dry slides overnight at 37°C.

Preparing solutions for decorin staining:

3% H_2O_2-Methanol – Make up fresh because hydrogen peroxide is sensitive to light. Both H_2O_2 and methanol are stored in the fridge. Prepare approximately 100 µL/slide. Example - 120 µL H_2O_2 and 1080 µL of methanol for 12 slides. Dispose of any extra H_2O_2-Methanol in the sink in the fume hood and rinse down.

5% Skimmilk-PBS – Make up fresh to avoid particles. Mix 0.5 g powdered milk with 10 mL PBS in a blue-cap centrifuge tube. Dispose extra solution in sink drain.

Goat serum-PBS – Stored in blue-capped centrifuge tubes in the freezer. If you need more, mix 3 drops of goat serum (from old Vectastain container in the fridge) to 10 mL of PBS. Store in freezer when finished.

Decorin Primary Antibody – The antibody LF-113 is diluted 1:300 in **10%** horse serum-PBS. Prepare 100 µL per slide. The horse serum-PBS mix is stored in the freezer and the primary antibody (for decorin) is stored in the freezer in 6 µL aliquots. Thaw each 6 µL aliquot, centrifuge and then add 900 µL of 10% horse serum-PBS. Vortex solution then transfer to blue-capped centrifuge tube. Add another 900 µL of 10% horse serum-PBS. Try to use as little antibody as possible; just enough to cover the samples. Pure serum vials are also stored in the freezer if more horse serum-PBS mix is needed.

Decorin Secondary Antibody – The antibody 550338 is diluted 1:200 in **10**% horse serum-PBS. Prepare 100 µL per slide. Example – 10 µL antibody and 1990 µL horse serum-PBS for 20 slides. The antibody is stored in the fridge and the serum is in the freezer. Parafilm seal the antibody container and immediately return the fridge after using.

Vectastain ABC – Prepare 30 minutes prior to use. Mix 1 drop Reagent A in 2.5 mL PBS and vortex. Add 1 drop Reagent B and vortex.

DAB – Prepare immediately before using. In 2.5 mL DI (or distilled) H_2O add 1 drop Buffer and vortex. Add two drops DAB solution and vortex. Add 1 drop hydrogen peroxide and vortex.

A20. Immunohistochemistry protocols – DAB intensity analysis

1. Place all images to be analyzed in one folder (for example, all images for one tendon location and one staining target)
2. Open MATLAB and set path to Y:\Software\Immuno
3. Run program immuno_analysis
4. Select the region that you want to analyze by creating a polygon by clicking the mouse button. Choose as many points as you need, then double click the last point to move on to the next image.
5. Continue until the last image is analyzed.
6. Copy the MATLAB output to a spreadsheet.
7. For each target, calculate the range of DAB intensities
8. Divide this range into 4 quartiles
9. Assign each quartile a grade (for example 0, 1, 2 and 3 or -, +, ++ and +++)
10. Assign each image a grade based on the appropriate range that its intensity value falls in.